P-V-T PROPERTIES OF METHYL CHLORIDE AT HIGH TEMPERATURES AND PRESSURES

A Dissertation

Presented to

the Faculty of the Graduate School

University of Missouri

In Partial Fulfillment

of the Requirements for the Degree

Doctor of Philosophy

---

by

Kyung Won Suh

June 1965

Truman S. Storvick Dissertation Supervisor

ACKNOWLEDGEMENTS

The author wishes to express his sincere appreciation to Dr. Truman S. Storvick of the Chemical Engineering Department for his invaluable assistance during the course of this project and to Mr. Joseph Twenter for the construction of the experimental apparatus.

The author also wishes to express his gratitude to the University of Missouri Computer Center for the use of their facilities, the National Science Foundation for financial support through grant G24480, and the Engineering Experiment Station for the financial assistance through research assistantships.

TABLE OF CONTENTS

CHAPTER PAGE

CHAPTER PAGE

LIST OF TABLES

LIST OF FIGURES

CHAPTER I

INTRODUCTION

The equation of state of a gas describes the relation between the three variables pressure, volume, and temperature. Many equations have been proposed which accurately describe the p-v-T relations of real gases (3,4,5,8,18,20, 26,31,32,39,51,58,70,74,90). Some of these are purely empirical while others are derived from the intermolecular properties.

A knowledge of the equation of state is necessary for obtaining equilibrium properties of pure substances. The volumetric behavior of non-polar gases may be described by the application of the principle of corresponding states, which has been successful in predicting compressibility factors and second virial coefficients for both pure gases and binary gas mixtures (19,24,25,34,35,49,54,59,63,66,67, 71). Polar gases deviate considerably from the principle of corresponding states, and require different treatment.

Two methods have been used in predicting the second virial coefficient of polar gases. The first method uses statistical mechanics and an intermolecular potential function based on a physical model. The second method is based on a hypothesis, first proposed by Eucken (21), that

polar gases undergo partial association due to dipole interaction or to hydrogen bonding, and that this is responsible for their deviation from the principle of corresponding states. This method of interpretation was originally applied by Alexander and Lambert to their results on acetaldehyde (1), and later by others to interpret the second virial coefficients (10,23,30,33,46,47). In this investigation the first approach was used to analyze the experimental second virial coefficient data.

The most general equation of state proposed by H. K. Onnes (32) can be written in the form

$$\frac{PV}{RT} = 1 + \frac{B(T)}{V} + \frac{C(T)}{V^2} + \ldots\ldots \qquad (1)$$

where B(T), C(T) ..... are the second,third,..... virial coefficients. The value of these coefficients provide the information for determining parameters in intermolecular potential functions. In recent years many attempts have been made to calculate these coefficients from a consideration of intermolecular forces (6,7,17,27,29,38,41,42,43, 44,48,52,53,68,73).

The most widely used potential function for monatomic molecules was originally introduced by Lennard-Jones (50) to represent an inverse sixth power attraction and an inverse twelfth power repulsion between spherical molecular pairs. Although the Lennard-Jones potential gives

satisfactory results for the inert gases, this type of potential is not as successful when the molecule becomes complex. Additional parameters related to the molecular geometry have been included to improve the representation of complex nonpolar molecules.

Kihara (40) has extended Lennard-Jones potential to nonspherical particles based on the geometry of convex bodies. The Kihara potential has been found to give better results than the Lennard-Jones potential for these nonspherical molecules (14,15,69,78).

Stockmayer (81) has also extended Lennard-Jones potential to include dipole interactions between polar molecules. This has since been applied by other investigators to the calculation of second virial coefficients (33,68,72,75) and transport properties (61).

In this investigation, the Kihara core model was used to represent the geometry of a polar molecule. A permanent point dipole was placed in the core and used to represent the polar contribution to the molecular pair force field. Pople's perturbation method (68) was used to obtain an expression for the second virial coefficient of a polar gas. Numerical methods were then used to evaluate the potential parameters for nine polar gases. Derived thermodynamic properties of methyl chloride were also

calculated from the calculated B(T) values for the modified Kihara potential and compared with those calculated from the p-v-T data.

Accurate experimental data are required to test these existing intermolecular force models. Extensive measurements of p-v-T properties over a wide range of conditions have been made on simple nonpolar gases and summarized by several authors (32,39,70). However, no systematic experimental studies over a wide range of conditions have been made on polar gases except for water and ammonia. It is the purpose of this investigation to measure the p-v-T properties of methyl chloride at pressures up to 5,000 psi and temperatures up to 350°C by the Burnett method.

In the conventional procedures for measuring p-v-T properties of a gas, it is necessary to determine the pressure, temperature, volume, and mass of the gas charged to the system. One major advantage of the Burnett method is that neither the volume nor the mass measurements are required. This advantage is somewhat offset by the fact that the apparatus is not suited for use in the liquid or two-phase regions.

The Burnett method (12) was introduced in 1936 and recently has been used by several investigators (9,28,45,

56,62,65,76,77,79,85,87,89). The equipment has been successfully modified to operate at temperatures from 80°F to 2,200°F (55,80,88).

The experimental apparatus consists of two chambers submerged in a constant temperature bath. The chambers are interconnected by an expansion valve. The gas to be studied is injected into chamber I to a pressure just below saturation and allowed to come to equilibrium and the pressure recorded. The expansion valve is then opened and the gas is allowed to expand into chamber II which has been evacuated. When the thermal equilibrium has been restored, the expansion valve is closed and the pressure is measured again. The evacuation, expansion, and pressure measurement is repeated until a pressure too low for accurate measurement is attained. These measurements can be reduced to compressibility factors or density data.

The apparatus in this work was designed for use in the range of pressures up to 7,000 psi and temperatures up to 700°F. The apparatus was tested by taking measurements on helium which has linear isotherms up to moderately high pressures. This makes it well suited as a calibrating gas for the Burnett apparatus. Experimental p-v-T measurements were then made on methyl chloride in the temperature range of 200°C to 350°C at pressures below 5,000 psi.

Tanner (82) has made p-v-T measurements on methyl chloride in the temperature range of -60°F to 170°F at pressures up to 310 psi. Additional measurements were made by Hsu and McKetta (36,37) over the temperature range from 35°C to 225°C and pressures up to 4,500 psi.

CHAPTER II

THEORY

A. The Second Virial Coefficients of Nonspherical Polar Gases

According to classical statistical mechanics, the second virial coefficient B(T) for a pure component gas is given by

$$B(T) = \frac{N}{2} \left\langle \int \left[1 - \exp\left(-\frac{U}{kT}\right) \right] d\tau \right\rangle_{av} \qquad (2)$$

In this expression $d\tau$ is the volume element occupied by the center of one molecule with respect to the other and $\langle\rangle_{av}$ represents the average over all orientations. For molecules that have spherically symmetric potential functions, U(r) depends only on the molecular separation r, Equation (2) then reduces to

$$B(T) = 2\pi N \int_0^{\infty} \left[1 - \exp\left(-\frac{U(r)}{kT}\right) \right] r^2 dr \qquad (3)$$

This equation has been integrated for several forms of U(r) and has given good results for substances with simple molecular structure. This work is summarized by Hirschfelder, Curtiss and Bird (32).

The development of intermolecular potential functions for more complex molecules has been based primarily on procedures that include molecular geometry as a parameter.

Kihara's work is based on an impenetrable molecular core that is defined by the atomic distances in the molecule and the application of measure theory developed in convex body geometry. The intermolecular potential $U(\rho)$ is a function of the minimum displacement ρ between the molecular cores. Equation (2) then becomes

$$B(T) = \frac{N}{2}\int_0^{\infty} \left[1 - \exp\left(-\frac{U(\rho)}{kT}\right)\right] \langle S_c + \rho + c \rangle_{av} \, d\rho + \langle V_c + c \rangle_{av} \qquad (4)$$

where $\langle V_c + c \rangle_{av}$ represents the average volume of convex body formed by the center of one molecule as it is moved around the other with core surfaces in contact with each other and this volume is excluded from the integration volume, $\langle S_c + \rho + c \rangle_{av}$ represents the average surface area of a convex body generated by the center of one molecule when it is moved around the second with a distance ρ between the two cores. These averages may be calculated for a convex core using the theorems of convex body geometry (39, 40).

Assuming the intermolecular potential function in the Kihara core model to be of the same form as the Lennard-Jones (12-6) potential and that it depends only on the core separation ρ, one obtains

$$U(\rho) = U_o \left[\left(\frac{\rho_o}{\rho}\right)^{12} - 2\left(\frac{\rho_o}{\rho}\right)^{6} \right] \qquad (5)$$

The core separation ρ_o occurs at the potential minimum U_o. Following Lennard-Jones (50), Kihara obtained

$$B(T) = \frac{2}{3}\pi N \rho_o^3 F_3(Z) + M_o N \rho_o^2 F_2(Z) + (S_o + M_o^2/4\pi) N \rho_o F_1(Z) + \left[V_o + (M_o S_o/4\pi)\right] N \qquad (6)$$

where $Z = U_o/kT$,

$$F_s(Z) = -\frac{s}{12} \sum_{P=0}^{\infty} \left(\frac{1}{P!}\right) (2)^P (Z)^{\frac{6P+s}{12}} \Gamma\left(\frac{6P-s}{12}\right)$$

for $s = 1,2,3$. These functions have been tabulated by Kihara and extended by Connolly and Kandalic (16). Γ is the gamma function and the fundamental measures of the core are the volume V_o, the surface area S_o, and the mean curvature integrated over the surface M_o. This expression reduces to the familiar Lennard-Jones expression for molecules represented by point centers of mass if $V_o = S_o = M_o = 0$.

In order to extend the core model to polar molecules, assume that a permanent point dipole of strength μ is embedded at the geometric center of the core. The orientation of the dipole within the core does not depend on the core shape but it is assumed to be fixed for any molecular species. The distance between the dipole pairs is r and the shortest distance between the cores is ρ as shown in Figure 6. The point dipole interaction energy can be

written as

$$(\mu^2/r^3)(2\cos\theta_1\cos\theta_2 - \sin\theta_1\sin\theta_2\cos\phi) = \frac{\mu^2}{r^3}g \qquad (7)$$

The dipole and core separation parameters r and ρ must be transformed to a common displacement in order to perform the integration in Equation (2). Figure 7 is a schematic representation of $U(\rho)$. The condition $U(0) = \infty$ and $U(\infty) = 0$ must be satisfied by this function. Since ρ represents the distance between cores, the average distance from a core surface to the embedded dipole may be approximated by a, the equivalent radius of the core. When $a = 0$, the limiting case $\rho = r$ can be represented by the Stockmayer potential

$$U = U_o \left[(r_o/r)^{12} - 2(r_o/r)^6 \right] - \mu^2 g/r^3 \qquad (8)$$

The potential function between pairs of molecules with $a \neq 0$ can be obtained by transforming the Stockmayer potential coordinates U and r to the new coordinates U' and r' with $U = U'$ and $r' = r + 2a$. This gives

$$U' = U'_o \left[\left(\frac{r'_o - 2a}{r' - 2a}\right)^{12} - 2\left(\frac{r'_o - 2a}{r' - 2a}\right)^6 \right] - \frac{\mu^2 g}{(r' - 2a)^3} \qquad (9)$$

For any polyhedral core, we can approximate r by $r \cong \rho + 2a$. In the new coordinates $r' \cong \rho' + 2a$ or $r \cong \rho' = \rho + 2a$. Using these relations, Equation (9) becomes

$$U'(\rho') = U'_o \left[\left(\frac{\rho'_o}{\rho'}\right)^{12} - 2\left(\frac{\rho'_o}{\rho'}\right)^{6} \right] - \frac{\mu^2 g}{\rho'^3} \qquad (10)$$

Equation (10) is exact for spherical cores and is an approximation for the nonspherical cores. This potential function can be written as the sum of the Kihara potential $U^{(o)}$ and the permanent dipole interaction $U^{(1)}$ which can be treated as a perturbation on the function $U^{(o)}$.

$$U' = U^{(o)} + U^{(1)} \qquad (11)$$

It is apparent from Figure 7 and Equation (4) that the integration of $U(\rho)$ from $\rho = -2a$ to $\rho = 0$ will make no contribution to B(T) except the term $\langle V_{c+c} \rangle_{av}$ since $U(\rho) = \infty$ for all $\rho \leq 0$.

Pople (68) has presented a solution for the second virial coefficient using the Stockmayer potential. If we calculate B(T) using Equation (10) in Equation (2) and expand $\exp\left(-\frac{U^{(1)}}{kT}\right)$ in a power series, we obtain

$$B(T) = \frac{N}{2}\left\langle \int \left[1 - \exp\left(-\frac{U^{(o)}}{kT}\right) - \sum_{n=1}^{\infty} \frac{1}{n!} \left(\frac{\mu^2}{\rho'^3}\right)^n g^n \left(-\frac{1}{kT}\right)^n \exp\left(-\frac{U^{(o)}}{kT}\right) \right] d\tau \right\rangle_{av} \qquad (12)$$

The first two terms in the bracket are identical to Equation (2). Equation (6) represents the integration of these two terms for a core with the same geometry as assigned to the polar molecule.

With g defined in Equation (7), integration over molecular orientations yields zero for the n = 1 term. Terminating the series with the first nonzero perturbation term in B(T), one obtains when n = 2

$$B(T) = B^{(o)} - \frac{(2)^{\frac{1}{2}}}{36}\pi N \rho_o'^{3} t'^{2} H_6(y) \qquad (13)$$

where $B^{(o)}$ is given by Equation (6) with ρ_o replaced by $\rho_o' = \rho_o + 2a$, $t' = \mu^2/(8)^{\frac{1}{2}}U_o'\rho_o'^{3}$ and $y = 2(U_o'/kT)^{\frac{1}{2}}$. The function $H_6(y)$ has been tabulated by Buckingham and Pople (11) and is given by

$$H_6(y) = y^{7/2} \sum_{p=0}^{\infty} \frac{y^p}{p!} \Gamma\left[\frac{(2p + 1)}{4}\right] \qquad (14)$$

The second virial coefficient for the Stockmayer potential is obtained from Equation (13) when the core is reduced to a point ($M_o = S_o = V_o = 0$).

B. Thermodynamic Properties in Terms of Equation of State and Virial Coefficients

The generalized expressions for the derived thermodynamic properties of gases are presented in terms of equation of state and the second virial coefficients. Detailed expressions are given in reduced units for

$$\frac{H - H^*}{RT_c}, \quad \frac{U - U^*}{RT_c}, \quad \frac{S - S^*}{R} \text{ and } \frac{f}{P}.$$

1. Enthalpy Deviations of Fluids from Ideal Gas Behavior

At moderate densities the p-v-T properties of all substances can be described by the virial equation of state truncated after the second virial coefficient.

$$\frac{PV}{RT} \cong 1 + \frac{B}{V} \tag{15}$$

The virial equation of state may also be expanded as a power series in pressure.

$$\frac{PV}{RT} \cong 1 + B'P \tag{16}$$

The second virial coefficients B and B' are related by the following expression

$$B' = \frac{B}{RT} \tag{17}$$

Making use of the combined first and second laws of thermodynamics, it follows that

$$\left(\frac{\partial H}{\partial P}\right)_T = \left[V - T\left(\frac{\partial V}{\partial T}\right)_P\right] \tag{18}$$

where $(\partial H/\partial P)_T$ represents the change of enthalpy with pressure at the constant temperature. The enthalpy of an ideal gas is independent of pressure (i.e., $(\partial H/\partial P)_T = 0$) and depends only on temperature. Substituting Equation (16) into Equation (18) and simplifying, we obtain

$$H - H^{\circ} = -\int_0^P RT^2 (dB'/dT)_P \, dP \tag{19}$$

At constant temperature Equation (19) can then be integrated between the limits of zero and P.

$$\frac{H - H^{\circ}}{RT} = -PT \left(\frac{dB'}{dT}\right)_P \tag{20}$$

Substituting Equation (17) into Equation (20) and dividing through by T_c, we obtain the final expression for the enthalpy deviation of real gases from the ideal gas behavior in a dimensionless form:

$$\frac{H - H^*}{RT_c} = \frac{P}{RT_c} \left(B - T\frac{dB}{dT}\right) \tag{21}$$

since $H^{\circ} = H^*$

2. Internal Energy Deviations of Fluids from Ideal Gas Behavior

The internal energy deviation of real gases from the ideal gas behavior at the constant temperature can be obtained by the following expression:

$$\left(\frac{\partial U}{\partial P}\right)_T = \left[\frac{\partial}{\partial P}(H - PV)\right]_T = \left(\frac{\partial H}{\partial P}\right)_T - \left(\frac{\partial (PV)}{\partial P}\right)_T \tag{22}$$

The substitution of Equations (16) and (18) into Equation (22) gives

$$\left(\frac{\partial U}{\partial P}\right)_T = \left[V - T\left(\frac{\partial V}{\partial T}\right)_P\right] - RTB' \tag{23}$$

Integrating Equation (23) between the limits of 0 and P

and simplifying, we obtain the result:

$$\frac{U - U^*}{RT_c} = - \frac{PT}{RT_c}\frac{dB}{dT} \tag{24}$$

since $U^o = U^*$

3. Entropy Deviations of Fluids from Ideal Gas Behavior

The entropy deviations of real gases from the ideal gas behavior at the constant temperature can be obtained by using Maxwell's relation

$$\left(\frac{\partial S}{\partial P}\right)_T = - \left(\frac{\partial V}{\partial T}\right)_P \tag{25}$$

The substitution of Equation (16) into Equation (25) gives

$$\left(\frac{\partial S}{\partial P}\right)_T = - \left[\frac{R}{P} + RB' + RT \frac{dB'}{dT} \right] \tag{26}$$

It is apparent that the integral in Equation (26) becomes indeterminate at the zero pressure. By a proper choice of the reference state, Equation (26) can be integrated between the limits of 0 and P. The ideal value S^o is defined in such a way that in the limit as $P \rightarrow 0$,

$$S \rightarrow S^o - R \ln P \tag{27}$$

thus,

$$\frac{S - S^o}{R} = -\left[\ln P + \frac{P}{R}\frac{dB}{dT}\right] \tag{28}$$

Equation (26) can be integrated also between the limits of 0 and P, if the ideal value S* is defined in such a way

that S* represents the property of hypothetical ideal gas at the same pressure as the real gas.

$$S - S^* = -\int_0^P \left[\left(\frac{\partial V}{\partial T}\right)_P - \frac{R}{P} \right] dP \qquad (29)$$

The integration leads to the final result

$$\frac{S - S^*}{R} = - \frac{P}{R} \frac{dB}{dT} \qquad (30)$$

Equation (30) was used in this work to calculate the entropy deviation.

4. Fugacity Coefficient

The fugacity coefficients of real gases can be evaluated by the relation

$$RT \, d \ln f = V \, dP \qquad (31)$$

The residual volume α is defined as

$$\alpha = \frac{RT}{P} - V \qquad (32)$$

When the residual volume is substituted in Equations (18), (25), and (31), we obtain the following expressions for the fugacity coefficient, enthalpy deviation, and entropy deviation, respectively:

$$\ln \left(\frac{f}{P}\right) = - \frac{1}{RT} \int_0^P \alpha \, dP \qquad (33)$$

$$H - H^* = \int_0^P \left[T\left(\frac{\partial \alpha}{\partial T}\right)_P - \alpha \right] dP \qquad (34)$$

$$S - S^* = \int_0^P \left[\left(\frac{\partial \alpha}{\partial T}\right)_P - \frac{\alpha}{T} \right] dP + \int_0^P \frac{\alpha}{T}\, dP \tag{35}$$

Thus

$$\ln \left(\frac{f}{P}\right) = \left(\frac{H - H^*}{RT}\right) - \left(\frac{S - S^*}{R}\right) \tag{36}$$

Substituting Equations (21) and (30) into Equation (36), we obtain

$$\ln \left(\frac{f}{P}\right) = \frac{PB}{RT} \tag{37}$$

In each case H*, U* and S* refer to the properties of the hypothetical ideal gas at the same pressure as the real gas. The expression for B is given by Equation (13), and the expression for dB/dT is given as follows:

$$\frac{dB}{dT} = \frac{2}{3}\pi N \rho'^3_o F'_3(Z) + M_o N \rho'^2_o F'_2(Z) + \left(S_o + \frac{M_o^2}{4\pi}\right) N \rho'_o F'_1(Z)$$

$$+ \left(V_o + \frac{M_o S_o}{4\pi}\right) N - \frac{\sqrt{2}}{36}\pi N \rho'^3 (t')^2 H'_6(y) \tag{38}$$

where

$$F'_s(Z) = \frac{dF_s(Z)}{dT} = \frac{dF_s(Z)}{dZ} \cdot \frac{dZ}{dT} \qquad s = 1,2,3 \tag{39}$$

or

$$F'_s(Z) = \left(\frac{s}{12}\right)\left(\frac{k}{U'_o}\right) \sum_{P=0}^{\infty} \frac{1}{P!}\, \Gamma\left(\frac{6P-s}{12}\right)(2)^P \left(\frac{6P+s}{12}\right) Z^{\left(\frac{6P+s+12}{12}\right)} \tag{40}$$

and

$$H'_6(y) = \frac{dH_6(y)}{dT} = \frac{dH_6(y)}{dy} \cdot \frac{dy}{dT} \tag{41}$$

or

$$H'_6(y) = -\frac{k}{8U'_o} \sum_{P=0}^{\infty} \Gamma\left(\frac{2P+1}{4}\right)\left(\frac{1}{P!}\right) \left(\frac{2P+7}{2}\right) y^{\left(\frac{2P+11}{2}\right)} \tag{42}$$

The functions $dF_s(Z)/dZ$ and $dH_6(y)/dy$ have been tabulated over the range of Z from 0.01 to 7.00 at intervals of 0.01 and summarized in Table XI.

C. The Compressibility of Polar Gases with the Burnett Apparatus

The compressibility factor of a gas is defined by the relation,

$$Z = \frac{PV}{nRT} \tag{43}$$

Let V_I and V_{II} be the volumes of chambers I and II of the Burnett apparatus. The apparatus constant is defined by

$$N = \frac{V_I + V_{II}}{V_I} \tag{44}$$

Then the number of moles of gas in the rth expansion may be expressed by the equation

$$n = \frac{P_{r-1}V_I}{Z_{r-1}RT} = \frac{P_r(V_I + V_{II})}{Z_r\ RT} \tag{45}$$

Substituting Equation (44) into Equation (45), we obtain

$$\frac{P_{r-1}}{P_r} = N\frac{Z_{r-1}}{Z_r} \tag{46}$$

Since $\lim_{P \to 0} Z = 1$, Equation (46) leads to the relation

$$\lim_{P_r \to 0} \frac{P_{r-1}}{P_r} = N \tag{47}$$

Using Equation (47) the apparatus constant N can be

evaluated by extrapolating the isothermal experimental pressure ratio data on a given gas to zero pressure. If the compressibility factor isotherm is linear with pressure up to moderately high pressures, then a plot of P_{r-1}/P_r vs P_r gives an accurate extrapolation. The value of N should not depend on the temperature of the series of expansions.

If Equation (46) is applied to the first, second, ..., rth expansions, the resulting equations may be combined to give the following relation.

$$P_r N^r = \frac{P_o}{Z_o} Z_r \tag{48}$$

It is apparent from Equation (43) that at low pressure $Z_r = 1$ and

$$\lim_{P_r \to 0} P_r N^r = P_o/Z_o \tag{49}$$

From Equation (49) the run constant, P_o/Z_o, may be evaluated by extrapolating the plot of $P_r N^r$ vs P_r to zero pressure. Contrary to the case of the apparatus constant, Equations (48) and (49) apply only to the pressure measurements in the same series of expansions on an isotherm.

When the Burnett apparatus is employed at high pressures, it is important to consider the deformation of the chambers due to pressure and its effect on the apparatus constant and on the run constant. In the treatment below, end effects have been neglected.

For a thick walled cylinder, the radial displacement of any point in the wall is given by the Lame formula (13,83).

$$\delta_r = \frac{1 - \nu}{E} \frac{R_i^2 P r}{R_o^2 - R_i^2} + \frac{1 + \nu}{E} \frac{R_o^2 R_i^2 P}{(R_o^2 - R_i^2) r} \qquad (50)$$

Considering the displacement of the wall at the inner radius and simplifying, we obtain

$$\delta_r \Big|_{r=R_i} = \frac{R_i P}{E} \left[\frac{R_o^2 + R_i^2}{R_o^2 - R_i^2} + \nu \right] \qquad (51)$$

If Hook's Law (stress is proportional to strain for small strains, $\sigma = E \epsilon$) is assumed to hold in the longitudinal as well as in the radial direction, the total longitudinal displacement is given by

$$\delta_l = L_o \left[\frac{S_o}{E} - \nu \frac{S_r}{E} - \nu \frac{S_t}{E} \right] \qquad (52)$$

These terms are given by the following formulas,

$$S_o = P R_i^2 / (R_o^2 - R_i^2) \qquad (53)$$

$$S_r = - P \qquad (54)$$

$$S_t = P(R_o^2 + R_i^2)/(R_o^2 - R_i^2) \qquad (55)$$

Substituting Equations (53), (54) and (55) into Equation (52),

$$\delta_l = L_o P R_i^2 (1 - 2\nu) / E(R_o^2 - R_i^2) \qquad (56)$$

The volume of the cylinder at zero pressure is given by

$$V_o = \pi R_i^2 L_o \tag{57}$$

The volume of the cylinder under pressure when the walls are displaced is given by

$$V = \pi (R_i + \delta_r)^2 (L_o + \delta_l) \tag{58}$$

Subtracting Equation (57) from Equation (58) and neglecting all correction terms higher than the first order, we obtain

$$\Delta V \cong \pi (2R_i \, \delta_r \, L_o + R_i^2 \, \delta_l) \tag{59}$$

Substituting Equation (51) and (56) into Equation (59) and dividing by Equation (57), we get

$$\frac{\Delta V}{V_o} = \frac{P}{E} \left[2\left(\frac{R_o^2 + R_i^2}{R_o^2 - R_i^2} + \nu\right) + \frac{R_i^2 (1 - 2\nu)}{R_o^2 - R_i^2} \right] \tag{60}$$

The volume of the chamber at any pressure P is given by

$$V = V_o \left(1 + \frac{\Delta V}{V_o}\right)_P \tag{61}$$

Applying this correction term to the apparatus constant, we get

$$N = \frac{\left[V_{oI}\left(1 + \frac{\Delta V}{V_o}\Big|_I\right)_{P_i} + V_{oII}\left(1 + \frac{\Delta V}{V_o}\Big|_{II}\right)_{P_i}\right]}{V_{oI}\left(1 + \frac{\Delta V}{V_o}\Big|_I\right)_{P_{i-1}}} \tag{62}$$

If $R_{iI} = R_{iII}$ and $R_{oI} = R_{oII}$, then Equation (62) reduces to

$$N = \frac{(V_{oI} + V_{oII})\left(1 + \frac{\Delta V}{V_o}\right)_{P_i}}{V_{oI}\left(1 + \frac{\Delta V}{V_o}\right)_{P_i - 1}} \tag{63}$$

or

$$N(P_i, P_{i-1}) = N_o \frac{(1 + \frac{\Delta V}{V_o})P_i}{(1 + \frac{\Delta V}{V_o})P_{i-1}} \tag{64}$$

N_o is obtained by a least square fit of Equation (47) to the experimental data (57). Equation (48) then becomes

$$P_r \prod_{i=1}^{r} N(P_i, P_{i-1}) = \frac{P_o}{Z_o} Z_r \tag{65}$$

and Equation (49) becomes

$$\lim_{P_r \to 0} P_r \prod_{i=1}^{r} N(P_i, P_{i-1}) = \frac{P_o}{Z_o} \tag{66}$$

Using Equation (65) and (66), the compressibility factor Z is obtained.

The Birlin expansion of the compressibility factor Z is represented by the following relation.

$$Z = 1 + B'P + C'P^2 + \ldots\ldots \tag{67}$$

Rewriting Equation (67), we get

$$\frac{Z - 1}{P} = B' + C'P + \ldots\ldots \tag{68}$$

Equation (68) shows that the second virial coefficient B' may be evaluated by extrapolating the plot of (Z-1)/P vs P for each isotherm to zero pressure. The second virial coefficient B can be obtained from B' using Equation (17).

CHAPTER III

EXPERIMENTAL APPARATUS AND PROCEDURE

The experimental apparatus can be divided into five basic parts: expansion cell, charging system, vacuum system, pressure measurement, and temperature measurement. A schematic diagram of the apparatus is shown in Figure 1 and a more detailed discussion of the experimental equipment is given in the Appendix.

A. Expansion Cell

The detailed construction of the expansion cell is shown in Figure 2. The expansion cell essentially consists of two chambers V_I and V_{II}, which are interconnected through an expansion valve. The cell is cylindrical and made of type 304 stainless steel. The overall length of the assembled cell is about 16" with an outside diameter of $4\frac{1}{2}$". The two chambers are 2" in diameter and about 5" long. They have nearly equal volumes (approximately 16 cubic inches). Three type 304 stainless steel cubes with a length of one edge equal to $1\frac{1}{4}$" were introduced into chamber II to reduce its effective volume to obtain evenly distributed data points on the isotherms over the full range of pressure to be studied. As shown in Figure 2, the upper chamber is welded closed while the lower chamber is closed by the compression-head type closure (13) and

sealed with a silver plated Inconel-X "O" ring. The metal "O" ring is made from a hollow, vented tubing with an outside diameter of 1/16 inch and wall thickness of 0.010". The metal "O" ring is compressed between the head and the end of the cell by twelve $\frac{1}{2}$" diameter cap screws bearing on a cap screw ring. There are five ports in the expansion cell for $\frac{1}{4}$" high pressure tubing, three entering chamber I and two entering chamber II. The valve I is the charging valve for chamber I. The valve 2 is the expansion valve connecting chambers I and II. The valve 3 is the evacuation valve for chamber II. The other port in chamber I is connected with the lower side of the high temperature differential pressure indicator. The expansion cell was washed with dilute nitric acid and then three times with benzene. A final washing with acetone was repeated until the effluent was absolutely clear.

The effect of internal pressure on the volume of either chamber has been calculated by the Lame's formula for thick-walled cylinders (83). At room temperature, the change in volume is approximately 0.1% at 7,000 psi internal pressure. At 700°F, this would be increased somewhat to 0.12%. The radial displacement of the cell at 7,000 psi internal pressure and room temperature is approximately 1.3×10^{-4} inch and the longitudinal displacement of the body at the same temperature and pressure is approximately

2.7×10^{-5} inch. Corrections for this volume change with pressure can be made when the data are reduced to obtain the compressibility factors. The procedure is described in the previous section.

Considerable effort was made to find a leak-tight valve for use at high temperatures. Commercially available high-pressure stainless steel needle valves with high temperature packing were initially installed. The packing was made of graphite impregnated asbestos. These valves were found unsatisfactory for use at high temperatures.

A special bellows type valve was designed to provide positive leak-tight closure after each expansion for use as an expansion valve. The bellows was 15/32" O.D., 0.005" in wall thickness, and had 14 convolutions which allowed a maximum stroke of 0.056". The bellows was made of type 321 stainless steel and welded to the stem at the lower end. The valve body was about 14" long and made from type 304 stainless steel. The two piece valve stem was made from type 416 stainless steel. "Teflon" packing was also provided at the top of the bonnet which was located outside of the temperature bath. A $\frac{1}{4}$" high pressure tubing fitting was provided to equalize the pressure differential across the bellows. This was connected to the nitrogen pressure system used in the upper side of the high temperature

differential pressure indicator. In order to seal the both sides of the bellows, two silver plated, vented, Inconel-X "O" rings were compressed between the flange of upper bonnet and the lower valve body. The valve body was closed with six 3/8" diameter Allen-head screws.

Two high temperature valves with extended bonnets manufactured by Autoclave Engineers, Inc. were used as block valves for charging the material to the chamber I and for evacuating the chamber II.

B. Charging System

The charging system is shown schematically in Figure 3. The charging surge tank (ST) was used to inject the test gas into chamber I at the desired initial pressure. This was usually higher than the shipping cylinder pressure. The surge tank was designed for a working pressure of 10,000 psia and had a volume of 19 cubic inches. This tank is made of type 304 stainless steel.

Mercury was supplied to the surge tank by a hand operated piston pump (MP), with a maximum stroke of 6" and a 5/8" diameter piston. The mercury level in the surge tank was calibrated against the mercury level in the mercury reservoir (MR) of the pump. A small stainless steel vessel (MT) was included in the charging line between the surge

tank and the chamber I to trap any mercury accidentally carried over into this line. Standard high pressure stainless steel $\frac{1}{4}$" tubing and valves were used throughout the charging system.

C. Vacuum System

The vacuum system is shown in Figure 3. A welch Duo-Seal vacuum pump (VP) with a pressure rating of 0.1 micron was used to evacuate the pressure cells. The pressure in chamber II can be reduced to below 50 microns in about 10 minutes. The low pressure vacuum was measured by a Virtis-McLeod Gauge (MG) with scale readings from 5 microns to 5 mm during the evacuation of the cell.

Standard high pressure stainless steel $\frac{1}{4}$" tubing and $\frac{1}{2}$" copper tubing were used in the vacuum system. A vacuum cold trap (VT) was used to remove most of the vapor ahead of the vacuum pump to reduce contamination of vacuum pump oil.

D. Pressure Measurement

A schematic diagram of the pressure measuring devices is shown in Figure 4. All pressures were measured with a dead weight gage (DWG) manufactured by the Ruska Instrument Corporation. Two separate dead weight gages were used in this experiment. Both the high and low range gage were

required to maintain precision and sensitivity over the entire pressure range since each expansion proceeds from high pressure to essentially atmospheric pressure. The low pressure gage ranges from 6 psig to 2,428 psig and the high pressure gage from 30 psig to 12,140 psig. The dead weight gages were calibrated by comparison with a master dead weight gage in the Ruska laboratory which was calibrated by the National Bureau of Standards. A set of English weights were used with both gages. All pressure measurements were corrected for the gage temperature, elastic distortion of the piston, gravity, and buoyancy. A more detailed description of the corrections to the pressure measurements is given in the Appendix B.

A mercury barometer was installed near the Burnett apparatus to obtain atmospheric pressure measurements for each run. These were used to convert each dead weight gage reading to absolute pressure.

Two differential pressure indicators (DPI) were required for the pressure measurement system. The high temperature differential pressure indicator was used to separate the substance on which p-v-T measurements were being made from the pressure transmitting fluid. The low temperature differential pressure indicator was used to separate the pressure transmitting fluid from the oil system of the dead weight gage. The differential pressure

indicator consists of two pressure chambers separated by a thin stainless steel diaphragm. A differential pressure across the diaphragm causes the diaphragm to deflect. The minute deflections of the metal diaphragm are detected by a linear differential transformer and the output produced by the diaphragm displacement is indicated by the electronic null indicator.

Since the high temperature differential pressure indicator was to be located in the bath, a standard low temperature differential pressure indicator was modified as shown in Figure 4. This indicator consists of two separate pressure cells connected by 9/16" O.D. high pressure tubing and special support fixtures. The electrical components were removed from the high temperature zone and placed in the upper body of the DP cell. The diaphragm was contained in the lower body of the DP cell which was completely submerged under the bath. A small air bath was provided to thermostat the upper body of the DP cell. The diaphragm connecting rod extended about 15" through a "Teflon" guide bushing mounted at the top of the 9/16" high pressure tubing. Four ½" stainless steel rods were used for aligning and supporting the two bodies. The high temperature DP cell was made of type 304L stainless steel, the standard low temperature DP cell was made of type 416 stainless steel. The differential pressure indicators and

the hand-operated, precision piston pumps to inject the pressure transmitting fluids were obtained from the Ruska Instrument Corporation. Nitrogen gas was used as a pressure transmitting fluid between the two differential pressure indicators.

A reference manometer was placed between the dead weight gage and differential pressure indicator, and another reference manometer in the charging line. With both sides of the differential pressure cell vented to the atmosphere, the electronic null indicator was adjusted to zero. This "zero adjustment" was made for each temperature. With the arrangement shown in Figure 4, it is possible to measure the pressure to within $\pm$ 0.02% at any pressure up to 7,000 psi. Standard high pressure stainless steel $\frac{1}{4}$" tubing and valves were used in the pressure measurement system.

E. Temperature Measurement

The temperature of the gas in the expansion cell was measured by a platinum resistance thermometer (T) inserted in a thermometer well in the wall of the expansion cell. This was calibrated by National Bureau of Standards at the oxygen, ice, steam, and sulphur points. The thermometer was surrounded with the bath fluid in the well as shown in Figure 5. The well was 5" deep and 5/16" in

diameter. A 5/8" standard steel pipe extended from the top of the cell to a compression fitting and adaptor provided at the top of the sensitive portion to protect the thermometer.

Resistances were measured with a Mueller Bridge (MB) to obtain temperatures of the gas in the cell. A high sensitivity reflecting galvanometer with an optical scale reading device was used to balance the Mueller Bridge. A variable resistance box was included between the galvanometer and Mueller Bridge to control the sensitivity of the galvanometer. Six 1.5 V batteries in parallel were used to supply the bridge current. A 2,000 ohm external resistor was placed between the bridge and batteries to reduce the self-heating of the platinum resistance thermometer. Temperature readings were made to the nearest $0.01^{\circ}C$, although temperature changes of $\pm$ $0.001^{\circ}C$ could be detected easily.

The constant temperature bath (2) was made of a stainless steel tank 18" in diameter and 30" deep with a fluid capacity of approximately 4 ft^3. It was insulated with a 3 inch layer of Careytemp and 3 inches of MW-one supplied by the Philip Carey Mfg. Company. The Careytemp is composed of expanded silica, special binders, and is reinforced with inorganic fibers and is recommended for

equipment operating from ambient temperature to 1,600°F. The MW-one is a combination insulation and finishing cement for temperatures up to 1,000°F. The insulation was held in place by an outer vessel made of 24 ga. stainless steel. Three casters were attached to the bottom of the bath. The bath was mounted in an angle iron frame and was raised or lowered by a manually operated hoist. During high temperature operation, the space over the top of the bath was partially filled with blocks of Careytemp insulation wrapped with aluminum foil.

A eutectic mixture of sodium nitrite, potassium and sodium nitrates was used as the bath fluid. The heat transfer salt (84) containing 40% sodium nitrite, 53% potassium nitrate and 7% sodium nitrate by weight melts at 288°F. The liquid density of the mixture is 1.86 at 600°F. The viscosity of the mixture is 2.9 centipoises at 600°F and decreases to 1.1 centipoises at 1,000°F. the salt bath was circulated with two stirrers each enclosed in a stainless steel tube 3" in diameter extending to within about 6" of the top and 5" of the bottom plate. Three propeller-type stirrers were mounted on the shafts which were centered and supported at the bottom end by cast iron bushings. The bath fluid was circulated from the top to the bottom of the tubes providing rapid circulation of the bath fluid. The agitators were driven

at about 1,700 rpm by induction motors.

All equipment in the constant temperature bath was supported by a $\frac{1}{4}$" thick stainless steel plate. This formed the stationary top of the constant temperature bath and was fastened to the wall with angle irons.

The salt bath was heated by two sets of heaters. Two internal immersion heaters (IH) were enclosed in the stirring tubes and the power to them is controlled by a Hallikainen Instruments Thermotrol general purpose laboratory temperature controller (TC). The temperature sensing element (TB) for the controller was a platinum resistance thermometer bulb. The power level of the two internal heaters could be continuously varied from zero to 250 watts by a variable transformer depending upon the operation of the temperature controller. With the system shown in Figure 5, the power level of 40 to 50 watts was used to control the bath temperature.

Five external heaters were used to raise the temperature of the bath. A thin asbestos cloth for temperatures up to 1,400^{o}F was wound around the inner vessel, and then five 40 ft, 25 ohm asbestos insulated resistance wires were wound around the bath and clamped at the top and bottom to lugs fastened to the vessel. The lead wire from the heaters to the studs on the asbestos

top of the bath was No. 10 Chromel A. The lead wires were clamped and also silver soldered to the ends of the heaters.

One of the five external heaters is controlled manually by a variable transformer. The external heaters were adjusted so that at steady state the temperature was slightly below the desired temperature. The final temperature control is achieved by internal heaters. With this arrangement, it is possible to control the bath temperature to within $\pm$ 0.01°C in the temperature range of 0°to 700°F.

F. Safety Precautions

All of the electrical equipment was protected by circuit breakers or time-delayed fuses located in the power control panel. A 45 amp., 220V. AC magnetic contactor supplied the power to the control panel. The holding circuit interlock had three emergency stop switches and a fenwal thermoswitch (FT) that opened on temperature rise. The thermoswitch was located in the constant temperature bath and set at 750 - 800°F and would cut off all power to the electrical control panel if a temperature excursion occured when the equipment was unattended. Two stop switches were located outside the laboratory to provide remote emergency shut-down. The only power activation switch was located on the power panel.

G. Experimental Procedure

The following experimental procedure was used to make one series of expansions on an isotherm with the Burnett apparatus.

After the heat transfer salt in the bath was melted with the external heaters, the constant temperature bath was raised into position and the circulation of the bath fluid was started. The air blowers were turned on to cool the agitators and to thermostat the upper body of high temperature differential pressure indicator. When the bath temperature approached the predetermined isothermal temperature, the thermotrol was turned on to control the bath temperature with the internal heaters. The isothermal temperature was attained in about five hours.

When the temperature remained constant for a period of 10 minutes, the electronic null indicators were adjusted to zero with both sides of the differential pressure cells vented to the atmosphere by means of manometers. The manometers were then closed off from the system.

The entire system was evaculated with the vacuum pump, purged twice with test gas, and re-evacuated to a pressure below 50 microns. The gas to be studied was

injected into the chamber I of the expansion cell to the desired pressure and allowed to come to equilibrium. The pressure was then measured. Four to five hours was usually required for charging the cell to 5,000 psi.

The expansion valve was opened and the gas was allowed to expand into chamber II which had been evacuated. When thermal equilibrium had been restored, the expansion valve was closed and the new pressure was measured. About one hour was required to make one expansion.

The intake valve of the vacuum pump was then closed and the vent was opened. The exhaust valve in the chamber II was cracked and the gas was allowed to vent to the atmosphere outside the building. The vent was closed when the pressure approached the atmospheric pressure and the chamber II was evacuated with the vacuum pump to a pressure below 50 microns. The pressure measurements were made during this evacuation to check for possible leaks through the expansion valve. The exhaust valve was then closed and the gas allowed to expand again. The above procedure was repeated until a final pressure of less than 100 psia was reached.

The pressure difference between both sides of the bellows in the expansion valve was kept as small as possible during the successive expansion and evacuation. This

was achieved by cracking both expansion valve and a valve leading to the expansion valve in the nitrogen system at the same time and by observing the pressure difference with the high temperature differential pressure indicator.

CHAPTER IV

RESULTS AND DISCUSSIONS

A. Theoretical Results

The Kihara core model has been extended to the nonspherical polar molecules. The experimental second virial coefficient data for nine polar gases were used to calculate the potential function parameters. The calculated values reproduced the second virial coefficient data within the limits of experimental errors. The potential function parameters and the second virial coefficients were compared to those obtained previously for the Stockmayer potential.

The derived thermodynamic properties of methyl chloride were also calculated for the modified Kihara core model. The calculated values were compared to those obtained from the p-v-T data.

The results obtained in this investigation are summarized in Tables VI through XII and illustrated in Figure 6 through 9 and 14.

1. The Second Virial Coefficients for the Modified Kihara Core Model

The molecular cores for the polar molecules were selected on the basis of the cores for the hydrocarbon

homomorph of the polar molecules. Although good agreement between experimental and calculated B(T) values for these hydrocarbons has been reported (15,69), this procedure was not successful for complex polar molecules. The core size and shape had to be adjusted to give good agreement between the experimental and calculated B(T) values. The size and shape of the core used in each calculation are given in Tables VI and VII. Figures 8 and 9 show typical cores used for chloroform and acetone.

The average percent deviation between experimental and calculated B(T) values are given in Table VIII. These are compared to the reported deviations obtained using the Stockmayer potential. The modified Kihara potential gives improved results for moderately polar substances which are nonspherical. No improvement resulted for strongly polar or associating molecules indicating that the perturbation solution is restricted to substances with smaller polar contributions than occur in ammonia and water.

Figure 14 shows the second virial coefficients of methyl chloride calculated from the p-v-T data and compared to B(T) values calculated for the modified Kihara core model and the Stockmayer potential. Since the second virial coefficients are more sensitive to the potential

function at low temperatures than at high temperatures, the experimental B(T) data at low temperatures reported by Hirschfelder (33) were used to calculate the potential function parameters for the two models. The modified Kihara core model gives better representation of experimental B(T) data of methyl chloride than the Stockmayer potential. The curvature of the calculated B(T) versus temperature for the Stockmayer potential is somewhat greater than that of the experimental B(T) values.

The shape of the potential energy well for the Stockmayer and the extended Kihara potential functions are compared in Table IX. The modified Kihara potential provides a means of controlling the slope of the repulsive wall and the width of the potential well by adjusting the core size and shape. For example, a pentagon core for ethyl chloride gives a steeper and narrower potential well than a rectangular core when fitted so that there is the same deviation between experimental and calculated B(T) values. A triangular prism core for methyl chloride gives a shallower and wider potential well than a rectangular core. This emphasizes the importance and need for a method to assign core geometry to the polar molecules.

The excellent representation obtained for chlorinated hydrocarbons using a core shape obtained from the

hydrocarbon homomorph indicates that further studies should be made of potential functions which include parameters for molecular shape and polar effects. Such work will require a more general solution of Equation (2). Additional B(T) data for both polar and nonpolar polyatomic substances will be required to test these methods.

2. Derived Thermodynamic Properties of Methyl Chloride

The derived thermodynamic properties of methyl chloride were calculated from the second virial coefficients for the modified Kihara core model. The thermodynamic excess functions, $(H^* - H)/RT$, $(U^* - U)/RT$, $(S^* - S)/R$, and the fugacity coefficients of methyl chloride have been tabulated over the range of temperatures from $-40^{\circ}C$ to $400^{\circ}C$ and pressures from 0.1 atmosphere to the saturation pressure below the critical temperature and from 1 atmosphere to 500 atmospheres at the interval of 5 atmospheres above the critical temperature. The calculated results are summarized in Table XII.

The saturated methyl chloride liquid at $-40^{\circ}F$ was chosen as the reference state and the vapor pressure at this temperature is 7.043 psia. The ideal gas heat capacities and the latent heat of vaporization of methyl chloride at the reference temperature together with the basic equations for the evaluation of thermodynamic

properties were given by Hsu and McKetta (37).

Table X shows the thermodynamic properties calculated from the second virial coefficients for the modified Kihara core model as compared to the properties calculated from the experimental p-v-T data reported by Hsu and McKetta (37). Excellent agreement was obtained between the two sets of values up to 0.8 of the critical temperature. Above this temperature, the thermodynamic properties calculated from the second virial coefficients tend to be lower and the percent difference between the two sets of values increases with the pressure. This disagreement can be attributed to the inability of the second virial coefficients alone to produce the point of inflection at the critical temperature. In addition, the contribution of the third term in the virial equation of state to the thermodynamic properties increases with pressure.

B. Experimental Results

The performance of the Burnett apparatus was tested by taking p-v-T measurements on helium at 200°C and 300°C. Helium was used as a calibrating gas for two reasons. First, helium possesses linear isotherms up to moderately high pressures which permits accurate extrapolation to zero pressure. Second, precise p-v-T data on helium are available in the literature which allowed a check on the

accuracy of the results. Four runs were made on helium for each temperature.

Compressibility factor isotherms for methyl chloride were determined from 200°C to 350°C at 25°C intervals. Two runs were made on methyl chloride for each temperature.

The results are summarized in Tables II through V and illustrated in Figures 10 through 14. The original data are presented in Table XIII. A discussion of errors is included in the Appendix C.

1. Calibration with Helium

The apparatus constant, N_o, was determined from the helium calibration data at 200°C and 300°C. The best straight line through the experimental points was obtained by a least square fit. It was desirable to weight the higher pressure points more than the lower pressure points since the high pressure points could be measured with greater precision. Each point was weighted in direct proportion to the absolute value of the pressure as shown on the abscissa in Figure 10. The cell constants so determined are given below:

$N_o = 1.599866$ at 200°C

$N_o = 1.599844$ at 300°C

The value of 1.599855 was selected as the apparatus constant

and used at all experimental temperatures as a convenience. The probable error of this value was estimated to be ±0.005% corresponding to an estimated probable error of 0.02% in the pressure measurements.

The compressibility factors of helium at 200°C and 300°C below 1,100 psia are presented in Table II and illustrated in Figure 12. The second virial coefficients of helium were also calculated and compared with the values reported by a number of other investigators in Table III. Good agreement between these values was obtained. However, the values reported by Silberberg (79) and by Keesom (79) seem to be low due to the presence of the mercury vapors in the system. The experimental points below 60 psia are widely scattered as shown in Figures 10 and 12. This may be attributed to the lack of resolution of the pressure balance at the low pressures.

2. Methyl Chloride Data

Compressibility factor isotherms for methyl chloride were determined over the temperature range of 200°C to 350°C at 25°C intervals and at the pressures up to 5,000 psia. The graphical method was used to evaluate the run constant, P_o/Z_o, and the second virial coefficients on a large scale plot which permits the intercept to be read to ± 0.005%.

The compressibility factors of methyl chloride are shown in Figure 13 and presented in Table IV. The compressibility factors at 200°C and 225°C are compared with the smoothed data reported by Hsu and McKetta (36). Excellent agreement was obtained for the compressibility factors at 200°C. However, these data at 225°C tend to be lower than those obtained in this work. This may be attributed to the presence of the mercury vapors in his system. The percent difference between the two sets of smoothed data is less than 0.2% at 200°C and 0.5% at 225°C in all cases.

The experimental points above 325°C are scattered widely as shown in Figures 11 and 13. This was due to the difficulty in obtaining the null reading of the high temperature differential pressure indicator due to the carbon deposits in the lower side of the diaphragm in the high temperature DPI. Evidently, methyl chloride started to decompose from 325°C in appreciable amounts and caused some difficulty in the pressure measurements.

Table V shows the second virial coefficients of methyl chloride reported by several investigators as compared to the values calculated from the potential functions. Good agreement between the experimental and theoretical values was obtained as illustrated in Figure 14.

CHAPTER V

CONCLUSIONS

The most significant conclusions that can be drawn from this investigation are summarized below:

1. The modified Kihara core model represents the second virial coefficients for the moderately polar substances by a factor of 3 to 5 better than the Stockmayer potential. No improvement over the Stockmayer potential was obtained for the strongly polar substances. This indicates that the perturbation solution of the (12-6) Kihara potential with dipole interactions is restricted to the moderately polar substances.

2. The improvement obtained with the modified Kihara core model over the Stockmayer potential for the polar gases is comparable to the improvement resulted with the Kihara potential over the Lennard-Jones potential for the nonpolar gases.

3. The thermodynamic properties of methyl chloride calculated from the second virial coefficients for the modified Kihara core model agrees with the values obtained from the experimental p-v-T data within the limits of experimental errors below the critical temperature. The third virial coefficients become important at higher

pressures and above the critical temperature in evaluating the derived thermodynamic properties.

4. The Burnett apparatus was calibrated with helium. The results were compared with the values reported in the literature. The second virial coefficients and the compressibility factors of helium agree with the reported values within the accuracy of experimental data.

5. The compressibility factors of methyl chloride were determined at 200, 225, 250, 275, 300, 325, and 350°C and pressures up to 5,000 psia. The maximum expected error in these values below 300°C is less than 0.1%. The compressibility factors above 325°C are not reliable due to decomposition of methyl chloride at higher temperatures.

CHAPTER VI

RECOMMENDATIONS

It is recommended that the following suggestions be thoroughly investigated in the future.

1. Evaluation of the third virial coefficients for the modified Kihara core model.

2. Recalculation of the generalized thermodynamic properties from the second and third virial coefficients for the modified Kihara core model.

3. Evaluation of the second virial coefficients for the modified Kihara core model using the technique of group contribution; namely, addition of the polar contribution term to the second virial coefficient of the homomorph.

4. Investigation of a new technique to evaluate Equation (2) for the modified Kihara core model.

5. Further investigation on other polar gases with high decomposition temperature so that the operating conditions may be extended to higher temperatures and pressures.

6. Modify the expansion cell to the completely enclosed type to reduce the possible leaks.

7. Improve the design of the expansion valve, charging valve and evacuation valve to allow better control of the gas flow during high pressure expansions.

APPENDIX

APPENDIX A

DETAILED DESCRIPTION OF THE APPARATUS

1. Pressure Measuring Equipment

The detailed description of the instrument is included in the test report supplied by the Ruska Instrument Corporation and summarized briefly in the following sections:

a. Dead Weight Gage

The piston in the Ruska Model 2400 Dead Weight Gage is made of tungsten carbide and has an enlarged section on its lower end for the purpose of overpressure protection. The cylinder is of the re-entrant type and made of A.I.S.I. type D2 steel. Tolerances on the piston diameter and roundness are of the order of 5×10^{-6} inch. During the operation of the dead weight gage, the piston is rotated either clockwise or counterclockwise by means of a pulley and motor arrangement. The rotation of the piston provides the alignment of the piston and cylinder due to the viscous forces in the annulus. This prevents the direct contact between the piston and the cylinder and thereby eliminates the friction. The clockwise and counterclockwise rotation also eliminates the screw effect which may arise from machining or polishing marks.

The gages are supplied with a set of English weights made of type 303 stainless steel. The calibration of the weights is made to a precision of one part in 50,000 for weights greater than 0.1 pound, one part in 20,000 for weights 0.01 to 0.1 pound and one part in 10,000 for weights 0.001 pound to 0.01 pound. Corrections to dead weight gage readings are discussed in Appendix B. The test report containing the constants and parameters necessary for the proper use of the gage is summarized below:

(i) Low - Range Dead Weight Gage (2400L):

Serial Number: 10211 Gage

Calibration Job Number: A3535/C2516

Cylinder Number: LC-147

Range: 6 to 2,428 psi

A_o: 0.130222 in^2

Reference Temperature: $25^{\circ}C$

b: -4.8×10^{-8}/psi

Thermal Coefficient (c): $1.7 \times 10^{-5}/\ ^{\circ}C$

Resolution* : Less than 5 PPM

Leak Rate: 0.02 in/min.

Plane of Reference: At the line on the sleeve weight

(ii) High-Range Dead Weight Gage (2400H)

Serial Number: 10210 Gage

Calibration Job Number: A3535/C2516

Cylinder Number: HC - 156

Range: 30 to 12,140 psi

A_o: 0.0260411 in^2

Reference Temperature: 25 °C

b: -3.6×10^{-8}/psi

Thermal Coefficient (c): 1.7×10^{-5}/ °C

Resolution* : Less than 5 PPM

Leak Rate: 0.02 in/min.

Plane of Reference: 0.03 inch below line on sleeve weight

* The resolution is defined as the smallest change in the mass of the test gage that will produce measurable change in the condition of equilibrium of the two gages and expressed as the ratio of change in mass to the total mass.

b. Differential Pressure Indicator

The DPI is a metal diaphragm assembly enclosed in a high pressure chamber which positions an iron core within a coil of a differential transformer also located inside the pressure chamber. The diaphragm displacement changes the transformer coil - core relationship which produces an electrical output. Axial adjustment of the transformer coil can be made through a hole offset from the center in the upper chamber. The rod is silver soldered into the diaphragm plug in the low temperature differential pressure

indicator.

In the high temperature DP cell, the rod is threaded into the diaphragm plug and extended about 15" to the iron core within the transformer coil located in the upper body of the DP cell. The type 321 stainless steel O-ring is used in the lower body of the high temperature DP cell.

A calibration curve for the zero shift as a function of operating pressure is supplied with each unit and reproduced in Figures 15 and 16. A brief summary of the DPI specifications is given below.

(i) Low Temperature Differential Pressure Indicator

Model: 2416.1

Cell: Cat. No. 2413, Serial No. 10312

Control Box: Cat. No. 2415, Serial No. 10322

Sensitivity: 1×10^{-4} psi/microamp.

Max. Operating Pressure: 15,000 psi

Max, Overpressure: 15,000 psi on either side of diaphragm

Temperature Range: $40^{\circ}F$ to $130^{\circ}F$

Accuracy: The accuracy of the null point is $\pm 1\frac{1}{2}$ scale divisions under the worst case of combined operating conditions of 10% line voltage variation, $20^{\circ}C$ to $40^{\circ}C$ temperature variation. This

corresponds to 0.0003 psi.

(ii) High Temperature Differential Pressure Indicator

Model: 216R

Cell: Cat. No. 216R, Serial No. 10878

Control Box: Cat. No. 2416, Serial No. 10744

Sensitivity: 4.6×10^{-4} psi/ μa

Temperaure Range: 40°F to 1,000°F

Max. Operating Pressure: 10,000 psia

Max. Overpressure: 10,000 psi

2. Temperature Measuring Equipment

a. Platinum Resistance Thermometer

The platinum resistance thermometer used in this work is designed for the range of -183°C to 500°C. The platinum resistor is made from fully annealed, high purity platinum wire. The platinum resistor is hermetically sealed within a closely fitting type 321 stainless steel well. The well is about $\frac{1}{4}$" in diameter and 18" long. The sensitive portion is located in the first 2 inches of the well. The thermometer has two current and two potential leads and the resistance between the lead junctions is measured.

A 2,000 ohm external resistor was used to reduce the self-heating of the thermometer. At 500°C, the

temperature rise of the platinum resistor above the temperature of the case is less than 0.2°C at a current of 0.02 amp. with no external resistor while the temperature rise is reduced to less than 0.0003°C at a current of 0.0007 amp. with a 2,000 ohm external resistor.

The thermometer has been calibrated by the National Bureau of Standards and certified at -183°C, 0.01°C, 100°C and 250°C. The thermometer has the following resistance versus temperature relationship:

$$R_t/R_o = 1 + \alpha\left[t - \delta\left(\frac{t}{100} - 1\right)\left(\frac{t}{100}\right) - \beta\left(\frac{t}{100} - 1\right)\left(\frac{t}{100}\right)^3\right]$$

where β is defined as zero when t is greater than 0°C, and

$$\alpha = 0.0039257_{62}$$

$$\delta = 1.491_{57}$$

$$\beta = 0.110_{42}$$

$$R_o = 25.550 \text{ abs. ohms}$$

Specifications

Manufacturer: Rosemont Engineering Company

Model: 162C

Serial No.: 49

NBS Calibration Test No.: 3.1/31709

Temperature Range: -200°C to 500°C

Stability: Better than 0.01°C

Insulation Resistance: Greater than 5,000 megohms at 100V DC at room temperature

Pressure Range: 0 to 2,000 psi

b. Mueller Bridge

The bridge comprises two ratio arms of 1,000 ohms each and a rheostat arm of 141.1110 ohms in steps of 0.0001 ohm. A built-in mercury-contact commutator for normal and reverse readings is provided to eliminate the lead resistance. The overall limit of error of the bridge is 0.02% of its setting or 0.00005 ohm, whichever is larger.

Manufacturer: Minneapolis-Honeywell Regulator Co., Rubicon Instruments

Cat. No.: 1551

Serial No.: 125202

c. Galvanometer

A reflecting high sensitivity galvanometer was used to balance the bridge. A damping key was provided in the galvanometer circuit to reduce the oscillation of the moving coil.

Manufacturer: Minneapolis-Honeywell Regulator Co., Rubicon Instruments

Cat. No.: 3201, Type T

Serial No.: 120375

Resistance: 11.5 ohms

Sensitivity per mm at 1 meter distance: 0.071 μV

Period: 10 seconds

Ext. Crit. Damp. Resistance: 17 ohms

Accessories

Cat. No.: 3910, Lamp and Scale Reading Device

3280, Right Angle Prism

3290, Galvanometer Bracket

d. Temperature Controller

A general purpose laboratory temperature controller was used to control the bath temperature in conjunction with a platinum resistance thermometer bulb as a sensing element. The Thermotrol is designed to control by any of three modes; on-off, proportional, or proportional with reset.

During proportional operation, a negative feedback signal is applied to produce an on period which is function of the bridge unbalance voltage. The sensitivity of the controller, expressed as the proportional band temperature differential, 0 - 100% duty cycle, can be adjusted in nine steps from 0.023°C to 5.888°C by the gain switch.

For reset operation, a positive feedback circuit with an appropriate time constant is added to the negative feedback circuit to restore the AC bridge unbalance to zero. This feature reduces the apparent proportional band by a factor of 100. For example, if the gain switch is set on the maximum gain, the proportional band temperature differential, 0 - 100% duty cycle, is 0.00023°C instead of

0.023°C. The reset rates provided on the Thermotrol may be set at eight different values from 6 to 90 seconds. Higher gains result in "hunting" or oscillations about the set point, while lower gains produce a proportional "offset" which is due to changes in load or heat demand of the system being controlled.

Thermotrol

Manufacturer: Hallikainen Instruments

Model: 1053A

Serial No.: 8379

Platinum Resistance Thermometer Bulb

Model: 11830

Serial No.: 8031

3. Material

The purity of the original methyl chloride sample was 99.7%. Further purification of the sample was accomplished by purging the first 10% or so of the vapor from the cylinder. This eliminated the majority of the volatile contaminants. After this point the vapor has a purity of at least 99.9% methyl chloride. In order to supply the methyl chloride to the surge tank as a liquid, the methyl chloride gas cylinder was inverted in an angle-iron fixture.

The purity of helium used in this work is 99.98%. and that of nitrogen is 99.996%. All of the cylinder gases were obtained from the Matheson Company.

APPENDIX B

Corrections to Pressure Measurements

The pressure measurements were obtained by applying the corrections discussed below to the dead weight gage readings. In addition hydraulic head corrections were made. With the exception of the treatment of the hydraulic head corrections, they are discussed in the order of their importance.

1. Corrections to the Dead Weight Gage Reading

a. Temperature

Dead weight gages are very sensitive to the temperature change and readings must be corrected to the operating temperature.

The change in effective area of the piston with temperature can be calculated by a straightforward application of the thermal coefficients of the materials of the piston and cylinder. The effective area of the piston at any temperature may be found by the relation

$$A_{o(t + \Delta t)} = A_{o(t = 25^{o}C)} (1 + c\,\Delta t) \qquad (69)$$

where c is the coefficient of superficial expansion and its value is given in Appendix A.

The order of magnitude of error due to a temperature change of 5°C for a tungsten carbide piston-tool steel cylinder combination is 0.08%. Gage temperatures were read to the nearest 0.1°C.

b. Elastic Distortion

The effective area of a piston gage is the mean of the areas of the cylinder and the piston, provided the piston is concentric with the cylinder and falling at such a rate that the volume displaced by the piston is equal to the volumetric leakage between them. In the piston gage the pressure varies along the length of the annulus between piston and cylinder. At the bottom it is equal to the pressure being measured; at the top it is zero. The stress set up by the pressure drop through the wall causes the cylinder to undergo a temporary strain in the direction of the bore. Consequently, the bore is reduced in diameter thereby reducing the effective area.

The distortion of the piston and cylinder may be calculated on the basis of an effective pressure in the annulus. This pressure is the mean between those at the two ends, provided that the pressure drop occurs in a region far from the ends of the piston and of the bore of the cylinder. The change in the diameter d of a piston subjected to the end pressure P and surrounded by the

effective pressure P_c may be represented by the relation

$$\Delta d/d = \nu P/E + (P_c/E)(\nu - 1) \qquad (70)$$

The above equation may be also written in terms of the effective area A_e,

$$\Delta A/A = 2\Delta d/d = bP \qquad (71)$$

or

$$A_e = A_o (1 + bP) \qquad (72)$$

at 7,000 psi this introduces an error of less than 0.025% with an estimated accuracy of about 0.001%.

c. Gravity

The pressure measured with a piston gage loaded with a particular set of dead weights is proportional to the local value of gravity g_l. The standard value of gravity g_s is chosen as 980.665 gm/sec^2. If the latitude ϕ and the elevation, h in meters, above sea level are known, the local gravitational constant can be calculated by the formula (22)

$$g_l = g_o - 0.0003086h \qquad (73)$$

where g_o is the local gravity at the sea level and given by

$$g_o = 978.0495 (1 + 0.0052892 \sin^2\phi - 0.0000073 \sin^2 2\phi) \qquad (74)$$

The local gravity in Columbia, Missouri (latitude = 38°56' and elevation = 743.5 ft) is then

$$g_l = 980.016 \text{ gm/sec}^2 \qquad (75)$$

The gage readings were corrected for the local gravity by

the following relation.

$$W = Mg_l / g_s \tag{76}$$

The estimated error is about 0.001%.

d. Buoyancy

Values for the weights under the heading "Apparent Mass vs Brass" as shown in Table I are those which the weights appear to have when compared in air against standard brass weights (density of 8.4 gm/cc). In precise work, the mass of the load on the piston should be reduced by an amount equal to the mass of the air displaced by the weights. The density of air is about 0.0012 gm/cc. An approximate correction may be made from the relation

$$W = M_a \left(1 - \frac{\text{density of air}}{\text{density of brass}} \right) \tag{77}$$

This approximation is good to about 1 PPM.

The corrections described above may all be combined to give

$$P = \frac{W}{A} = \frac{M_a\left(\frac{g_l}{g_s}\right)\left(1 - \frac{\rho_{air}}{\rho_{brass}}\right)}{A_{o(25^oC)}\ (1 + c\,\Delta t)(1 + bP)} \tag{78}$$

If the absolute value of the corrections described above is taken, they add up to about 0.01%.

2. Hydraulic Head Corrections

The hydraulic heads as shown in Figure 4 are

distances above an arbitrary reference plane in the laboratory. Since the upper expansion cell has its reference plane (about middle of the chamber I) above that of the dead weight gage, it is necessary to apply corrections to the gage readings for the pressure gradient throughout the hydraulic system. The density of the gage oil is approximately 0.85 gm/cc which corresponds to a pressure gradient of 0.031 psi for each inch of vertical dimension of the oil system. Because the density of the gage oil is considerably larger than that of the gas, the hydraulic head correction for each unit distance in the oil system is correspondingly greater than that in the gas system. Therefore, hydraulic heads can be entirely eliminated in the oil system by installing the two dead weight gages and the low temperature DPI in such a way that their reference planes coincide.

The dead weight gage is provided with a post with an index line representing the plane of reference. When the index line on the sleeve weight and that of the post coincide, the pressure measurement is referenced directly to the test system. The reference plane of the piston slowly changes its position during a pressure measurement because of the oil leakage by the piston. Therefore, the pressure is raised until the weights are floating at a position somewhat above the line on the post so that the

entire system will have time to reach equilibrium before the two index lines coincide.

A second set of index lines is located on the main housing and weight table drive pins. When the pressure is less than that requiring the sleeve weight, the position of the piston is determined by the second set of index lines.

The pressure exerted by a hydraulic head may be calculated by the following relation:

$$P = dh \frac{g}{g_c} \tag{79}$$

The pressure exerted at the diaphragm of the high temperature differential pressure cell by the hydraulic heads illustrated in Figure 4 is given by

$$P_h = d_{N_2(T_{av})}(H_2 - H_1)\, g/g_c + d_{N_2(T_{room})}(H_o - H_2)\, g/g_c \tag{80}$$

where

$H_o = 0$ (reference plane)

$H_1 = 16\frac{1}{2}"$

$H_2 = 37\frac{3}{4}"$

$d_{N_2(T_{av})}$ = density of nitrogen at P and

$$T_{av} = \frac{T_{bath} + T_{room}}{2}$$

$d_{N_2(T_{room})}$ = density of nitrogen at P and room temperature

Since half of the high temperature differential pressure indicator was submerged in the bath and half was located

outside, the density of nitrogen in this vertical section of the line was determined at the average temperature between the bath and the room.

The hydraulic pressure corresponding to the zero reading of the differential pressure indicator must also be determined at each temperature. The zero correction which must be applied to all pressure measurements is the negative of Equation (80) evaluated at the atmospheric pressure. The density of nitrogen was obtained from the reported experimental data (9,60).

The order of magnitude of the hydraulic head correction is about 0.007% while that of zero correction varies from about 0.007% at low pressure to about 1.5×10^{-5}% at 7,000 psi. Therefore, the zero correction is negligible at high pressures. At low pressures the combined zero correction and hydraulic head correction is negligibly small. This combined uncertainty amounts to about 0.002% at 50 psi and decreases rapidly with pressure.

3. Zero Shift as a Function of Operating Pressure

The diaphragm assembly in the differential pressure indicator expands with pressure resulting in a zero shift due to the change in the position of the core within a transformer coil. The "zero" shifts approximately 0.016

psi as the operating pressure is varied from zero to 7,000 psi in the low temperature differential pressure cell and 0.75 psi in the case of high temperature differential pressure cell. The calibration curves for the two differential pressure indicators are given in Figures 15 and 16. The estimated accuracy of these curves is about 0.002%.

The corrections described above may be combined to give the following final result:

$$P = \text{corrected gage pressure} + \text{hydraulic head correction} + \text{zero correction} + \text{zero shift} + \text{barometric pressure} \quad (81)$$

The barometric pressures can be read with an accuracy of 0.01%. This uncertainty introduces an error of 0.004% at 50 psi and decreases rapidly with pressure. Therefore, the probable error in all pressure measurements is less than $\pm$ 0.02%.

APPENDIX C

Discussion of Errors

In addition to the usual experimental errors in the measurement, calibration, etc., are some sources of errors unique to the determination of the final results. The errors discussed here comprise a brief description of the systematic errors introduced by some of the assumptions made in the calculation of results and by the incomplete evacuation of the chamber II of the expansion cell.

The first error of importance is that of the apparatus constant calculated by Equation (64) using Hook's Law and neglecting end effects. The fractional change in volume of the cell with internal pressure corresponds to about 0.08% at 7,000 psi and reduces to 0.0006% at 50 psi. The uncertainty in the apparatus constant due to this elastic distortion of the cell amounts to about 0.001%.

The second source of error comes from the change in the line voltage. This changes the power input to the temperature bath, which causes some difficulty in controlling the temperature of the bath. The change in the line voltage also changes the null setting of the differential pressure indicators and of the temperature controller. The observed variation in the line voltage was about 2%.

The third source of error comes from the change in the room temperature. This changes the null setting of the differential pressure indicators. The zero setting in the Mueller Bridge is also disturbed by the change in the lead resistances due to the temperature change. The room temperature was controlled within $\pm$ 1°C at all times.

Incomplete evacuation of the chamber II of the expansion cell also leads to another source of error. When the first expansion is completed, the number of moles remaining in the chamber I is given by

$$n_1 = (n_o + n_x)/ N(P_i, P_{i-1}) \qquad (82)$$

If the above equation is applied repeatedly to the first, second,... rth expansions assuming that the chamber II is evacuated to the same pressure (50 microns) each time, the resulting equations may be combined. The relationship so obtained, after substituting PV = ZnRT and simplifying, is given by

$$P_r \prod_{i=1}^{r} N(P_i, P_{i-1}) = \frac{P_o}{Z_o} Z_r \left\{ 1 + \frac{P_x Z_o}{Z_x P_o} \left[\prod_{i=1}^{r} N(P_i, P_{i-1}) - 1 \right] \right\} \qquad (83)$$

comparing Equations (65) and (83), the relative error in the compressibility factor due to the incomplete evacuation of the chamber II is given by

$$\frac{Z_r - Z'_r}{Z'_r} = P_x \frac{Z_o}{P_o} \left[\prod_{i=1}^{r} (P_i, P_{i-1}) - 1 \right] \qquad (84)$$

where Z_r' is the corrected compressibility factor.

The order of magnitude of this error is less than 0.00001% for all cases. The major error in the compressibility factor due to the incomplete evacuation of the chamber II is in the low pressure region where the number of expansion r is large as shown in Equation (84).

The probable error in the temperature measurements is approximately $\pm$ 0.01°C which corresponds to a relative error of $\pm$ 0.005% at the lowest temperature. Error in the pressure measurements have been discussed in Appendix B.

Finally, a single value of N obtained from the helium calibration runs was used at all experimental temperatures as a convenience. This introduces some error in the apparatus constant. The order of magnitude of this error is probably less than 0.005%. The error in the apparatus constant together with that due to the elastic distortion of the cell are propagated to the evaluated run constant P_o/Z_o by the subsequent expansions. The probable error in the compressibility factor from this source after r expansions is rE_N which amounts to approximately 0.06%. Therefore, the estimated overall error in the compressibility factor is less than $\pm$ 0.1%. With the experimental apparatus shown in Figure 1, this error could be reduced

to some extent by improving the precision of the experimental data.

APPENDIX D

Determination of Potential Parameters

High-speed computational methods were applied to determine the potential parameters ρ_o', U_o' and t' from the experimental B(T) data. The average percent deviation was the criterion for the optimum agreement between experimental and calculated B(T) values.

For a given set of predetermined values of M_o, S_o and V_o, the following procedure was used to determine the potential parameters.

(1) A trial value of ρ_o' was selected.

(2) For the highest value of T, t' was obtained such that the calculated B(T) agreed with the experimental value within the experimental accuracy.

(3) U_o' was then determined

(4) B(T) values were calculated for each T.

(5) ρ_o' was then increased or decreased by discrete amount depending on the curvature of the potential function.

(6) the above steps were repeated until the minimum average percent deviation between experimental and calculated B(T) values was obtained.

Each step of this procedure was done automatically using IBM 1620-II. The results are listed in Tables VI and VII.

APPENDIX E

Sample Calculations

The initial pressure P_o of Run number 14 at 250°C will be used to demonstrate the sample calculations for methyl chloride except where noted.

Corrections to the Dead Weight Gage Reading

The combined corrections for the temperature, elastic distortion, local gravity and buoyancy to the dead weight gage reading can be calculated from Equation (78).

$$P = \frac{M_a\left(\frac{g_l}{g_s}\right)\left(1 - \frac{\rho_{air}}{\rho_{brass}}\right)}{A_{o(25^\circ C)}(1 + c\,\Delta t)(1 + bP)}$$

$$= \frac{(98.41634)\left(\frac{980.016}{980.665}\right)\left(1 - \frac{0.0012}{8.4}\right)}{(0.0260411)(1-1.7\times10^{-5}\times0.1)(1-3.6\times10^{-8}\times3780)}$$

$$= \underline{3776.615 \text{ psi}}$$

Hydraulic Head Correction

The hydraulic head correction can be obtained by using Equation (80).

$$P_h = d_{N_2(T_{av})}(H_2 - H_1)\frac{g}{g_c} + d_{N_2(T_{room})}(H_o - H_2)$$

$$d_{N_2(137.35^\circ C)} = 6.73 \times 10^{-3} \text{ lb/in}^3$$

$$d_{N_2(24.7^\circ C)} = 9.61 \times 10^{-3} \text{ lb/in}^3$$

$$P_h = (6.73 \times 10^{-3})(21.25) - (9.61 \times 10^{-3})(37.75)$$
$$= - \underline{0.220 \text{ psi}}$$

Zero Correction

The Hydraulic pressure corresponding to the zero reading of the differential pressure indicator is the negative of Equation (80).

d_{N_2} at 137.5°C and 1 atm = 2.97×10^{-5} lb/in^3

d_{N_2} at 25°C and 1 atm = 4.10×10^{-5} lb/in^3

$$P_{h(zero)} = - (2.97 \times 10^{-5})(21.25) + (4.10 \times 10^{-5})(37.75)$$
$$= \underline{0.00092 \text{ psi}}$$

Zero Shifts

The zero shifts of the differential pressure indicators are given in Figures 15 and 16. If subscript 1 refers to high temperature DPI and subscript 2 refers to low temperature DPI, then the pressure in the lower chamber of DPI can be expressed as the sum of the pressure in the upper chamber of the DPI, P_u, and the zero shift, ΔP. Thus,

$$P_{\ell 2} = P_{u2} + \Delta P_2$$

Since $P_{\ell 2} = P_{u1}$ and P_{u2} = corrected DWG pressure,

$$P_{\ell 1} = P_{u1} + \Delta P_1 = P_{\ell 2} + \Delta P_1 = P_{u2} + \Delta P_1 + \Delta P_2$$

Therefore, the zero shifts must be added to the corrected dead weight gage pressure to obtain the pressure in the expansion cell.

$$\Delta P_1 = 0.402 \text{ psi}$$

$$\Delta P_2 = 0.009 \text{ psi}$$

Barometric Pressure

$$\frac{748.2}{760.0} \times 14.696 = \underline{14.467 \text{ psi}}$$

The correct pressure can be calculated from Equation (81).

P_o = corrected gage pressure + hydraulic head correction + zero correction + zero shift + barometric pressure

= 3776.615 - 0.220 + 0.001 + 0.402 + 0.009 + 14.467 = <u>3791.274 psia</u>

Similarly, P_1, P_2,... P_r can be calculated from Equation (81).

Compressibility Factor

The apparatus constant for P_1 can be obtained from Equation (64).

$$N = N_o \frac{(1 + 1.313875 \times 10^{-7} P_1)}{(1 + 1.313875 \times 10^{-7} P_o)}$$

$$= 1.599855 \frac{(1 + 1.313875 \times 10^{-7} \times 2354.290)}{(1 + 1.313875 \times 10^{-7} \times 3791.274)}$$

$$= 1.599553$$

Substituting the values of the apparatus constant into Equation (65), we obtain for P_1,

$$P_r \prod_{i=1}^{r} N(P_i, P_{i-1}) = (2354.290)(1.599553) = \underline{3765.812}$$

Similarly, a set of values required to determine the run constant can be obtained.

Having obtained the run constant P_o/Z_o from Equation (66), the compressibility factor can be calculated from Equation (65).

$$Z_1 = \frac{Z_o}{P_o} P_r \prod_{i=1}^{r} N(P_i, P_{i-1}) = \frac{3765.8}{6053.2} = \underline{0.62212}$$

A table of sample calculation data is given below.

Sample Calculation

$T = 250^{\circ}$ C

Run No.	r	P(psia)	N	$P_r \prod_{i=1}^{r} N(P_i, P_{i-1})$	P_o/Z_o	Z	$-B \times 10^3$ (atm^{-1})
13	0	4999.394	1.000000	4999.394		0.70828	
	1	2667.229	1.599365	4265.873		0.60436	
	2	1870.876	1.599688	4786.607		0.67813	
	3	1325.198	1.599740	5423.917		0.76842	
	4	909.424	1.599768	5954.641		0.84361	
	5	605.376	1.599791	6341.291	7058.5	0.89839	2.2000
	6	394.062	1.599811	6603.674		0.93556	
	7	252.696	1.599825	6774.730		0.95980	
	8	160.453	1.599836	6882.034		0.97500	
	9	101.265	1.599843	6948.732		0.98445	
	10	63.663	1.599847	6988.948		0.99015	
14	0	3791.274	1.000000	3791.274		0.62633	
	1	2354.290	1.599553	3765.812		0.62212	
	2	1676.121	1.599712	4288.900		0.70853	
	3	1176.759	1.599750	4817.040	6053.2	0.79578	2.1613
	4	798.982	1.599776	5232.254		0.86438	
	5	527.462	1.599798	5525.965		0.91290	
	6	341.414	1.599816	5722.269		0.94533	
	7	218.079	1.599829	5847.556		0.96603	
	8	138.145	1.599838	5926.138		0.97901	
	9	87.049	1.599844	5974.177		0.98695	
	10	54.671	1.599848	6002.748		0.99167	

NOMENCLATURE

NOMENCLATURE

a	Equivalent radius of Kihara core
B	Second Virial Coefficient
E	Young's modulus
f	Fugacity
g	Gravitational acceleration
g_c	Gravitational conversion factor
H	Enthalpy
H^o	Enthalpy at ideal gas state($P = 0$)
H^*	Enthalpy of hypothetical ideal gas at the same pressure as real gas
k	Boltzmann constant
L_o	Original length of cylinder at zero pressure
M_o	Surface integral of mean curvature of Kihara core
N	Avogadro's number, apparatus constant
n	Number of moles of gas
n_o	Original moles of gas in chamber I
n_i	Moles of gas in chamber I after first expansion
n_x	Moles of gas in chamber II after evacuation
P	Pressure
P_o	Initial pressure in chamber I
P_x	Pressure in chamber II after evacuation
r	Radius, intermolecular separation
r_o	Distance of separation corresponding to potential minimum
R_i	Inner radius

R_o	Outer radius, resistance at 0^oC
R_t	Resistance at temperature t
R	Universal gas constant
S	Entropy
S^o	Entropy at ideal gas state
S*	Entropy of hypothetical ideal gas at the same pressure as real gas
S_o	Surface area of Kihara core, longitudinal stress
S_r	Radial stress
S_t	Hoop stress
t	Temperature
T	Absolute temperature
T_c	Critical temperature
t'	Reduced dipole moment
U	Intermolecular potential energy
U_o	Minimum potential energy
U^o	Internal energy at ideal gas state (P = 0)
U*	Internal energy of hypothetical ideal gas at the same pressure as real gas
V	Molar volume
V_o	Volume of Kihara core, volume of cylinder at zero pressure
W	Weight
Z	Compressibility factor
Z_o	Compressibility factor at P_o
Z_x	Compressibility factor at P_x

Greek Letters

α	Residual volume
ρ	Shortest distance between molecular cores
ρ_o	Shortest distance between molecular cores at potential minimum
θ_1	Angle between dipole axis of molecule 1 and intermolecular axis
θ_2	Angle between dipole axis of molecule 2 and intermolecular axis
ϕ	Azimuthal angle between two dipole axis
μ	Dipole moment
ν	Poisson's ratio

BIBLIOGRAPHY

BIBLIOGRAPHY

1. Alexander, E. A., and Lambert, J. D., Trans. Faraday Soc., 37, 421 (1941).

2. Beattie, J. A., Rev. Sci. Instr., 2, 458 (1931).

3. Beattie, J. A., and Bridgeman, O. C., J. Am. Chem. Soc., 49, 1665 (1927).

4. Benedick, M., Webb, G. B., and Rubin, L. C., J. Chem. Phys., 8, 334 (1940).

5. Bird, R. B., Hirschfelder, J. O., and Curtiss, C. F., University of Wisconsin, CM-758, Nord-9937 Task Wis-1-c, November, 1952.

6. Bird, R. B., and Spotz, E. L., University of Wisconsin, CM-599, (1950).

7. Bird, R. B., Spotz, E. L., and Hirschfelder, J. O., J. Chem. Phys., 18, 1395 (1950).

8. Black, C., Ind. Eng. Chem., 50, 391 (1958).

9. Bloomer, O. T., Inst. Gas Tech. Res. Bul,, 13, 1 (May, 1952).

10. Bondi, A., and Simkin, D. J., A.I.Ch.E.J., 3, 473 (1957).

11. Buckingham, A. D., and Pople, J. A., Trans. Faraday Soc., 51, 1173 (1955).

12. Burnett, E. S., J. Applied Mech., 58, A136 (1936).

13. Comings, E. W., High Pressure Technology, McGraw-Hill, New York, 1956.

14. Connolly, J. F., Virial Coefficients of Carbon-monoxide-Hydrocarbon Mixtures, Private Communication, April, 1964.

15. Connolly, J. F., and Kandalic, G. A., Phys. Fluids, 3, 463 (1960).

16. Connolly, J. F., and Kandalic, G. A., Documentation Institute, Library of Congress, Document No. 6307.

17. Corner, J., Proc. Roy. Soc. (London), A192, 275 (1948).

18. De Boer, J., and Michels, A., Physica, 5, 945, 949 (1938).

19. Edmister, W. C., Petrol. Refiner, 37, No. 4, 173 (1958).

20. Eubank, P. T., and Smith, J. M., A.I.Ch.E.J., 8, 117 (1962).

21 Eucken, A., and Meyer, L., Z. Physik. Chem. B., 5, 452 (1929),

22. Forsythe, W. E., Smithsonian Physical Tables, P. 714, 1954.

23. Ginell, R., J. Chem. Phys., 23, 2395 (1955).

24. Guggenheim, E. A., Mixtures, P. 154, Clarendon Press, Oxford, 1952.

25. Guggenheim, E. A., and McGlashan, M. L., Proc. Roy. Soc., A206, 448 (1951).

26. Hall, N. A., and Ibele, W., A.S.M.E. Trans., 77, 1003 (1955).

27. Hamann, S. D., and Lambert, J. A., Australian J. Chem., 7, 1 (1954).

28. Harper, R. C., Jr., and Miller, J. G., J. Chem. Phys., 27, 36 (1957).

29. Harris, F. E., and Alder, B. J., J. Chem. Phys. 21, 1351 (1953).

30. Hildebrand, J. H., and Scott, R. L., The Solubilities of Non-electrolytes, Reinhold Publishing Corporation, New York, P. 194, 1950.

31. Hirschfelder, J. O., Buehler, R. J., McGee, H. A., Jr., and Sutton, J. R., Ind. Eng. Chem., 50, 375 (1958).

32. Hirschfelder, J. O., Curtiss, C. F., and Bird, R. B., Molecular Theory of Gases and Liquids, John Wiley, New York, 1954.

33. Hirschfelder, J. O., McClure, F. T., and Weeks, I. F., J. Chem. Phys., 10, 201 (1942).

34. Hooper, E. D., and Jaffe, J., J. Chem. Eng. Data, 5, 155 (1960).

35. Hougen, O. A., and Watson, K. M., Chemical Process Principles, Part II, P. 488, John Wiley, New York, 1949.

36. Hsu, C. C., and McKetta, J. J., J. Chem. Eng. Data, 9 45 (1964).

37. Hsu, C. C., and McKetta, J. J., A.I.Ch.E.J., 9, 794 (1963).

38. Kahn, B., and Uhlenbeck, G. E., Physica, 5, 399 (1938).

39. Kihara, T., "Convex Molecules in Gaseous and Crystalline States", Advances in Chemical Physics, 5, Interscience Publisher's, Inc., New York, 1958.

40. Kihara, T., Rev. Mod. Phys., 25, 831 (1953).

41. Kihara, T., Rev. Mod. Phys., 27, 412 (1955).

42. Kirkwood, J. G., J. Chem. Phys., 1, 597 (1933).

43. Kirkwood, J. G., Phys. Rev., 44, 31 (1933).

44. Konowalow, D. D., Taylor, M. H., and Hirschfelder, J. O., Phys. Fluids, 4, 622, 629 (1961).

45. Kramer, G. M., and Miller, J. G., J. Phys. Chem., 61, 785 (1957).

46. Lambert, J. D., Roberts, G. A., Rowlinson, J. S., and Wilkinson, V. J., Proc. Roy. Soc., A196, 113 (1949).

47. Lambert, J. D., Disc. Faraday Soc., 15, 226 (1953).

48. Lambert, J. D., and Fox, H. P., Proc. Roy. Soc. (London), A210, 557 (1951).

49. Leland, T. W., and Mueller, W. H., Ind. Eng. Chem., 51, 597 (1959).

50. Lennard-Jones, J. E., Proc. Roy. Soc. (London), A106, 463 (1924).

51. Lennard-Jones, J. E., Physica, 4, 941 (1937).

52. London, F., Trans. Faraday Soc., 33, 8 (1937).

53. Lunbeck, R. J., and Ten Seldam, C. A., Physica, 17, 788 (1951).

54. Lyderson, A. L., Greenkorn, R. A., and Hougen, O. A., "Generalized Thermodynamic Properties of Pure Fluids," University of Wisconsin Eng. Exp. Station, Report No. 4, Madison, Wisconsin, 1955.

55. MacCormack, K. E., and Schneider, W. G., J. Chem. Phys., 18, 1269 (1950).

56. MacCormack, K. E., and Schneider, W. G., J. Chem. Phys., 19, 845 (1951).

57. Marcus, Leo, General Motors Engineering Journal, 16 (April-May-June, 1957).

58. Martin, J. J., and Hou, Y. C., A.I.Ch.E.J., 1, 142 (1955).

59. Meissner, H. P., and Seferian, R., Chem. Eng. Prog., 47, 579 (1951).

60. Michels, A., Lunbeck, R. J., and Wolkers, G. J., Physica, 17, 801 (1951).

61. Monchick, L., and Mason, E. A., J. Chem. Phys. 35, 1676 (1961).

62. Mueller, W. H., Ph.D. Thesis in Chemical Eng., The Rice Institute, Houston, Texas, 1959.

63. Nelson, L., and Obert, E. F., A.I.Ch.E.J., 1, 74 (1955).

64. Pauling, L., The Nature of the Chemical Bond, Cornell University Press, Ithaca, New York, 1940.

65. Pfefferle, W. C., Goff, J. A., and Miller, J. G., J. Chem. Phys., 23, 509 (1955).

66. Pitzer, K. S., J. Chem. Phys., 7, 583 (1939).

67. Pitzer, K. S., J. A.C.S., 77, 3427, 3433 (1955).

68. Pople, J. A., Proc. Roy. Soc. (London), A221, 498 508 (1954).

69. Prausnitz, J. M., and Myers, A. L., A.I.Ch.E.J., 9, 5 (1963).

70. Prigogine, I., The Molecular Theory of Solutions, North-Holland Publishing Co., Amsterdam, 1957.

71. Riedel, L., Chem. Ing. Tech., 26, 83 (1954).

72. Rowlinson, J. S., Trans. Faraday Soc., 45, 974 (1949).

73. Rowlinson, J. S., Trans. Faraday Soc., 47, 120 (1951).

74. Rowlinson, J. S., Trans. Faraday Soc., 51, 1317 (1955).

75. Saxena, S. C., and Joshi, K. M., Phys. Fluids, 5, 1217 (1962).

76. Schneider, W. G., Can. J. Research, B27, 339 (1949).

77. Schneider, W. G., and Duffie, J. A. H., J. Chem. Phys., 17, 751 (1949).

78. Sherwood, A. E., and Prausnitz, J. M., J. Chem. Phys., 41, 429 (1964).

79. Silberberg, I. H., Kobe, K. A., and McKetta, J. J., J. Chem. Eng. Data, 4, 314, 323 (1959).

80. Stevens, A. B., and Vance, H., Oil Weekly, 106, 21 (1942).

81. Stockmayer, W. H., J. Chem. Phys., 9, 398 (1941).

82. Tanner, H. G., Benning, A. F., and Mathewson, W. F., Thermodynamic Properties of Methyl Chloride, E. I. Du Pont de Nemours & Co., Wilmington, Delaware, 1939.

83. Timoshenko, S., Strength of Materials, Part II, Advanced Theory and Problems, P. 208, D. Van Nostrand, New York, 1930.

84. Voznick, H. P., and Uhl, V. W., "Molten Salt as a Heat Transfer Medium", Private Communication, 1962.

85. Watson, G. M., Stevens, A. B., Evans, R. B., III, and Hodges, D., Jr., Ind. Eng. Chem., 46, 362 (1954).

86. Wesson, L. G., Tables of Electric Dipole Moments, Technology Press, Cambridge, Mass., 1948.

87. Whalley, E., Lupien, Y., and Schneider, W. G., Can J. Chem., 31, 722 (1953).

88. Yntema, J. L., and Schneider, W. G., J. Chem. Phys., 18, 641 (1950).

89. Zimmerman, R. H., and Beitler, S. R., Trans. A. S. M. E., 74, 945 (1952).

90. Zwanzig, R. W., J. Chem. Phys., 23, 1915 (1955).

FIGURES AND TABLES

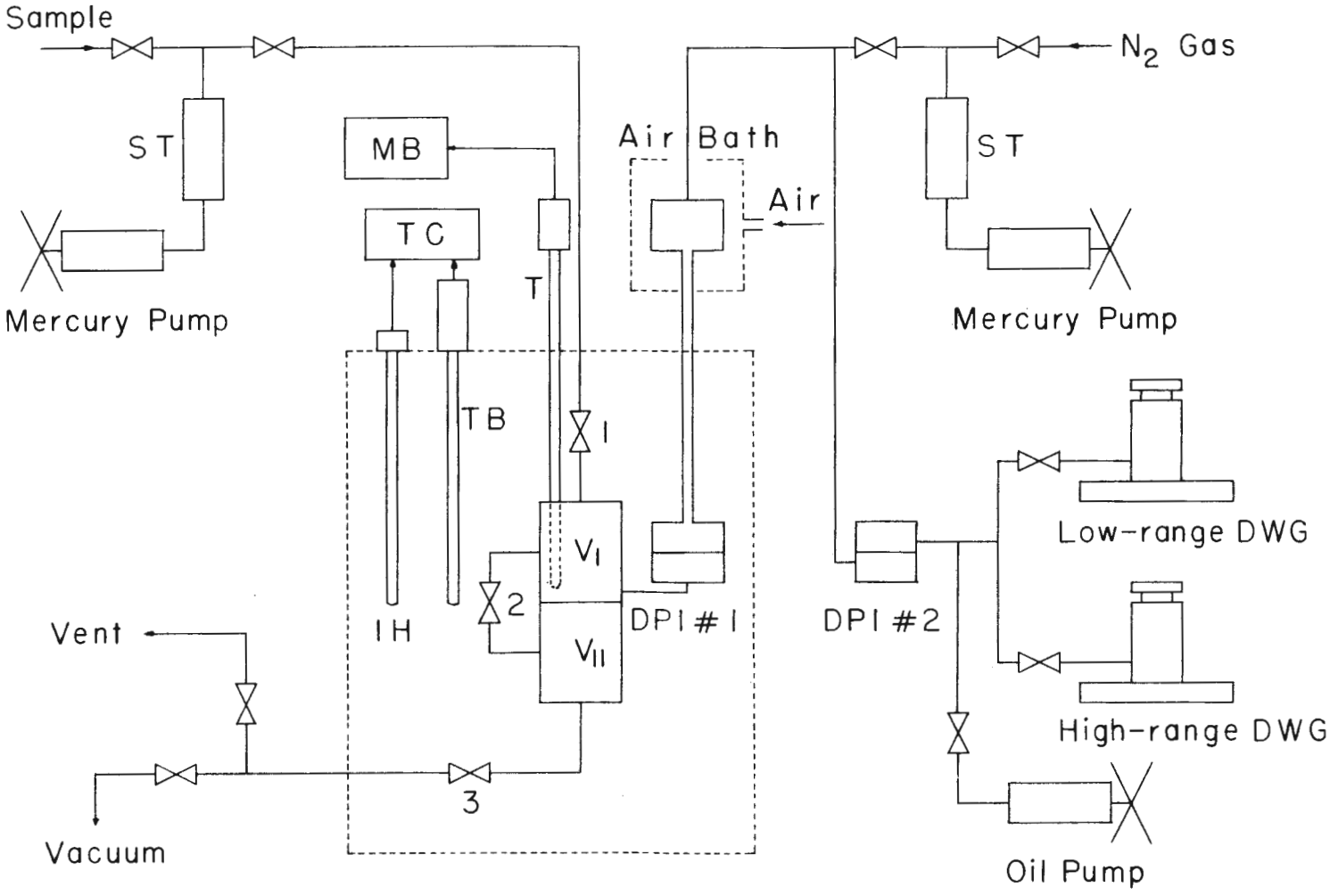

FIGURE I. Schematic Diagram of Apparatus

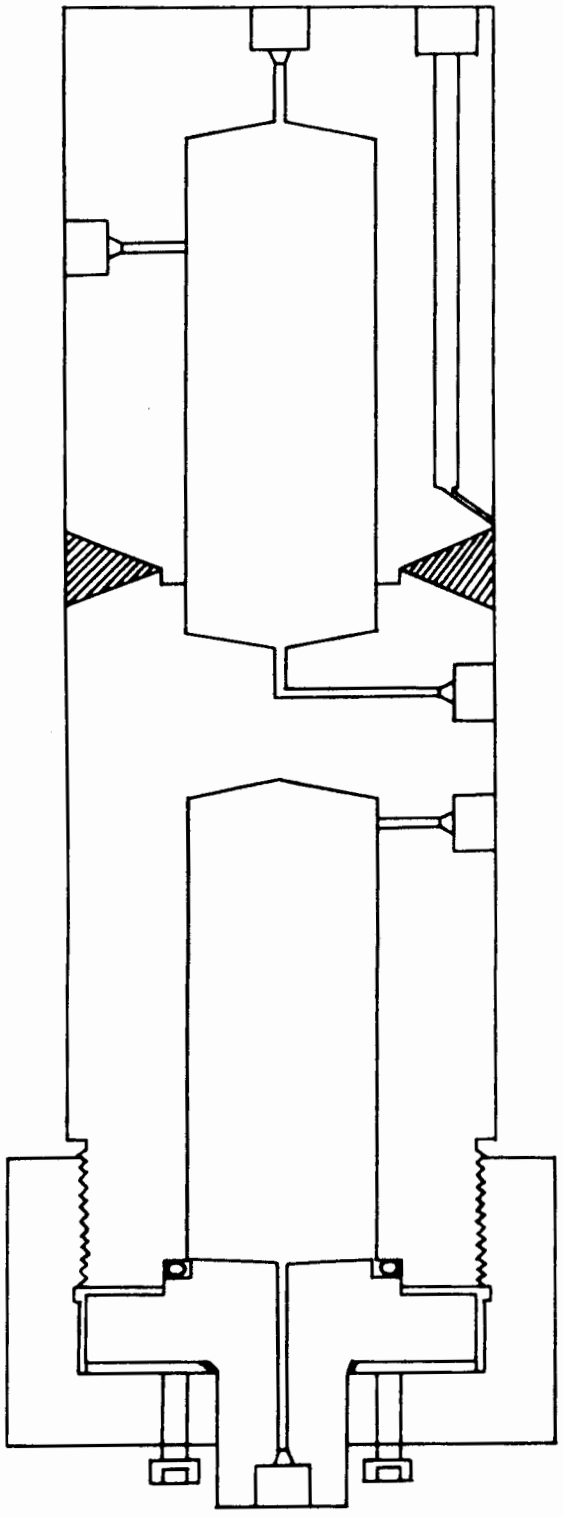

FIGURE 2. Expansion Cell

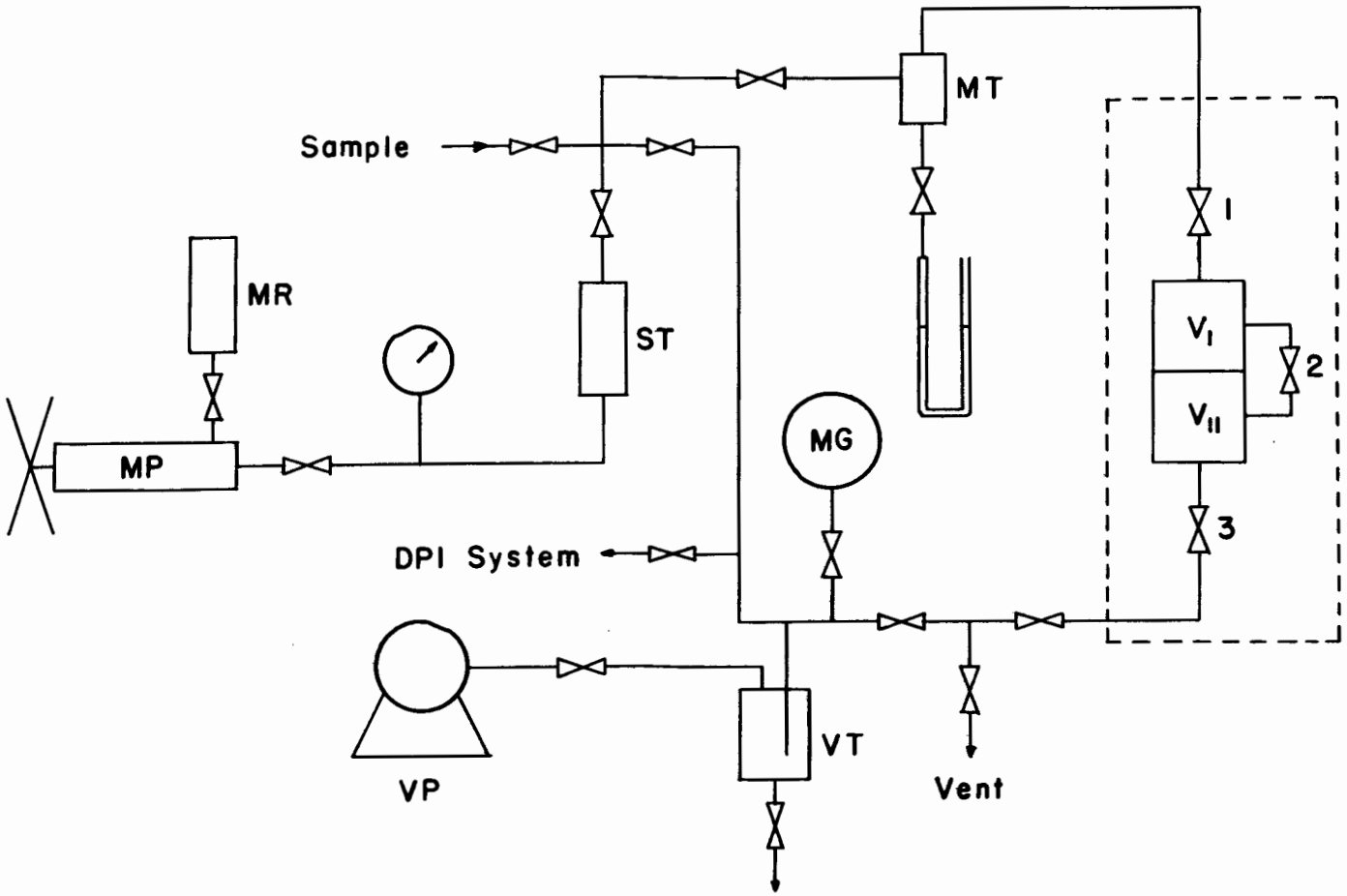

FIGURE 3. Schematic Diagram of Charging and Vacuum System

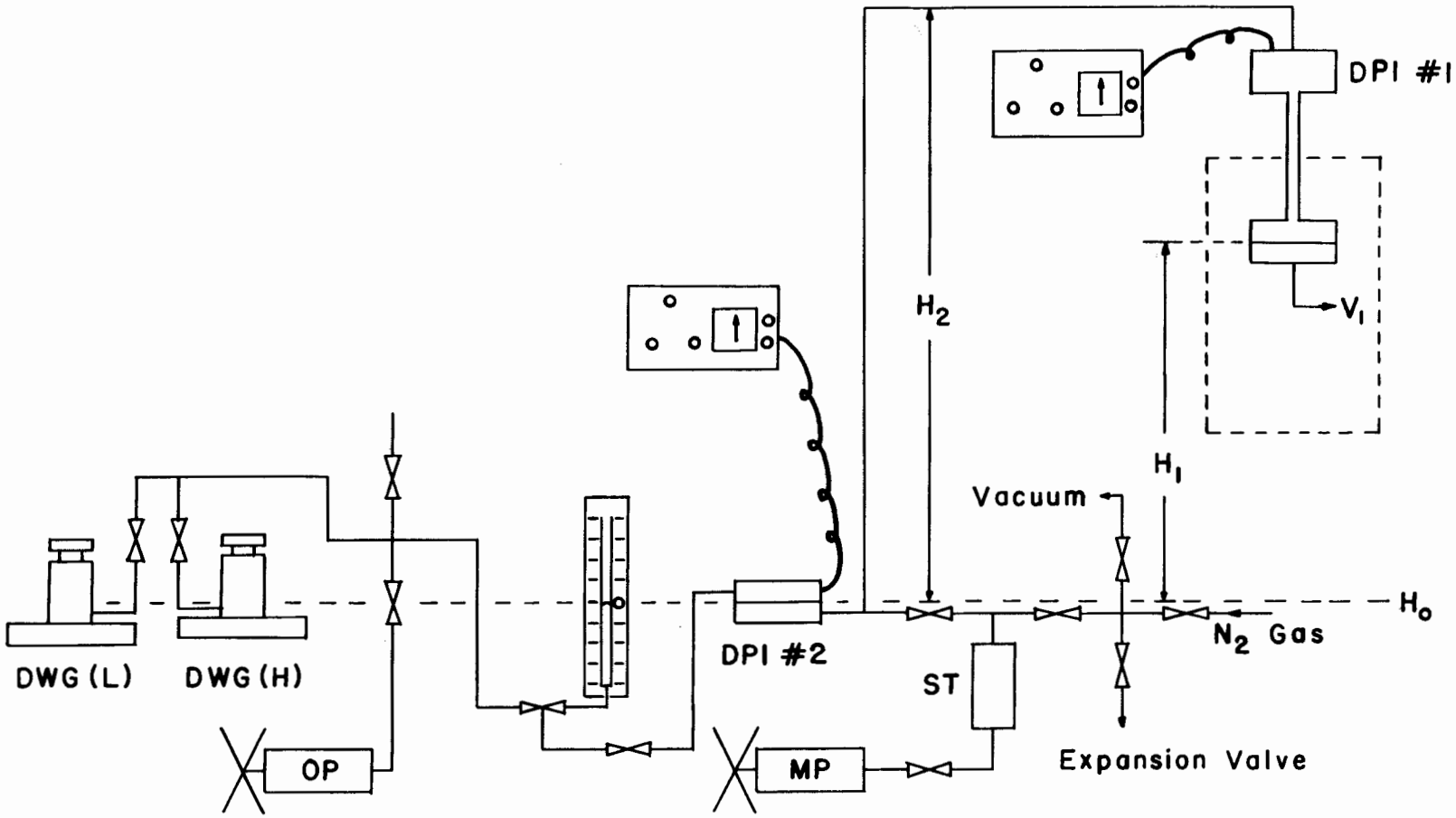

FIGURE 4. Pressure Measurement

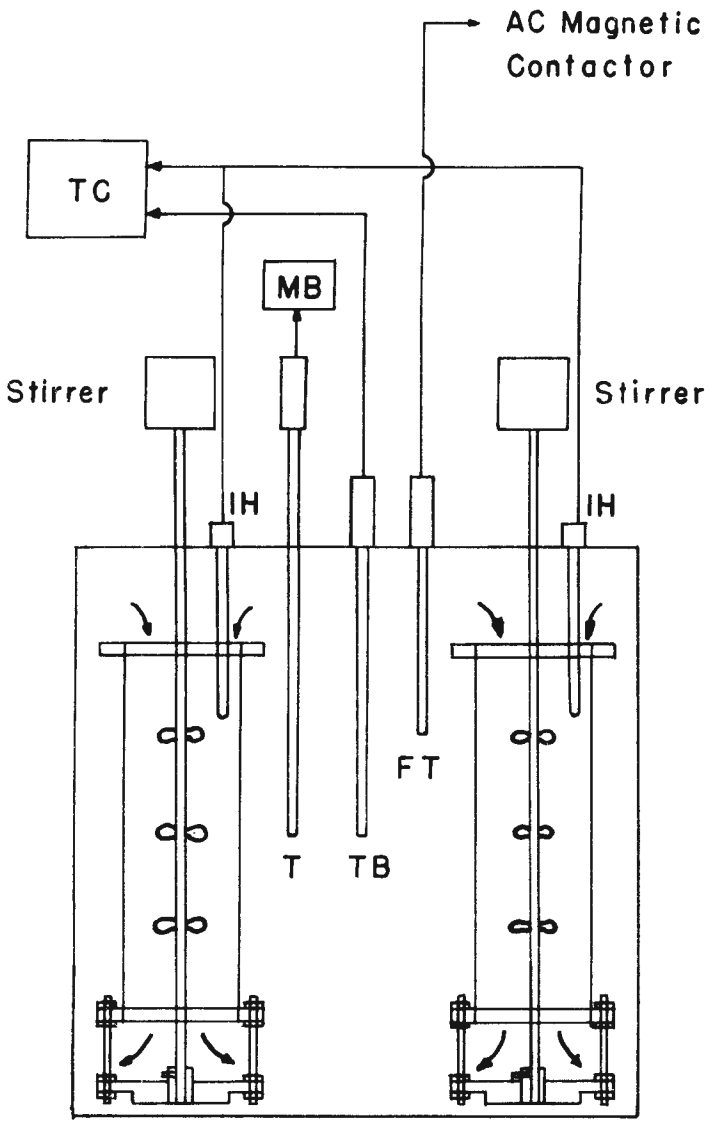

FIGURE 5. Temperature Measurement

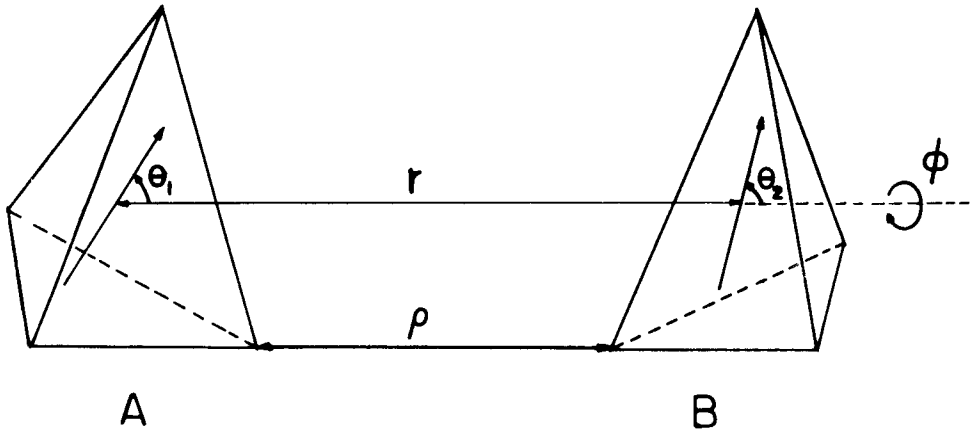

FIGURE 6. The Coordinates Describing the Mutual Orientation of Two Polar Molecules. A and B are Tetrahedron Cores Assigned to the Two Polar Molecules.

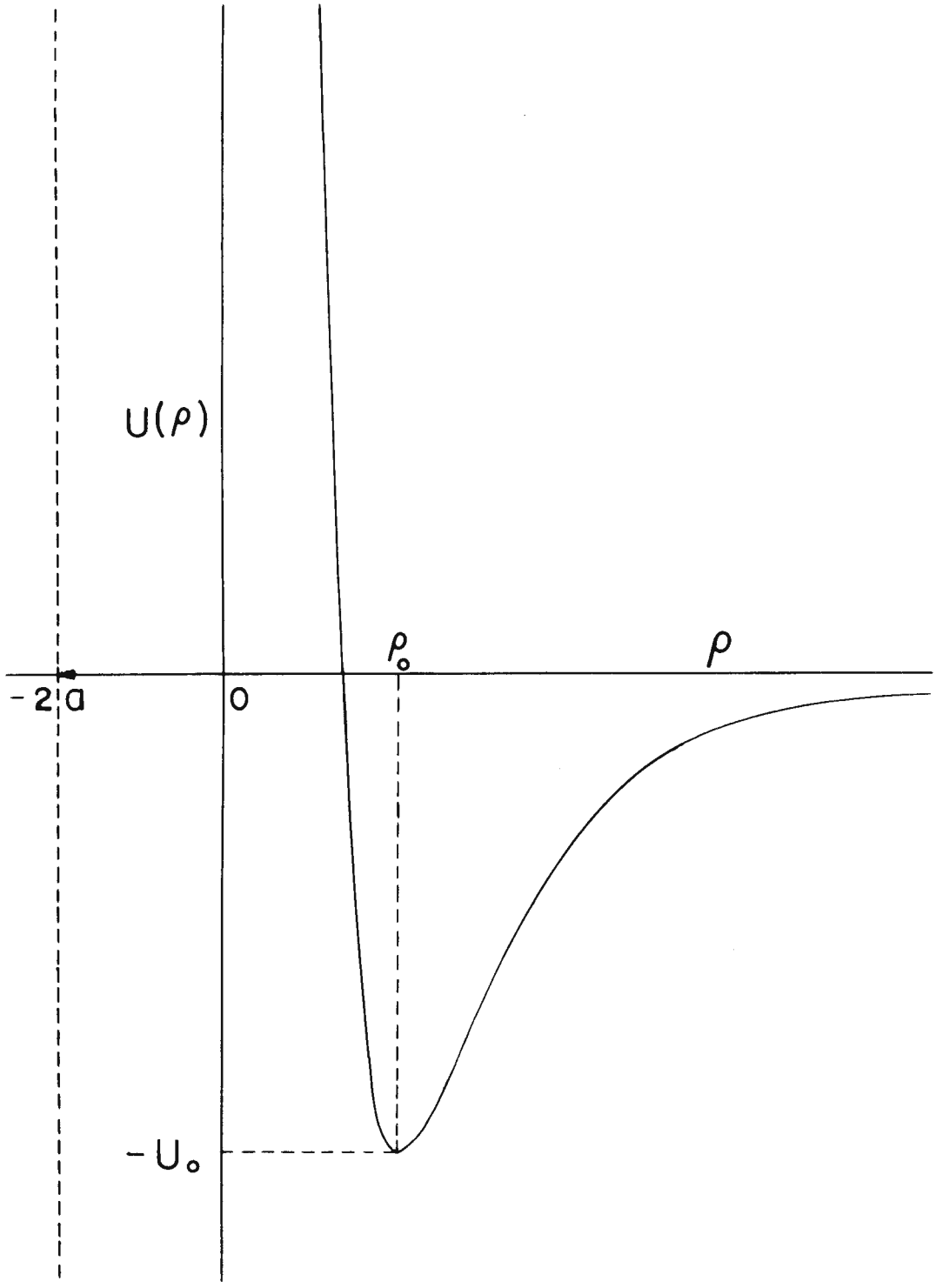

FIGURE 7. Potential Energy of Interaction Between Two Molecules for Kihara Potential.

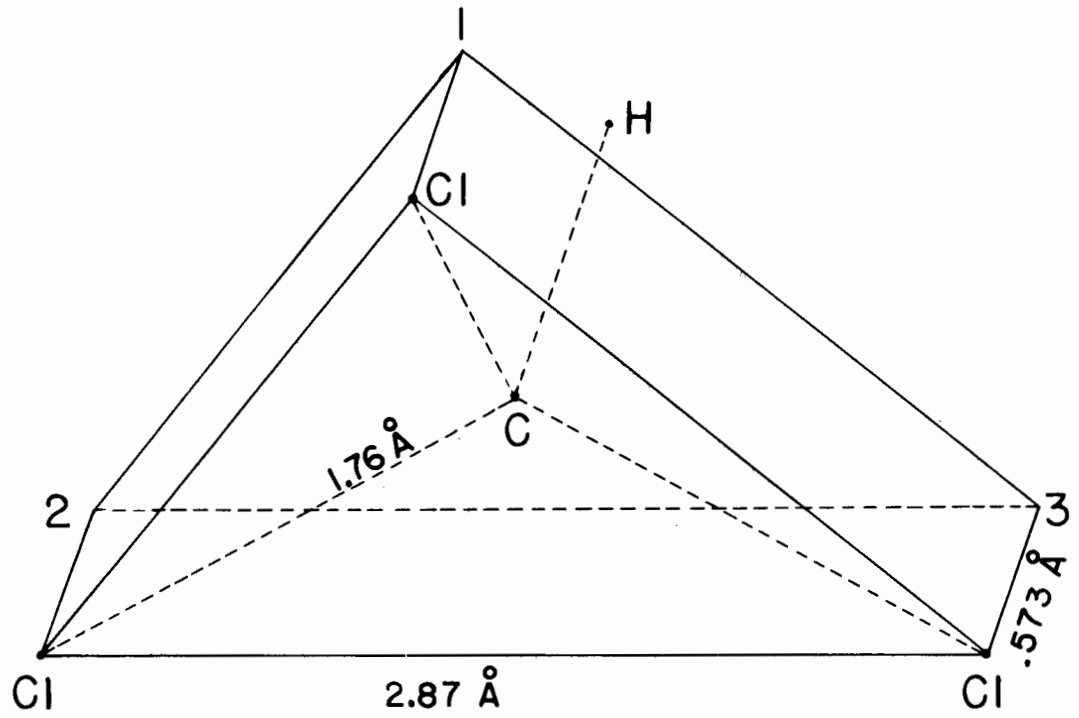

FIGURE 8. Triangular Prism Core for Chloroform, Points 1, 2, 3 and C are Coplanar.

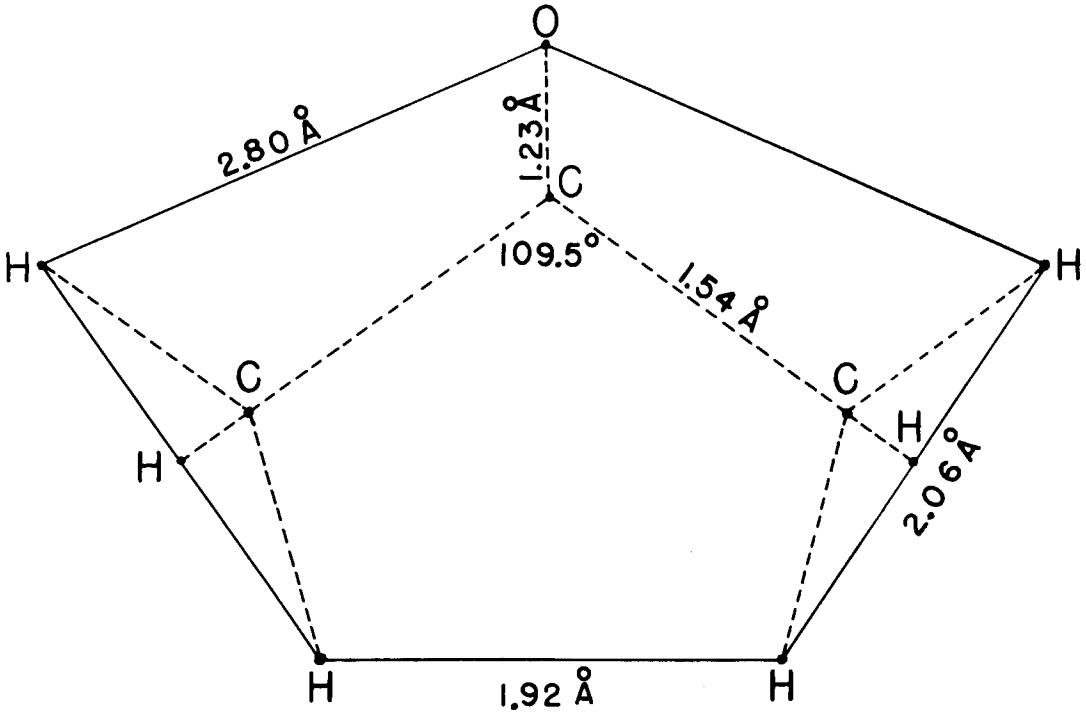

FIGURE 9. Pentagon Core for Acetone

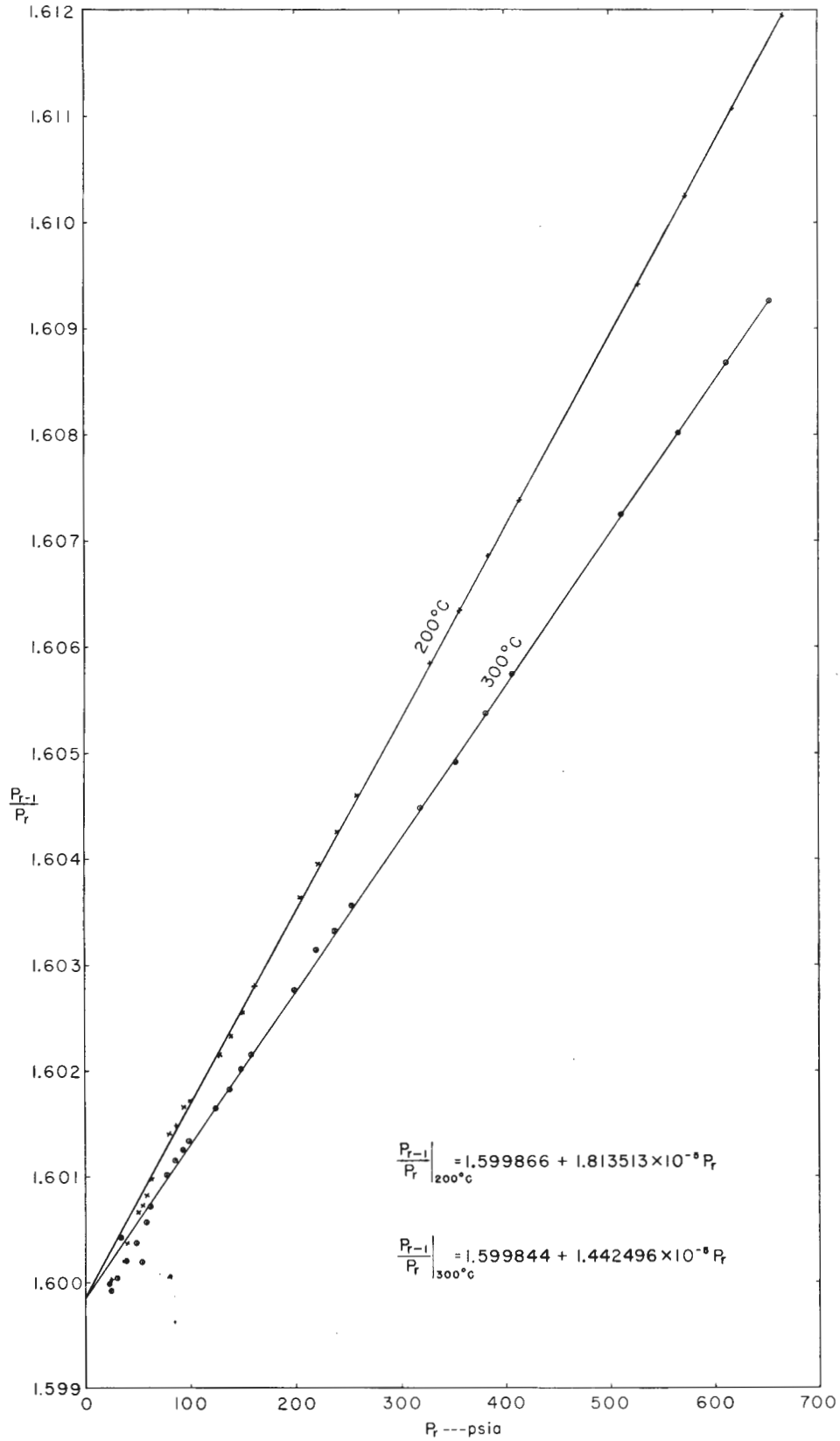

FIGURE 10. $\frac{P_{r-1}}{P_r}$ vs P_r for Helium

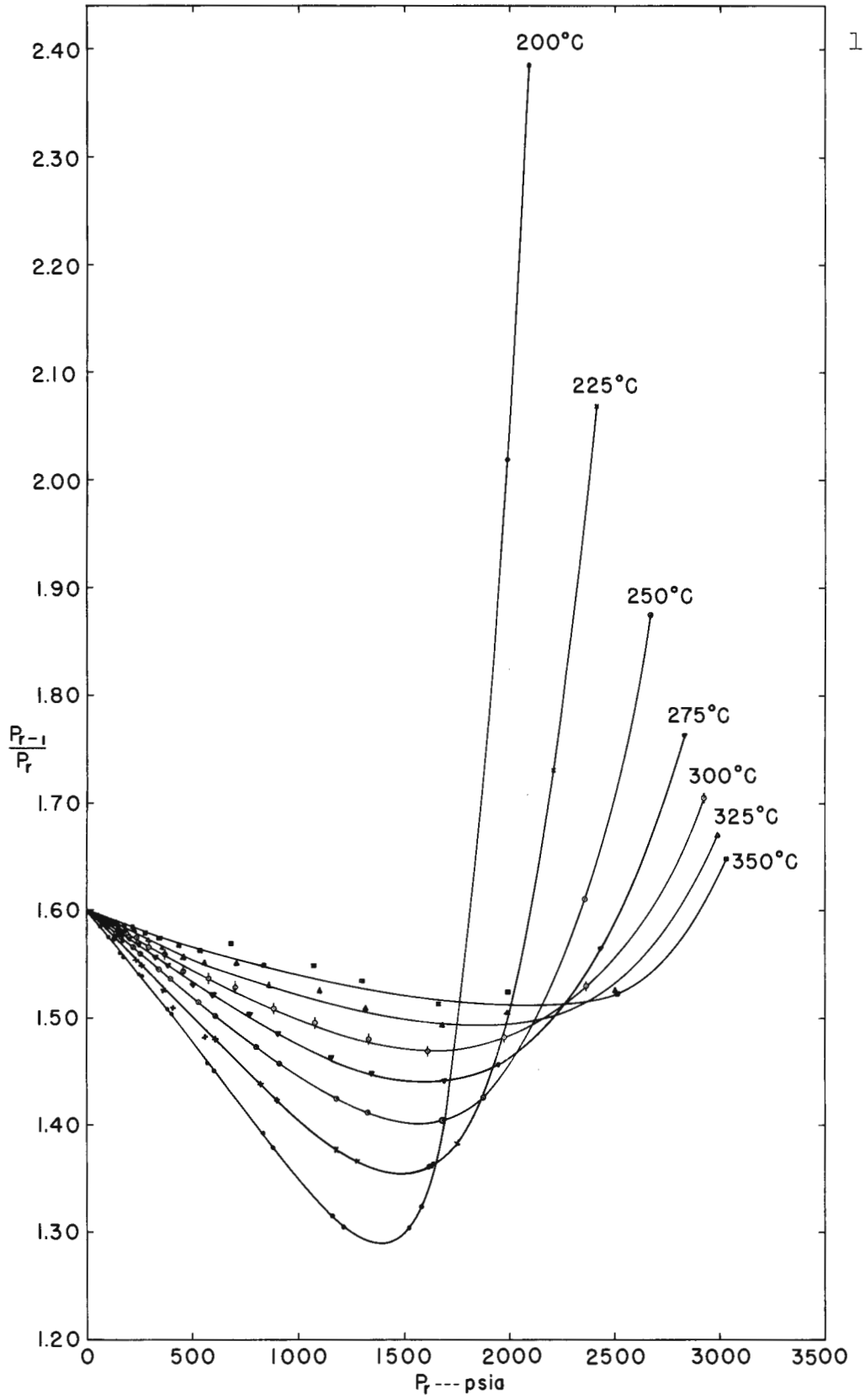

FIGURE 11. $\frac{P_r - 1}{P_r}$ vs P_r for Methyl Chloride

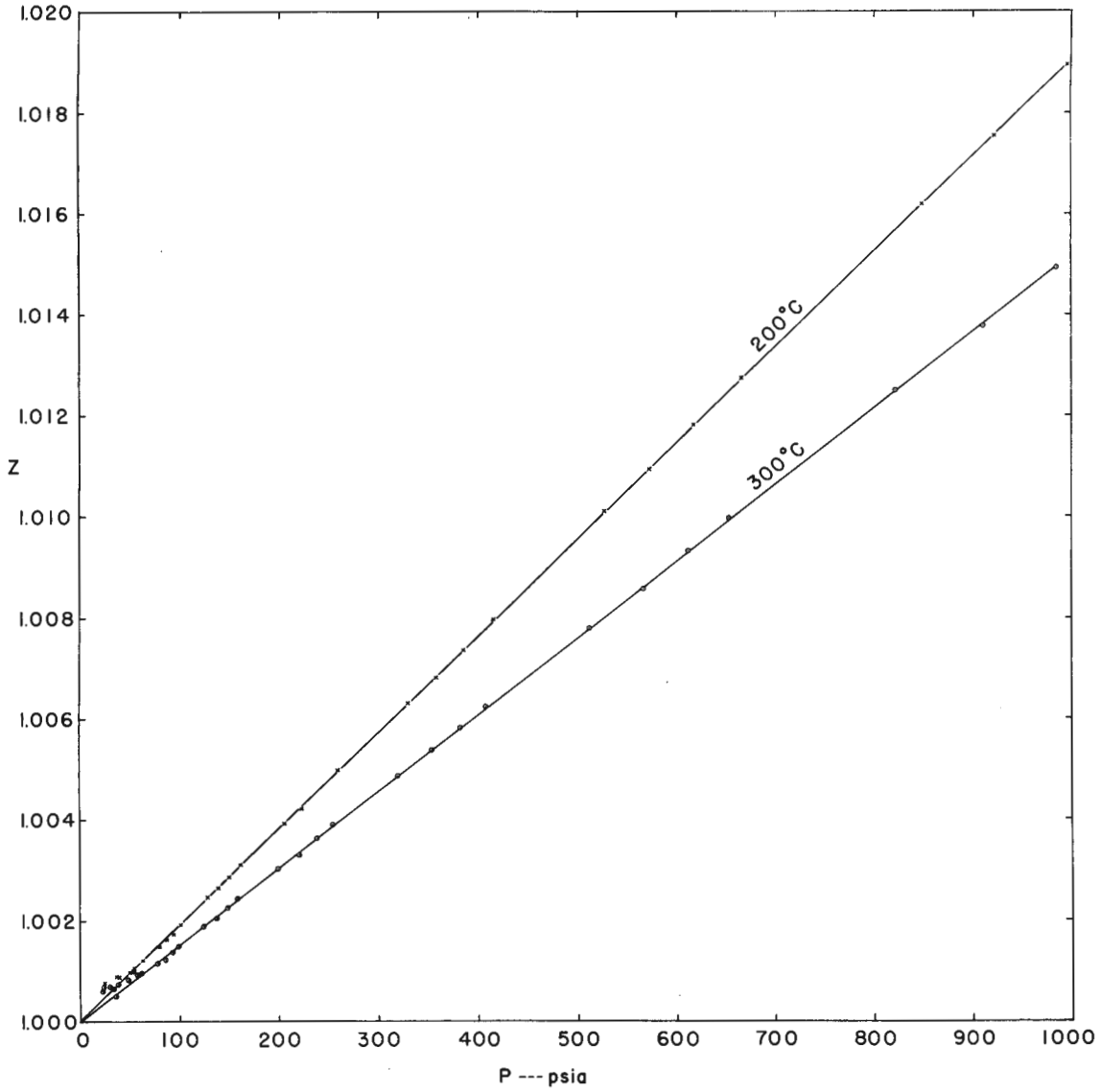

FIGURE 12. Compressibility Factor of Helium

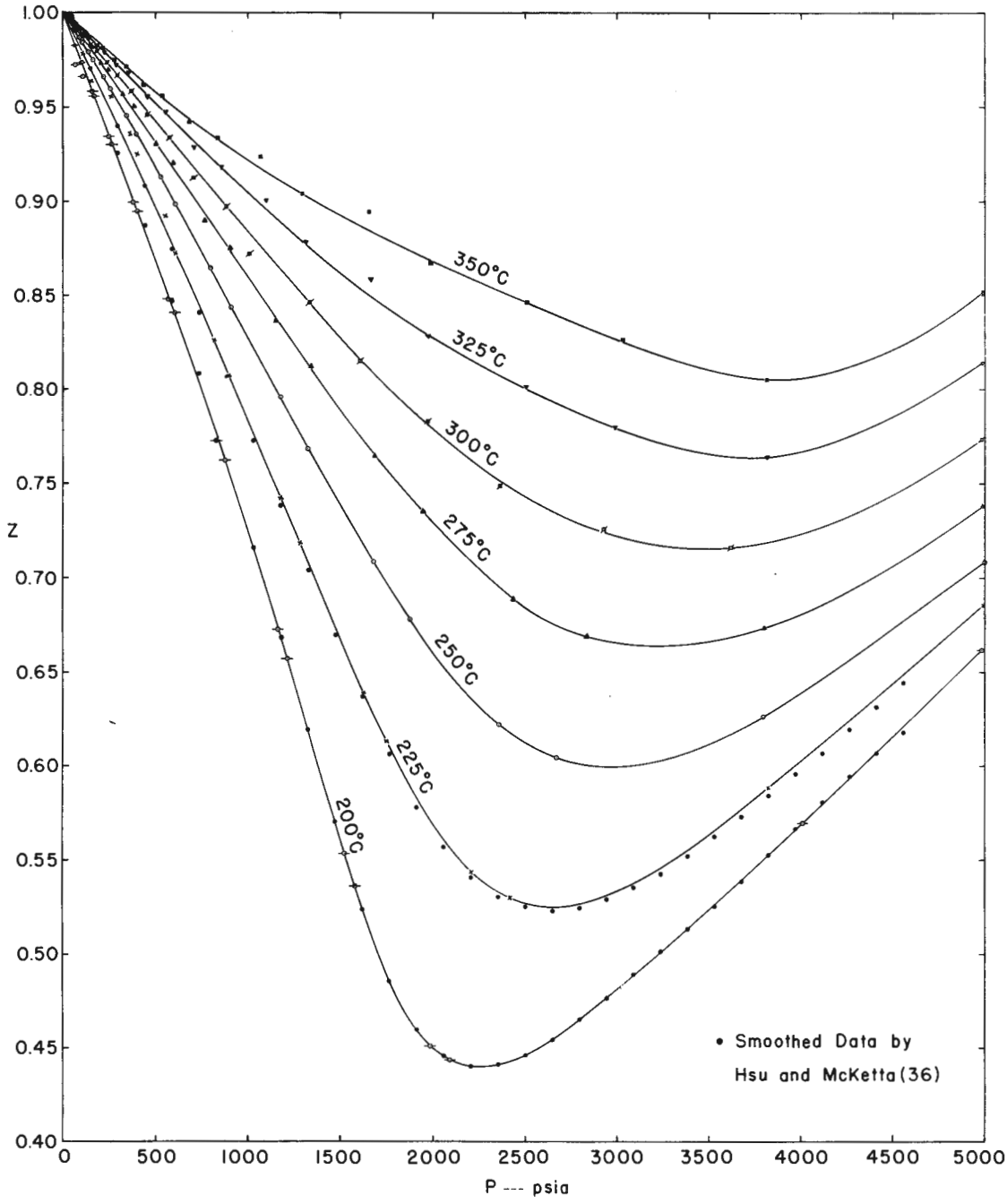

FIGURE 13. Compressibility Factor of Methyl Chloride

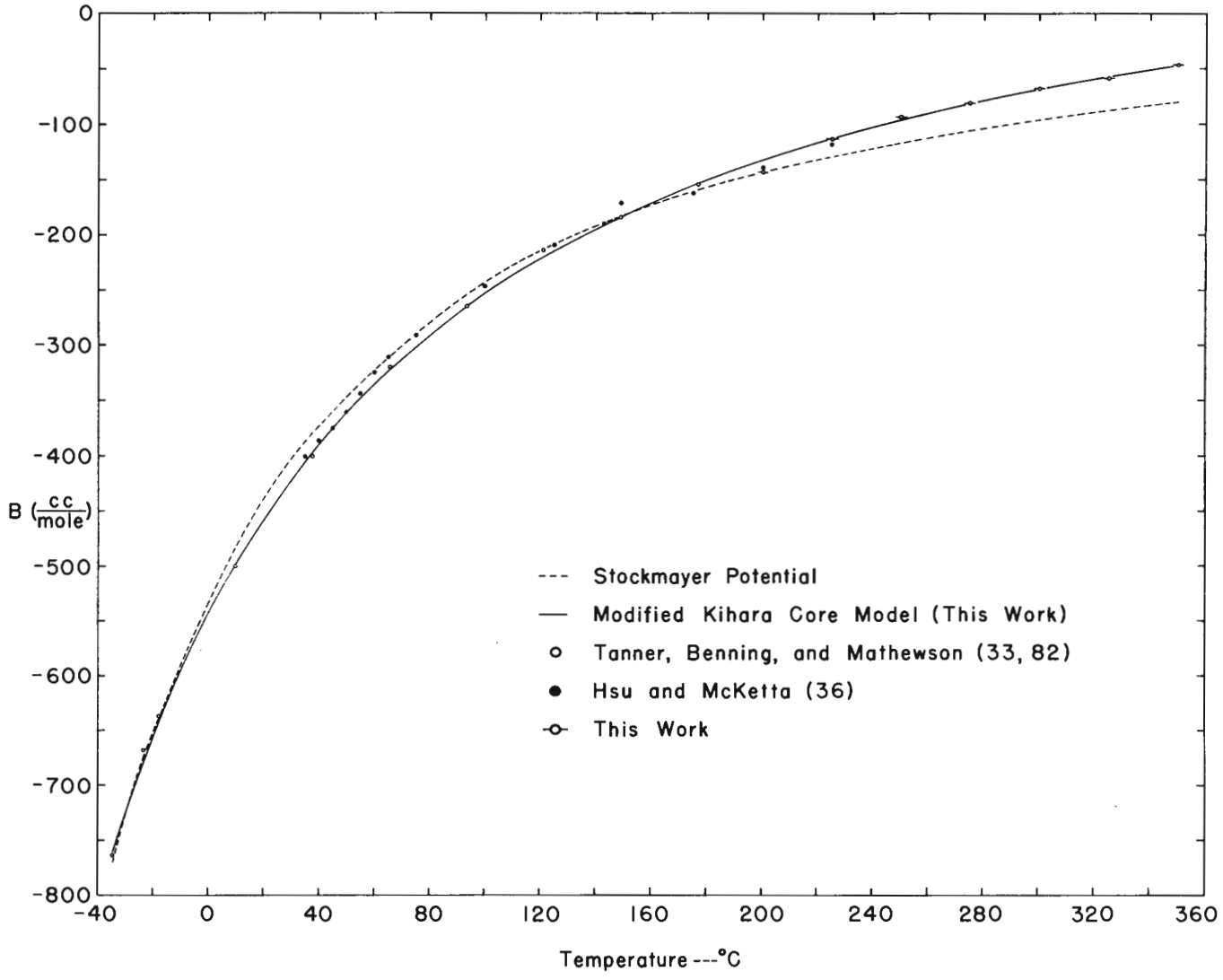

FIGURE 14. Second Virial Coefficients of Methyl Chloride

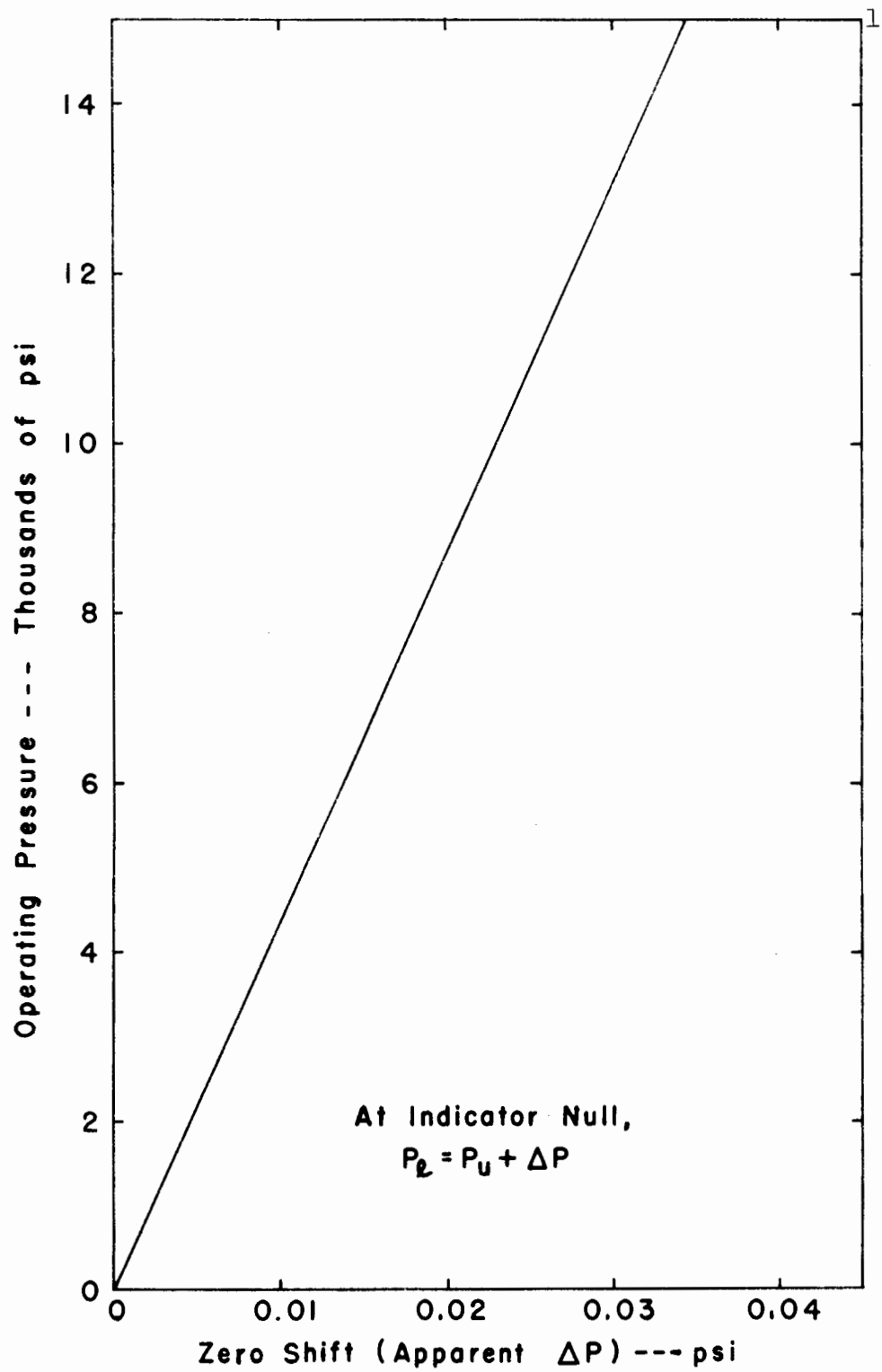

FIGURE 15. Zero Shift as a Function of Operating Pressure for Low Temperature DPI

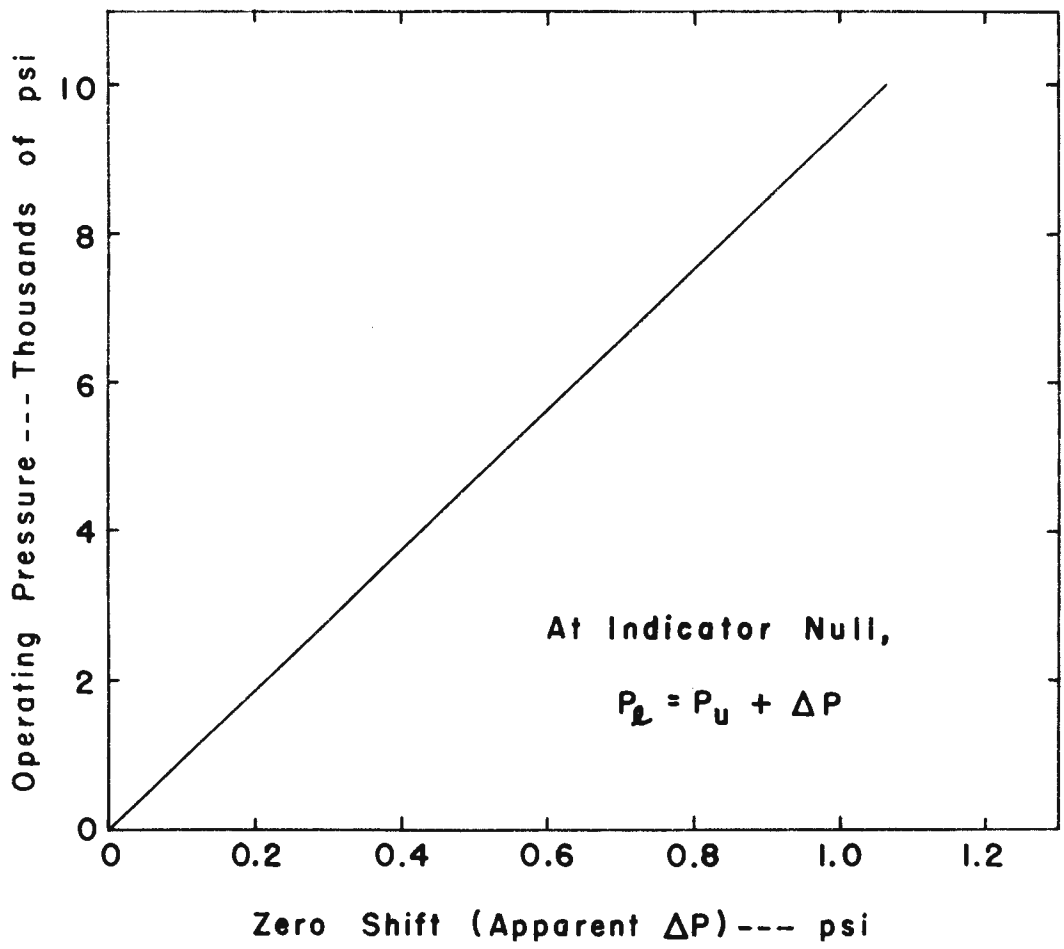

FIGURE 16. Zero Shift as a Function of Operating Pressure for High Temperature DPI

TABLE I

Calibration - Pressure Gage Weights

Serial No.: 12123

Source: Taken from the test report supplied by the Ruska Instrument Corporation

Designation			Apparent Mass vs Brass (M_A) Pounds
	High-range	Low-range	
Tare	30 psi	6 psi	0.78107
A	1000	200	26.03608
B	1000	200	26.03606
C	1000	200	26.03600
D	1000	200	26.03594
E	1000	200	26.03602
F	1000	200	26.03612
G	1000	200	26.03596
H	1000	200	26.03599
I	1000	200	26.03577
J	1000	200	26.03622
K	1000	200	26.03588
L	500	100	13.01828
M	200	40	5.20698
N	200	40	5.20709
O	100	20	2.60359
P	50	10	1.30182
Q	20	4	0.52074
R	20	4	0.52072
S	10	2	0.26038
T	5	1	0.13017
U	2	0.4	0.05210
V	2	0.4	0.05209
W	1	0.2	0.02605
X	0.5	0.1	0.01302

TABLE II

Helium Calibration Data

Temperature: 200°C

Run No.	r	P (psia)	P_{r-1}/P_r	$P_r \prod_{i=1}^{r} N(P_i, P_{i-1})$	P_o/Z_o	Z	$B \times 10^4$ (atm^{-1})
1	0	849.113	---	849.113		1.016184	
	1	527.590	1.609418	844.032		1.010103	
	2	328.544	1.605843	840.863		1.006310	
	3	204.874	1.603639	838.865	835.590	1.003919	2.8360
	4	127.874	1.602155	837.652		1.002468	
	5	79.851	1.601408	836.835		1.001489	
	6	49.886	1.600670	836.405		1.000976	
2	0	922.470	---	922.470		1.017544	
	1	572.873	1.610252	916.472		1.010928	
	2	356.632	1.606342	912.745		1.006816	
	3	222.345	1.603958	910.394	906.565	1.004223	2.8175
	4	138.763	1.602336	908.974		1.002657	
	5	86.646	1.601493	908.038		1.001625	
	6	54.129	1.600732	907.537		1.001072	

TABLE II (Continued)

Temperature: 200°C

Run No.	r	P (psia)	P_{r-1}/P_r	$P_r \prod_{i=1}^{r} N(P_i, P_{i-1})$	P_o/Z_o	Z	$Bx10^4$ (atm^{-1})
3	0	995.761	---	995.761		1.018942	
	1	618.077	1.611063	988.785		1.011803	
	2	384.649	1.606860	984.444		1.007361	
	3	239.768	1.604255	981.725	977.250	1.004579	2.8231
	4	149.616	1.602556	980.059		1.002874	
	5	93.413	1.601661	978.946		1.001736	
	6	58.353	1.600826	978.348		1.001124	
	7	36.466	1.600203	978.133		1.000903	
4	0	1074.313	---	1074.313		1.020458	
	1	666.467	1.611952	1066.193		1.012746	
	2	414.630	1.607378	1061.168		1.007973	
	3	258.400	1.604605	1058.005	1052.775	1.004968	2.8342
	4	161.217	1.602809	1056.042		1.003103	
	5	100.652	1.601727	1054.800		1.001923	
	6	62.869	1.600980	1054.053		1.001214	
	7	39.284	1.600372	1053.710		1.000888	
	8	24.552	1.600033	1053.591		1.000775	

TABLE II (Continued)

Temperature: 300°C

Run No.	r	P (psia)	P_{r-1}/P_r	$P_r \prod_{i=1}^{r} N(P_i, P_{i-1})$	P_o/Z_o	Z	$Bx10^4$ (atm^{-1})
5	0	822.577	---	822.577		1.012490	
	1	511.795	1.607239	818.764		1.007797	
	2	318.979	1.604479	816.384		1.004867	
	3	199.018	1.602765	814.889	812.430	1.003027	2.2497
	4	124.258	1.601651	813.967		1.001892	
	5	77.612	1.601015	813.372		1.001160	
	6	48.496	1.600379	813.103		1.000828	
	7	30.309	1.600053	813.000		1.000702	
6	0	911.207	---	911.207		1.013770	
	1	566.668	1.608009	906.546		1.008584	
	2	353.084	1.604910	903.665		1.005379	
	3	220.245	1.603142	901.796	898.830	1.003300	2.2443
	4	137.496	1.601828	900.676		1.002053	
	5	85.873	1.601155	899.938		1.001233	
	6	53.664	1.600198	899.742		1.001014	
	7	33.531	1.600429	899.416		1.000652	

TABLE II (Continued)

Temperature: 300°C

Run No.	r	P (psia)	P_{r-1}/P_r	$P_r \prod_{i=1}^{r} N(P_i, P_{i-1})$	P_o/Z_o	Z	$Bx10^4$ (atm^{-1})
7	0	985.327	---	985.327		1.014935	
	1	612.510	1.608671	979.879		1.009323	
	2	381.538	1.605371	976.483		1.005825	
	3	237.967	1.603323	974.352		1.003630	
	4	148.542	1.602018	973.025	970.828	1.002263	2.2528
	5	92.766	1.601255	972.167		1.001380	
	6	57.958	1.600573	971.727		1.000926	
	7	36.219	1.600210	971.509		1.000701	
	8	22.637	1.599991	971.424		1.000614	
8	0	1051.849	---	1051.849		1.015960	
	1	653.624	1.609257	1045.649		1.009972	
	2	407.055	1.605739	1041.784		1.006238	
	3	253.845	1.603557	1039.357		1.003895	
	4	158.440	1.602152	1037.854	1035.325	1.002443	2.2627
	5	98.942	1.601342	1036.882		1.001504	
	6	61.811	1.600718	1036.318		1.000959	
	7	38.627	1.600202	1036.090		1.000739	
	8	24.143	1.599925	1036.043		1.000693	

N_o at 200°C = 1.599866

N_o at 300°C = 1.599844

N_o av = 1.599855

TABLE III

Comparison of Second Virial Coefficients of Helium

T (°C)	Source	$10^4 B$ (atm^{-1})	B (cc/mole)
200	This work	2.8277	10.979
	Silberberg (79)	2.774	10.77
	Keesom (79)	2.60	10.10
	Otto (77,79)	2.851	11.07
	Schneider (77,79)	2.853	11.08
	Wiebe (77,79)	2.758	10.71
300	This work	2.2524	10.594
	Otto (77)	2.233	10.50
	Schneider (77)	2.288	10.76

TABLE IV

Experimental Methyl Chloride Data

Run No.	T (°C)	r	P (psia)	Z
9	200	0	4008.274	0.56952
		1	1985.278	0.45117
		2	1522.076	0.55336
		3	1156.874	0.67285
		4	830.489	0.77273
		5	569.603	0.84787
		6	377.693	0.89943
		7	245.253	0.93436
		8	157.228	0.95831
		9	99.826	0.97341
		10	62.988	0.98263
10	200	0	4985.086	0.66178
		1	2090.349	0.44379
		2	1578.540	0.53613
		3	1209.764	0.65731
		4	876.841	0.76217
		5	604.490	0.84059
		6	402.112	0.89457
		7	261.323	0.93007
		8	167.850	0.95573
		9	106.058	0.96613
		10	66.713	0.97225
11	225	0	3817.795	0.58850
		1	2206.097	0.54394
		2	1620.240	0.63907
		3	1176.817	0.74257
		4	818.449	0.82619
		5	552.432	0.89214
		6	362.167	0.93569
		7	233.133	0.96361
		8	147.848	0.97766
		9	93.088	0.98479
		10	58.088	0.98314

TABLE IV (Continued)

Run No.	T (°C)	r	P (psia)	Z
12	225	0	4992.622	0.68571
		1	2413.850	0.53022
		2	1745.766	0.61344
		3	1278.068	0.71844
		4	897.700	0.80729
		5	606.298	0.87226
		6	401.965	0.92516
		7	259.548	0.95570
		8	165.310	0.97382
		9	103.794	0.97820
		10	65.190	0.98291
13	250	0	4999.394	0.70828
		1	2667.229	0.60436
		2	1870.876	0.67813
		3	1325.198	0.76842
		4	909.424	0.84361
		5	605.376	0.89839
		6	394.062	0.93556
		7	252.696	0.95980
		8	160.453	0.97500
		9	101.265	0.98445
		10	63.663	0.99015
14	250	0	3791.274	0.62633
		1	2354.290	0.62212
		2	1676.121	0.70853
		3	1176.759	0.79578
		4	798.982	0.86438
		5	527.462	0.91290
		6	341.414	0.94533
		7	218.079	0.96603
		8	138.145	0.97901
		9	87.049	0.98695
		10	54.671	0.99167

TABLE IV (Continued)

Run No.	T(°C)	r	P (psia)	Z
15	275	0	4986.802	0.73791
		1	2828.276	0.66936
		2	1942.308	0.73534
		3	1341.389	0.81240
		4	903.247	0.87514
		5	593.661	0.92018
		6	383.250	0.95035
		7	244.430	0.96968
		8	154.657	0.98157
		9	97.378	0.98876
		10	61.129	0.99301
16	275	0	3799.283	0.67375
		1	2428.599	0.68890
		2	1685.353	0.76477
		3	1152.025	0.83628
		4	766.328	0.88994
		5	500.860	0.93053
		6	321.898	0.95676
		7	204.646	0.97311
		8	130.101	0.98972
		9	81.883	0.99656
		10	51.446	1.00171
17	300	0	4984.476	0.77363
		1	2923.196	0.72566
		2	1971.853	0.78303
		3	1332.305	0.84635
		4	882.926	0.89727
		5	574.453	0.93394
		6	368.473	0.95838
		7	233.999	0.97369
		8	147.687	0.98316
		9	92.892	0.98932
		10	58.390	0.99489

TABLE IV (Continued)

Run No.	T(°C)	r	P (psia)	Z
18	300	0	3614.517	0.71610
		1	2362.359	0.74865
		2	1607.917	0.81514
		3	1075.093	0.87190
		4	703.299	0.91247
		5	455.724	0.94591
		6	291.152	0.96680
		7	184.443	0.97984
		8	116.192	0.98752
		9	73.017	0.99282
		10	45.877	0.99798
19	325	0	4987.379	0.81411
		1	2986.230	0.77965
		2	1983.855	0.82853
		3	1314.656	0.87832
		4	859.140	0.91825
		5	553.996	0.94725
		6	353.942	0.96819
		7	223.742	0.97915
		8	140.936	0.98673
		9	88.588	0.99227
		10	55.631	0.99690
20	325	0	3816.353	0.76399
		1	2502.400	0.80131
		2	1675.795	0.85842
		3	1098.892	0.90049
		4	708.392	0.92866
		5	455.551	0.95540
		6	289.738	0.97213
		7	183.064	0.98265
		8	115.134	0.98873
		9	72.365	0.99421
		10	45.445	0.99889

TABLE IV (Continued)

Run No.	T(°C)	r	P (psia)	Z
21	350	0	4991.270	0.85175
		1	3028.632	0.82664
		2	1986.422	0.86729
		3	1294.311	0.90401
		4	835.504	0.93355
		5	534.745	0.95587
		6	339.738	0.97155
		7	214.479	0.98125
		8	134.970	0.98789
		9	84.842	0.99348
		10	53.280	0.99814
22	350	0	3816.069	0.80508
		1	2507.046	0.84604
		2	1656.985	0.89450
		3	1069.666	0.92375
		4	681.817	0.94196
		5	435.124	0.96171 →
		6	275.689	0.97482
		7	173.865	0.98354
		8	109.285	0.98904
		9	68.650	0.99397
		10	43.124	0.99892 →

TABLE V

Second Virial Coefficients of Methyl Chloride

-B (cc/mole)

T (°C)	Experimental Data Source			Stockmayer Potential Model Source	Modified Kinara Core Model
	(33)	(36)**	This work	(72)	This work
-34.45	764			770	760.6
-23.34	668			675	678.6
-17.78	637			640	642.5
10	500			482	498.7
35		401			406.0
37.78	401			380	397.2
40		387			390.4
45		376			375.6
50		361			361.6
55		344			348.3
60		325			335.7
65		311			323.6
65.55	320			310	322.3
75		291			301.2
93.33	265			260	265.0
100		247			253.3
121.11	214			210	220.0
125		209			214.4
143.1		190			190.7
148.89	184			185	183.7
150		172			182.4
175		163			155.6
176.66	155			160	154.0
200		140	144.2	146*	132.8
225		119	113.7	130*	113.3
250			93.62	117*	96.37
275			81.19	106*	81.57
300			68.50	96.4*	68.53
325			58.71	88.0*	56.97
350			47.05	80.3*	46.65

TABLE V (Continued)

* The values were calculated using the potential parameters reported in the reference.

** The values were obtained graphically from the p-v-T data reported by Hsu and McKetta (36).

Note: Potential parameters for the Stockmayer potential and the modified Kihara core model were determined from the observed second virial coefficients reported by Hirshfelder (33).

TABLE VI

Potential Parameters for the Modified Kihara Potential

Substance	Homo-morph	Core	μ (debye)	M_o (Å)	S_o (Å^2)	V_o (Å^3)
CCl_2F_2	--	Tetrahedron	0.51	16.450	14.267	2.786
$CHCl_2F$	--	Tetrahedron	1.29	0.160	0.00135	0.00000254
$CHCl_3$	--	Triangular Prism	1.05	15.325	12.067	2.0437
	$CH(CH_3)_3$	Triangular Prism		13.427	9.2607	1.3732
C_2H_5Cl	--	Pentagon	2.02	11.891	7.3145	0
	--	Rectangle		9.965	3.8822	0
CH_3Cl	--	Triangular Prism	1.89	10.3217	5.9107	0.6739
	C_2H_6	Triangular Prism		10.170	5.7700	0.653
	--	Rectangle		9.349	4.0142	0
	C_2H_4	Rectangle		8.800	3.4800	0
CH_3COCH_3	--	Pentagon	2.74	41.14	89.02	0
CH_3OH	--	Tetrahedron	1.66	0.160	0.00135	0.00000254
	--	Tetrahedron		0.640	0.0216	0.00016
CH_3F	--	Tetrahedron	1.82	5.120	1.380	0.084
NH_3	--	Triangular Prism	1.47	7.2257	2.8235	0.2547

TABLE VI (Continued)

Substance	Homo-morph	Core	t'	ρ'_o (Å)	U'_o/k (^oK)	Ref. for B(T) Data
CCl_2F_2	--	Tetrahedron	0.04383636	3.1076476	506.31	33
$CHCl_2F$	--	Tetrahedron	0.07123908	5.381482	383.85	32.33
$CHCl_3$	--	Triangular Prism	0.15441743	2.7406551	888.23	
	$CH(CH_3)_3$	Triangular Prism	0.14372497	2.7860481	908.42	72
C_2H_5Cl	--	Pentagon	0.2165	5.0745293	369.37	
	--	Rectangle	0.18914748	5.4117626	348.57	72
CH_3Cl	--	Triangular Prism	0.45235695	3.7967296	369.50	33
	C_2H_6	Triangular Prism	0.47062109	3.7414776	371.13	
	--	Rectangle	0.51424595	3.6302060	371.85	
	C_2H_4	Rectangle	0.561	3.525	372.30	
CH_3COCH_3	--	Pentagon	0.6522573	3.91	493.13	72
CH_3OH	--	Tetrahedron	0.490	2.490	932.89	72
	--	Tetrahedron	0.782344	2.2176561	827.07	
CH_3F	--	Tetrahedron	0.97553338	3.4054665	220.18	53
NH_3	--	Triangular Prism	1.1433785	2.4890202	313.88	33

TABLE VII

The Second Virial Coefficients (ml./mole)

Model I--Present Work, and Model II--(12,6,3) Stockmayer Potential

CCl_2F_2

(I) Tetrahedron Connecting 4 Cl's

T(°C)	-B(exp.)	-B(calc.)	$\frac{B_{exp} - B_{calc}}{B_{exp}} \times 100$
-34.45	637	651.67	-2.30
-28.89	604	616.70	-2.10
-23.34	586	584.50	0.25
-17.78	560	554.67	0.95
10.00	454	434.17	4.36
37.78	347	347.20	-0.05
			Av. = 1.67

TABLE VII (Continued)

$CHCl_2F$

(I) Tetrahedron Connecting Points at 1/64 of C-H Distance				(II)	
T(°C)	-B(exp.)	-B(calc.)	$\frac{B_{exp}- B_{calc}}{B_{exp}}$ x 100	-B(calc.)	$\frac{B_{exp}-B_{calc}}{B_{exp}}$ x 100
-34.45	766	839.74	-9.62	838	-9.40
-23.34	734	722.64	-5.26	769	-4.77
10.00	616	617.08	-0.17	616	0.0
37.78	528	523.16	0.91	522	1.14
65.55	446	450.28	-0.95	448	-0.45
93.33	403	392.10	2.70	393	2.48
121.11	354	344.65	2.63	345	2.54
148.89	310	305.23	1.53	305	1.61
176.66	271	271.99	-0.36	271	0.0
			Av.= 2.68		Av.= 2.38

TABLE VII (Continued)

$CHCl_3$

(I) Triangular Prism Core Formed by C and 3 Cl's

T(°C)	50	70	90	110	
-B(exp.)	1000	840	730	630	
-B(calc.)	995.23	842.83	724.10	629.51	
$\frac{B_{exp} - B_{calc}}{B_{exp}} \times 100$	0.47	-0.33	0.80	0.07	Av. = 0.42

(I) Triangular Prism Core of Homomorph, $CH(CH_3)_3$, Formed by 4C's

-B(calc.)	995.00	842.62	724.31	630.31	
$\frac{B_{exp} - B_{calc}}{B_{exp}} \times 100$	0.49	-0.31	0.77	-0.04	Av. = 0.41
(II) -B(calc.)	1010	850	730	630	
$\frac{B_{exp} - B_{calc}}{B_{exp}} \times 100$	-1.00	-1.19	0.0	0.0	Av. = 0.55

TABLE VII (Continued)

C_2H_5Cl

(I) Pentagon Core Formed by Points Midway between C-H Distance

T(°C)	50	70	90	110	130	
-B(exp.)	580	510	450	390	350	
-B(calc.)	582.79	508.73	446.17	392.67	346.43	
$\frac{B_{exp} - B_{calc}}{B_{exp}} \times 100$	-0.48	0.24	0.85	-0.68	1.01	Av. = 0.65

(I) Rectangular Core Formed by Points Midway between C-H Distance

-B(calc.)	579.19	508.28	448.08	396.37	351.50	
$\frac{B_{exp} - B_{calc}}{B_{exp}} \times 100$	0.13	0.33	0.42	-1.63	-0.43	Av. = 0.59
(II) -B(calc.)	560	500	450	410	370	
$\frac{B_{exp} - B_{calc}}{B_{exp}} \times 100$	3.45	1.96	0.0	-5.13	-5.71	Av. = 3.25

TABLE VII (Continued)

CH_3Cl

(I) Triangular Prism Core Formed by Midpoints of C-H and Cl				(I) Triangular Prism Core of Homomorph, C_2H_6, Formed by Midpoints of C-H	
T(°C)	-B(exp.)	-B(calc.)	$\frac{B_{exp} - B_{calc}}{B_{exp}} \times 100$	-B(calc.)	$\frac{B_{exp} - B_{calc}}{B_{exp}} \times 100$
-34.45	764	760.56	0.45	763.29	0.09
-23.34	668	678.61	-1.58	680.38	-1.85
-17.78	637	642.51	-0.86	643.90	-1.08
10.00	500	498.71	0.25	498.91	0.21
37.78	401	397.22	0.94	396.93	1.01
65.55	320	322.32	-0.72	321.88	-0.59
93.33	265	265.03	-0.01	264.63	0.13
121.11	214	219.97	-2.79	219.69	-2.66
148.89	184	183.70	0.16	183.60	0.21
176.66	155	153.95	0.67	154.04	0.61
			Av. = 0.84		Av. = 0.84

TABLE VII (Continued)

CH_3Cl

(I) Rectangular Core Formed by Midpoints of C-H and Cl.			(I) Rectangular Core of Homomorph, C_2H_4, Formed by Midpoints of C-H		(II)	
T(°C)	-B(calc.)	$\frac{B_{exp} - B_{calc}}{B_{exp}}$ x 100	-B(calc.)	$\frac{B_{exp} - B_{calc}}{B_{exp}}$ x 100	-B(calc.)	$\frac{B_{exp} - B_{calc}}{B_{exp}}$ x 100
-34.45	757.86	0.80	761.24	0.36	770	-0.79
-23.34	674.56	-0.98	676.32	-1.24	675	-1.05
-17.78	638.00	-0.15	639.13	-0.33	640	-0.47
10.00	493.34	1.33	492.57	1.48	482	3.60
37.78	392.32	2.16	390.86	2.52	380	5.24
65.55	318.46	0.47	316.93	0.95	310	3.13
93.33	262.42	0.97	261.12	1.46	260	1.89
121.11	218.66	-2.18	217.74	-1.75	210	1.87
148.89	183.67	0.17	183.19	0.43	185	-0.54
176.66	155.14	-0.09	155.13	-0.08	160	-3.23
		Av. = 0.93		Av. = 1.06		Av. = -2.18

TABLE VII (Continued)

CH_3COCH_3

(I) Pentagon Core Formed by 6H's and O (each length is increased by a factor of 2.25)

$T(^{\circ}C)$		30	50	70	90	110	130	
$-B(exp.)$		1860	1560	1280	1040	850	700	
$-B(calc.)$		1902.89	1549.38	1268.53	1040.92	853.29	696.34	
$\frac{B_{exp} - B_{calc}}{B_{exp}}$	x 100	-2.30	0.68	0.89	-0.08	-0.38	0.52	Av. = 0.81
(II) $-B(calc.)$		1900	1530	1230	1010	850	730	
$\frac{B_{exp} - B_{calc}}{B_{exp}}$	x 100	-2.15	1.92	3.91	2.88	0.0	-4.29	Av. = 2.53

TABLE VII (Continued)

CH_3OH

(I) Tetrahedron Core Formed by Points at 1/16 of C-H Distance

T(°C)	60	80	100	120	
-B(exp.)	1220	1000	790	620	
-B(calc.)	1177.04	952.43	785.63	658.76	
$\frac{B_{exp} - B_{calc}}{B_{exp}} \times 100$	3.52	4.75	0.55	-6.25	Av. = 3.77

(I) Tetrahedron Core Formed by Points at 1/64 of C-H Distance

-B(calc.)	1187.60	954.70	783.87	655.26	
$\frac{B_{exp} - B_{calc}}{B_{exp}} \times 100$	2.65	4.52	0.77	-5.68	Av. = 3.41

(II) -B(calc.)	1270	980	760	590	
$\frac{B_{exp} - B_{calc}}{B_{exp}} \times 100$	-4.10	2.00	3.80	4.84	Av. = 3.69

TABLE VII (Continued)

CH_3F

(I) Tetrahedron Core Connecting Midpoints of C-H				(II)	
T(°C)	-B(exp.)	-B(calc.)	$\frac{B_{exp} - B_{calc}}{B_{exp}} \times 100$	-B(calc.)	$\frac{B_{exp} - B_{calc}}{B_{exp}} \times 100$
0	259.99	263.18	-1.23	265.66	-2.18
24.61	209.47	213.36	-1.85	210.37	-0.43
49.60	171.22	174.99	-2.20	170.93	0.17
74.76	142.71	144.98	-1.59	141.77	0.66
99.62	120.97	121.39	-0.35	119.18	1.48
124.49	102.86	102.24	0.59	101.54	1.28
149.55	87.30	86.34	1.09	87.11	0.22
			Av. = 1.27		Av. = 0.92

TABLE VII (Continued)

NH_3

(I) Triangular Prism Core formed by 3H's and N (each length is reduced by a factor of 0.80)

T(°C)	-B(exp.)	-B(calc.)	$\frac{B_{exp} - B_{calc}}{B_{exp}} \times 100$
0	345	325.48	5.65
25	261	259.06	0.74
50	209	210.49	-0.71
100	142	145.37	-2.37
150	101	104.59	-3.56
200	75	77.17	-2.89
250	58	57.71	0.48
300	44	43.34	1.49
			Av. = 2.24

TABLE VIII

Comparison of Second Virial Coefficients

Substance	Average % Deviation between Experimental and Calculated B(T)		Curvature of Calculated B(T) Curve Compared with that of Experimental B(T) Curve	
	This Work	Stockmayer Potential (12-6-3)	This Work	Stockmayer Potential (12-6-3)
$CHCl_2F$	2.68 %	2.38 %	greater	greater
$CHCl_3$	0.41	0.55	same	same
C_2H_5Cl	0.59	3.25	same	smaller
CH_3Cl	0.84	2.18	same	greater
CH_3COCH_3	0.81	2.53	greater	smaller
CH_3OH	3.41	3.69	smaller	greater
CH_3F	1.27	0.92	greater	greater

TABLE IX

Comparison of Potential Parameters between

Stockmayer Potential and This Work

Substance	$\frac{t - t'}{t}$ x 100	$\frac{r_o - \rho'_o}{r_o}$ x 100	$\frac{(U_o/k) - (U'_o/k)}{(U_o/k)}$ x 100	Shape of Potential "well" Compared with that of Stockmayer Potential
$CHCl_2F$	29	-1	-1	shallower
$CHCl_3$	-54	17	16	steeper and narrower
C_2H_5Cl [a]	-8	6	-15	steeper and narrower
C_2H_5Cl [b]	5	-0.04	-9	steeper
CH_3Cl [c]	25	-5	3	shallower and wider
CH_3Cl [b]	14	-1	2	shallower
CH_3COCH_3	7	0	5	shallower
CH_3OH	2	11	-31	steeper and narrower
CH_3F	9	1	-6	shallower
NH_3	-14	6	2	steeper and narrower

a: Pentagon Core b: Rectangular Core c: Triangular Prism Core

TABLE X

Comparison of Thermodynamic Properties

T (°C)	P (atm)	$(f/P)_{pot.fun.}^{*} = a$	$(f/P)_{p\text{-}v\text{-}T}^{**} = b$	$\frac{b - a}{b} \times 100$ (%)
35	3	0.95297	0.9528	-0.02
	6	0.90816	0.9063	-0.20
40	3	0.95544	0.9564	0.10
	6	0.91287	0.9127	-0.02
45	3	0.95775	0.9568	-0.10
	6	0.91729	0.9149	-0.26
	9	0.87853	0.8740	-0.52
50	3	0.95991	0.9596	-0.03
	6	0.92143	0.9202	-0.13
	9	0.88449	0.8815	-0.34
55	3	0.96194	0.9621	0.02
	6	0.92532	0.9250	-0.03
	9	0.89010	0.8885	-0.18
	12	0.85622	0.8521	-0.48
60	6	0.92898	0.9297	0.08
	12	0.86300	0.8610	-0.23
65	6	0.93241	0.9336	0.13
	12	0.86940	0.8685	-0.10
75	6	0.93870	0.9363	-0.26
	12	0.88116	0.8780	-0.36
	18	0.82715	0.8196	-0.92
100	3	0.97549	0.9758	0.03
	12	0.90551	0.9050	-0.06
	21	0.84055	0.8359	-0.56
	30	0.78026	0.7675	-1.66
125	15	0.90624	0.9046	-0.18
	30	0.82127	0.8139	-0.91
	45	0.74427	0.7234	-2.89
143.1 (T_c)	15	0.91968	0.9183	-0.15
	30	0.84581	0.8401	-0.68
	120	0.51178	0.4108	-24.58
	150	0.43287	0.3512	-23.25
	240	0.26192	0.2642	0.86
	255	0.24088	0.2563	6.02
	300	0.18737	0.2381	21.30

TABLE X (Continued)

T (°C)	P (atm)	$(f/P)_{pot.fun.} = a$	$(f/P)_{p\text{-}v\text{-}T} = b$	$\frac{b - a}{b} \times 100$ (%)
150	15	0.92423	0.9229	-0.14
	30	0.85419	0.8469	-0.86
	120	0.53238	0.4374	-21.72
	150	0.45476	0.3748	-21.33
	225	0.30667	0.2932	-4.59
	240	0.28343	0.2835	0.02
	255	0.26196	0.2750	4.74
	300	0.20681	0.2556	19.09
175	15	0.93851	0.9351	-0.36
	30	0.88080	0.8734	-0.85
	120	0.60188	0.5368	-12.12
	150	0.53013	0.4645	-14.13
	225	0.38599	0.3667	-5.26
	240	0.36226	0.3548	-2.10
	255	0.33998	0.3444	1.28
	300	0.28104	0.3203	12.26
200	15	0.94998	0.9466	-0.36
	30	0.90246	0.8952	-0.81
	120	0.66330	0.6195	-7.07
	150	0.59860	0.5487	-9.09
	225	0.46313	0.4414	-4.92
	240	0.43996	0.4278	-2.84
	255	0.41795	0.4160	-0.47
	300	0.35832	0.3883	7.72
225	15	0.95928	0.9566	-0.28
	30	0.92021	0.9142	-0.66
	120	0.71706	0.6807	-5.34
	150	0.65985	0.6185	-6.69
	225	0.53600	0.5113	-4.83
	240	0.51417	0.4968	-3.50
	255	0.49323	0.4841	-1.89
	300	0.43540	0.4539	4.08

TABLE X (Continued)

T (°F)	P (psi)	$H^{*}_{pot.fun.} = a$ (Btu/lb)	$H^{**}_{p\text{-}v\text{-}T} = b$ (Btu/lb)	$\frac{b-a}{b} \times 100$ (%)	$S^{*}_{pot.fun.} = a$ (Btu/lb.°R)	$S^{**}_{p\text{-}v\text{-}T} = b$ (Btu/lb.°R)	$\frac{b-a}{b} \times 100$ (%)
300	50	254.4	258.7	1.66	0.4894	0.4953	1.19
	500	199.3	238.9	16.6	0.3326	0.3850	13.6
	1000	138.0	195.8	29.5	0.2318	0.3088	24.9
	2000	15.5	131.0	88.2	0.0574	0.2131	73.1
420	50	283.9	289.0	1.76	0.5262	0.5323	1.15
	500	227.8	278.5	18.2	0.3754	0.4335	13.4
	1000	165.5	267.9	38.2	0.2813	0.3992	29.5
	2000	40.8	224.4	81.8	0.1203	0.3307	63.6

* Thermodynamic properties calculated from the second virial coefficients for the modified Kihara Potential.

** Thermodynamic properties calculated from the experimental p-v-T data reported by Hsu and McKetta (37).

TABLE XI

Z	$dF_1(Z)/dZ$	$dF_2(Z)/dZ$	$dF_3(Z)/dZ$	$H_6(y)$	$dH_6(y)/dy$
0.01	44.423159E-01*	57.484286E-01	51.271910E-01	13.915138E-03	24.861678E-02
0.10	-23.289895E-03	-39.011743E-02	-12.433926E-01	93.126111E-02	55.645712E-01
0.20	-27.456449E-02	-79.474501E-02	-17.413111E-01	35.410747E-01	15.614092E+00
0.30	-37.188159E-02	-96.623982E-02	-19.746891E-01	79.924070E-01	29.886049E+00
0.40	-43.493014E-02	-10.852960E-01	-21.484209E-01	14.554443E+00	48.843775E+00
0.50	-48.671357E-02	-11.877141E-01	-23.043851E-01	23.558380E+00	73.186269E+00
0.60	-53.474962E-02	-12.854719E-01	-24.569403E-01	35.395565E+00	10.379814E+01
0.70	-58.229171E-02	-13.838843E-01	-26.126707E-01	50.522607E+00	14.174773E+01
0.80	-63.106796E-02	-14.858639E-01	-27.752765E-01	69.469338E+00	18.830261E+01
0.90	-68.216667E-02	-15.933135E-01	-29.472885E-01	92.847258E+00	24.495395E+01
1.00	-73.636849E-02	-17.076541E-01	-31.307143E-01	12.136175E+01	31.344259E+01
1.10	-79.432131E-02	-18.301056E-01	-33.272674E-01	15.582558E+01	39.579853E+01
1.20	-85.661334E-02	-19.618056E-01	-35.386191E-01	19.717075E+01	49.438331E+01
1.30	-92.379835E-02	-21.038509E-01	-37.664574E-01	24.646846E+01	61.192889E+01
1.40	-99.644549E-02	-22.573811E-01	-40.124673E-01	30.494803E+01	75.160329E+01
1.50	-10.751478E-01	-24.235847E-01	-42.784787E-01	37.401424E+01	91.706733E+01
1.60	-11.605199E-01	-26.037433E-01	-45.664306E-01	45.527754E+01	11.125566E+02
1.70	-12.532304E-01	-27.991910E-01	-48.784558E-01	55.057837E+01	13.429355E+02
1.80	-13.539965E-01	-30.114060E-01	-52.167603E-01	66.202370E+01	16.138235E+02
1.90	-14.636054E-01	-32.419833E-01	-55.838292E-01	79.200890E+01	19.316963E+02
2.00	-15.828910E-01	-34.926845E-01	-59.823801E-01	94.327574E+01	23.039715E+02
2.10	-17.127805E-01	-37.653646E-01	-64.152868E-01	11.189459E+02	27.391927E+02
2.20	-18.542821E-01	-40.621074E-01	-68.857670E-01	13.225853E+02	32.471572E+02
2.30	-20.085091E-01	-43.851729E-01	-73.973125E-01	15.582356E+02	38.391387E+02
2.40	-21.766478E-01	-47.370692E-01	-79.537413E-01	18.305105E+02	45.279840E+02
2.50	-23.600248E-01	-51.204495E-01	-85.593099E-01	21.446511E+02	53.284588E+02
2.60	-25.600848E-01	-55.382989E-01	-92.184759E-01	25.066329E+02	62.574520E+02
2.70	-27.784263E-01	-59.938635E-01	-99.362970E-01	29.232041E+02	73.343344E+02
2.80	-30.167585E-01	-64.907434E-01	-10.718314E+00	34.020599E+02	85.811096E+02
2.90	-32.769929E-01	-70.327663E-01	-11.570454E+00	39.519271E+02	10.023035E+03

TABLE XI (Continued)

Z	$dF_1(Z)/dZ$	$dF_2(Z)/dZ$	$dF_3(Z)/dZ$	$H_6(y)$	$dH_6(y)/dy$
3.00	-35.612135E-01	-76.242315E-01	-12.499339E+00	45.827235E+02	11.688899E+03
3.10	-38.717062E-01	-82.698235E-01	-13.512185E+00	53.056364E+02	13.611654E+03
3.20	-42.110054E-01	-89.747260E-01	-14.616896E+00	61.334043E+02	15.828668E+03
3.30	-45.818140E-01	-97.444816E-01	-15.822240E+00	70.804268E+02	18.382688E+03
3.40	-49.871675E-01	-10.585299E+00	-17.137563E+00	81.630280E+02	21.322398E+03
3.50	-54.303730E-01	-11.503949E+00	-18.573343E+00	93.997387E+02	24.703211E+03
3.60	-59.150974E-01	-12.507859E+00	-20.141012E+00	10.811350E+03	28.588402E+03
3.70	-64.452675E-01	-13.605268E+00	-21.853222E+00	12.421554E+03	33.049428E+03
3.80	-70.252769E-01	-14.804958E+00	-23.723502E+00	14.257147E+03	38.168040E+03
3.90	-76.599551E-01	-16.116807E+00	-25.767021E+00	16.348253E+03	44.037225E+03
4.00	-83.545226E-01	-17.551644E+00	-28.000314E+00	18.729036E+03	50.762059E+03
4.10	-91.147807E-01	-19.121158E+00	-30.441647E+00	21.438048E+03	58.462336E+03
4.20	-99.470793E-01	-20.838380E+00	-33.110715E+00	24.518906E+03	67.274224E+03
4.30	-10.858373E+00	-22.717516E+00	-36.029444E+00	28.020797E+03	77.351701E+03
4.40	-11.856377E+00	-24.774196E+00	-39.221793E+00	31.999073E+03	88.870412E+03
4.50	-12.949414E+00	-27.025666E+00	-42.714058E+00	36.516353E+03	10.202796E+04
4.60	-14.146746E+00	-29.490592E+00	-46.535381E+00	41.643280E+03	11.704996E+04
4.70	-15.458499E+00	-32.189695E+00	-50.717029E+00	47.459400E+03	13.419129E+04
4.80	-16.895810E+00	-35.145681E+00	-55.293973E+00	54.054682E+03	15.374089E+04
4.90	-18.470968E+00	-38.383470E+00	-60.304405E+00	61.529832E+03	17.602679E+04
5.00	-20.197288E+00	-41.930614E+00	-65.790240E+00	69.999045E+03	20.141848E+04
5.10	-22.089573E+00	-45.816875E+00	-71.797896E+00	79.590512E+03	23.033562E+04
5.20	-24.164036E+00	-50.075415E+00	-78.377359E+00	90.448754E+03	26.325291E+04
5.30	-26.438480E+00	-54.742498E+00	-85.584394E+00	10.273690E+04	30.070736E+04
5.40	-28.932462E+00	-59.857950E+00	-93.479975E+00	11.663753E+04	34.330796E+04
5.50	-31.667640E+00	-65.465834E+00	-10.213104E+01	13.235667E+04	39.173779E+04
5.60	-34.667389E+00	-71.613800E+00	-11.161177E+01	15.012647E+04	44.677463E+04
5.70	-37.957784E+00	-78.354895E+00	-12.200215E+01	17.020777E+04	50.929570E+04
5.80	-41.567374E+00	-85.747173E+00	-13.339132E+01	19.289473E+04	58.029172E+04
5.90	-45.527468E+00	-93.854393E+00	-14.587675E+01	21.851540E+04	66.088030E+04

TABLE XI (Continued)

Z	$dF_1(Z)/dZ$	$dF_2(Z)/dZ$	$dF_3(Z)/dZ$	$H_6(y)$	$dH_6(y)/dy$
6.00	-49.872574E+00	-10.274664E+01	-15.956569E+01	24.744168E+04	75.232649E+04
6.10	-54.640568E+00	-11.250110E+01	-17.457592E+01	28.009001E+04	85.605595E+04
6.20	-59.873101E+00	-12.320237E+01	-19.103668E+01	31.692820E+04	97.367675E+04
6.30	-65.615970E+00	-13.494360E+01	-20.909040E+01	35.848321E+04	11.070071E+05
6.40	-71.919424E+00	-14.782701E+01	-22.889306E+01	40.534558E+04	12.580965E+05
6.50	-78.838897E+00	-16.196502E+01	-25.061665E+01	45.817894E+04	14.292550E+05
6.60	-86.435149E+00	-17.748137E+01	-27.444976E+01	51.772835E+04	16.230874E+05
6.70	-94.775065E+00	-19.451183E+01	-30.059978E+01	58.483089E+04	18.425325E+05
6.80	-10.393209E+01	-21.320577E+01	-32.929472E+01	66.042665E+04	20.909050E+05
6.90	-11.398719E+01	-23.372741E+01	-36.078515E+01	74.556840E+04	23.719311E+05
7.00	-12.502917E+01	-25.625716E+01	-39.534651E+01	84.144011E+04	26.898175E+05

* 44.423159E-01 = 44.423159×10^{-1}

TABLE XII

Thermodynamic Properties of Methyl Chloride for the Modified Kihara Potential

$T(^{\circ}C)$	$P_{(atm)}$	f/P	$(U^*- U)/RT_c$	$(H^*- H)/RT_c$	$(S^*- S)/R$
-40	0.1	99.578943E-02	82.823882E-04	10.645835E-03	14.786528E-03
-35	0.1	99.609299E-02	79.768040E-04	10.216548E-03	13.941990E-03
-30	0.1	99.636778E-02	77.035146E-04	98.291513E-04	13.187469E-03
-25	0.1	99.661722E-02	74.587160E-04	94.788277E-04	12.511142E-03
-20	0.1	99.684425E-02	72.391627E-04	91.614533E-04	11.903041E-03
-15	1.0	97.090194E-02	70.420263E-03	88.734326E-03	11.354640E-02
-10	1.0	97.274794E-02	68.648627E-03	86.116516E-03	10.858670E-02
- 5	1.0	97.444264E-02	67.055583E-03	83.734008E-03	10.408919E-02
0	1.0	97.600140E-02	65.622648E-03	81.563166E-03	10.000030E-02
10	1.0	97.876408E-02	63.174467E-03	77.775745E-03	92.869769E-03
20	1.0	98.112672E-02	61.196856E-03	74.615796E-03	86.893857E-03
30	1.0	98.316037E-02	59.606247E-03	71.974894E-03	81.843570E-03
40	1.0	98.492131E-02	58.336863E-03	69.767225E-03	77.542798E-03
50	1.0	98.645454E-02	57.336213E-03	67.923988E-03	73.854352E-03
60	1.0	98.779622E-02	56.562245E-03	66.389815E-03	70.670549E-03
70	1.0	98.897583E-02	55.980694E-03	65.119357E-03	67.905713E-03
80	1.0	99.001750E-02	55.563615E-03	64.075444E-03	65.491310E-03
90	1.0	99.094104E-02	55.287974E-03	63.227346E-03	63.371994E-03
100	1.0	99.176296E-02	55.134644E-03	62.549387E-03	61.502701E-03
110	1.0	99.249703E-02	55.087657E-03	62.020044E-03	59.846512E-03
120	1.0	99.315478E-02	55.133587E-03	61.621162E-03	58.372948E-03
130	1.0	99.374597E-02	55.261085E-03	61.337313E-03	57.056704E-03
140	1.0	99.427887E-02	55.460474E-03	61.155300E-03	55.876605E-03
143.1	1.0	99.443336E-02	55.535573E-03	61.117756E-03	55.535575E-03
150	1.0	99.476053E-02	55.723553E-03	61.063870E-03	54.814935E-03

TABLE XII (Continued)

$T(^{\circ}C)$	$P_{(atm)}$	f/P	$(U^*- U)/RT_c$	$(H^*- H)/RT_c$	$(S^*- S)/R$
175	1.0	99.577810E-02	56.615608E-03	61.170673E-03	52.585716E-03
200	1.0	99.658472E-02	57.776844E-03	61.665610E-03	50.828872E-03
225	1.0	99.723218E-02	59.145516E-03	62.462495E-03	49.421697E-03
250	1.0	99.775760E-02	60.676896E-03	63.498325E-03	48.278472E-03
275	1.0	99.818810E-02	62.337909E-03	64.726099E-03	47.337965E-03
300	1.0	99.854383E-02	64.103612E-03	66.110110E-03	46.555535E-03
325	1.0	99.883998E-02	65.954929E-03	67.622830E-03	45.898087E-03
350	1.0	99.908816E-02	67.877011E-03	69.242688E-03	45.340658E-03
375	1.0	99.929739E-02	69.858211E-03	70.952627E-03	44.864199E-03
400	1.0	99.947470E-02	71.889203E-03	72.738920E-03	44.453919E-03

TABLE XIII

Original Data

A. Helium Calibration Data

T: 200°C Date: 10/30/64 $T_{air\ bath}$: 86°F

Run No.	r	T_{DWG}(°C)	T_{room} (°C)	P_{atm} (mm Hg)	DWG Reading (Low)
1	0	25.2	25.2	747.4	A,B,C,D,O,Q,R,T,U,X,$\overline{A}$,$\overline{B}$
	1	25.2	25.3	747.6	A,B,L,Q,S,T,U,W,$\overline{A}$,$\overline{A}$,$\overline{C}$
	2	25.5	25.6	747.4	A,L,Q,R,U,$\overline{B}$,$\overline{C}$,300 mg
	3	25.7	25.8	747.2	L,M,N,Q,U,W,$\overline{A}$
	4	25.9	26.0	747.2	L,Q,S,T,U,X,$\overline{A}$,$\overline{C}$
	5	26.1	26.2	747.0	M.P.Q.R.T.U.$\overline{A}$.A
	6	26.2	26.3	747.0	O,Q,R,T,U,$\overline{A}$,$\overline{A}$
	Date: 10/31/64			Thermotrol Setting: 636c/430f	Heater: 1 & 5 (40%)
2	0	25.7	25.8	747.8	A,B,C,D,L,S,U,$\overline{V}$,X,$\overline{A}$,$\overline{A}$,$\overline{C}$
	1	25.7	25.8	747.8	A,B,L,M,P,S,T,$\overline{B}$,300 mg
	2	25.8	26.0	747.6	A,L,O,P,Q,S,U,X,$\overline{A}$,$\overline{C}$,200 mg
	3	26.0	26.3	747.5	A,S,X,$\overline{B}$,300 mg
	4	26.3	26.5	747.3	L,P,Q,R,U,$\overline{A}$,$\overline{C}$
	5	26.4	26.6	747.2	M,O,Q,S,W,$\overline{A}$,$\overline{A}$
	6	26.5	26.6	747.2	O,P,S,T,U,W,X,$\overline{B}$,300 mg

TABLE XIII (Continued)

T: 200°C Date: 11/1/64 $T_{air\ bath}$: 86°F

Run No.	r	T_{DWG}(°C)	T_{room} (°C)	P_{atm}(mm Hg)	DWG Reading (Low)
3	0	25.1	25.3	747.3	A,B,C,D,L,M,O,P,Q,S,W,X,$\overline{A}$,$\overline{B}$
	1	25.1	25.3	747.4	A,B,L,M,N,P,Q,R,W,$\overline{A}$,$\overline{A}$
	2	25.2	25.4	747.3	A,L,M,O,Q,U,W,300 mg
	3	25.3	25.6	747.2	A,P,Q,R,T,U,X,$\overline{A}$,$\overline{B}$,$\overline{C}$
	4	25.6	25.8	747.0	L,O,Q,R,T,W,X,$\overline{B}$
	5	25.8	26.0	746.9	M,O,P,S,T,$\overline{A}$,$\overline{B}$
	6	26.0	26.2	746.8	O,P,Q,S,T,U,V,X,$\overline{A}$,$\overline{B}$
	7	26.2	26.3	746.7	P,Q,S,$\overline{A}$,$\overline{C}$
	Date: 11/2/64				
4	0	25.6	26.0	746.9	A,B,C,D,E,M,P,Q,T,$\overline{C}$
	1	25.8	26.1	746.6	A,B,C,M,Q,S,U,W,X,$\overline{B}$,$\overline{C}$
	2	26.0	26.2	746.4	A,L,M,N,P,Q,U,W,$\overline{A}$
	3	26.2	26.4	746.3	A,O,P,Q,R,W,$\overline{A}$,200 mg
	4	26.3	26.5	746.2	L,M,U,V,X,$\overline{A}$,$\overline{C}$,200 mg
	5	26.4	26.6	746.1	M,N,W,X,$\overline{B}$,250 mg
	6	26.6	26.8	746.0	M,S,U,X
	7	26.8	26.9	745.8	P,Q,R,U,V,$\overline{A}$,$\overline{A}$,$\overline{C}$
	8	27.0	27.1	745.6	Q,X,$\overline{A}$,300 mg

TABLE XIII (Continued)

T: 300°C Date: 11/4/64 $T_{air\ bath}$: 91°F

Run No.	r	T_{DWG}(°C)	T_{room} (°C)	P_{atm}(mm Hg)	DWG Reading (Low)
5	0	25.4	25.5	746.8	A,B,C,D,S,T,$\overline{C}$
	1	25.4	25.5	746.8	A,B,M,N,P,T,U,V,**X**
	2	25.4	25.6	746.9	A,M,N,P,Q,R,U,V,$\overline{A}$,$\overline{B}$,$\overline{C}$,200 mg
	3	25.5	25.7	746.7	L,M,O,P,Q,R,U,W,X,$\overline{A}$,$\overline{A}$,250 mg
	4	25.6	25.9	746.5	L,S,T,U,V,X,$\overline{A}$,250 mg
	5	25.8	26.0	746.4	M,P,Q,S,T,W,$\overline{A}$,$\overline{C}$
	6	26.0	26.2	746.4	O,Q,R,X
	7	26.2	26.3	746.5	Q,R,T,U,V,$\overline{A}$,$\overline{A}$,$\overline{C}$
	Date: 11/5/64		Thermotrol Setting: 677c/847f		Heater: 1,2 & 5 (40%)
6	0	24.3	24.4	747.1	A,B,C,D,M,N,P,T,U,W,X,$\overline{C}$,200 mg
	1	24.3	24.4	747.1	A,B,L,M,Q,S,U,V,$\overline{C}$,250 mg
	2	24.4	24.6	747.2	A,L,O,P,S,U,V,X,$\overline{A}$,$\overline{A}$,$\overline{C}$
	3	24.5	24.7	747.1	A,$\overline{B}$,250 mg
	4	24.7	24.9	747.0	L,P,Q,S,T,X,$\overline{A}$,$\overline{A}$,200 mg
	5	24.9	25.1	746.7	M,O,Q,T,U,X,$\overline{C}$,250 mg
	6	25.1	25.2	746.5	O,P,S,T,W,$\overline{A}$,$\overline{B}$
	7	25.2	25.3	746.3	P,S,T,X,$\overline{B}$

TABLE XIII (Continued)

T: 300°C Date: 11/6/64 $T_{air\ bath}$: 91°F

Run No.	r	T_{DWG}(°C)	T_{room} (°C)	P_{atm}(mm Hg)	DWG Reading (Low)
7	0	25.9	25.9	745.9	A,B,C,D,L,M,O,Q,T,U,V,X,$\overline{A}$,$\overline{C}$,300 mg
	1	25.9	25.9	746.1	A,B,L,M,N,P,S,U,W,X,$\overline{A}$
	2	26.o	26.1	746.0	A,L,M,O,T,U,X,$\overline{B}$
	3	26.1	26.2	745.8	A,P,Q,S,T,U,W,X,$\overline{A}$,$\overline{A}$,$\overline{C}$,350 mg
	4	26.2	26.4	745.5	L,O,Q,R,W,$\overline{A}$,$\overline{B}$,$\overline{C}$,300 mg
	5	26.3	26.5	745.2	M,O,P,S,U,$\overline{A}$,350 mg
	6	26.5	26.7	745.2	O,P,Q,S,T,U,X,$\overline{A}$,$\overline{A}$,$\overline{C}$,350 mg
	7	26.6	26.8	745.1	P,Q,T,U,V,$\overline{B}$,$\overline{C}$,250 mg
	8	26.8	27.0	745.0	S,W,$\overline{A}$
	Date: 11/7/64				
8	0	25.4	25.4	746.6	A,B,C,D,E,O,P,S,U,X,$\overline{B}$,200 mg
	1	25.4	25.4	746.6	A,B,C,O,P,S,T,U,V,$\overline{A}$,$\overline{A}$,200 mg
	2	25.4	25.5	746.4	A,L,M,N,Q,S,T,$\overline{A}$,$\overline{C}$,250 mg
	3	25.5	25.7	746.3	A,O,P,S,T,U,W,$\overline{A}$,$\overline{A}$
	4	25.6	25.8	746.2	L,O,P,Q,R,X,$\overline{A}$,$\overline{B}$,$\overline{C}$
	5	25.7	25.9	746.1	M,O,P,Q,R,U,W,X
	6	25.9	26.1	745.8	M,T,U,$\overline{A}$,250 mg
	7	26.1	26.2	745.7	P,Q,R,W,$\overline{B}$,$\overline{C}$,200 mg
	8	26.2	26.2	745.5	S,T,U,W,X,$\overline{B}$,$\overline{C}$,400 mg

TABLE XIII (Continued)

B. Methyl Chloride Data

T: 200°C Date: 11/11/64 $T_{air\ bath}$: 86°F

Run No.	r	T_{DWG}(°C)	T_{room} (°C)	P_{atm}(mm Hg)	DWG Reading	
9	0	25.4	25.5	734.0	A,B,C,L,M,N,P,S,T,U,$\overline{A}$,$\overline{A}$	(High)
	1	25.3	25.4	734.0	A,L,M,N,Q,R,U,X,$\overline{A}$,$\overline{A}$	"
	2	25.2	25.3	734.5	A,M,N,P,Q,T,U,V,$\overline{A}$,$\overline{B}$	"
	3	25.2	25.4	734.8	A,O,S,U,W,X,$\overline{A}$,$\overline{C}$	"
	4	25.5	25.2	737.6	A,B,C,D,P,T,X,$\overline{C}$	(Low)
	5	25.5	25.0	737.5	A,B,L,M,Q,R,T,U,V,X,$\overline{A}$,$\overline{C}$	"
	6	25.5	25.0	737.7	A,L,M,P,Q,S,T,U,V,$\overline{B}$,$\overline{C}$	"
	7	25.5	25.1	738.0	A,O,Q,T,W,$\overline{A}$	"
	8	25.5	25.0	738.3	L,O,P,Q,S,T,X,$\overline{C}$	"
	9	25.5	25.0	738.6	M,O,P,Q,R,T,U,W,$\overline{A}$	"
	10	25.3	24.9	740.2	M,S,U,W,X,$\overline{B}$,$\overline{C}$	"
	Date: 11/12/64		Thermotrol Setting: 636c/430f		Heater: 1 & 5(40%)	
10	0	24.7	24.7	746.4	A,B,C,D,L,M,N,Q,R,U,V,X,$\overline{B}$	(High)
	1	24.8	24.9	746.3	A,B,Q,R,T,U,X,$\overline{A}$,$\overline{B}$	"
	2	24.9	25.0	746.4	A,L,Q,S,T,X,$\overline{C}$	"
	3	24.9	25.0	746.5	A,O,P,S,T,W,$\overline{A}$,$\overline{A}$,$\overline{C}$	"
	4	25.2	25.0	746.8	A,B,C,D,M,P,Q,S,T,W,X,$\overline{B}$,$\overline{C}$	(Low)
	5	25.2	25.0	747.4	A,B,L,M,N,Q,U,W,$\overline{A}$,$\overline{A}$	"
	6	24.9	24.9	747.7	A,L,M,N,S,$\overline{A}$,$\overline{A}$	"
	7	25.1	24.9	747.7	A,M,T,X,$\overline{A}$	"
	8	25.1	24.9	747.8	L,M,Q,S,T,U,X,$\overline{A}$,$\overline{B}$	"
	9	25.1	24.9	747.9	M,N,Q,T,U,W,X,$\overline{A}$,$\overline{C}$	"
	10	25.0	24.8	747.9	M,Q,S,W,X,$\overline{C}$	"

TABLE XIII (Continued)

T: 225°C Date: 11/14/64 $T_{air\ bath}$: 87°F

Run No.	r	T_{DWG}(°C)	T_{room} (°C)	P_{atm}(mm Hg)	DWG Reading	
11	0	24.1	24.2	747.3	A,B,C,L,M,P,Q,T,$\underline{W}$,X	(High)
	1	24.1	24.2	747.3	A,B,O,P,S,U,$\underline{W}$,$\underline{X}$,$\overline{B}$	"
	2	24.1	24.3	747.1	A,L,P,Q,T,U,$\underline{A}$,$\underline{C}$	"
	3	24.2	24.5	747.1	A,O,Q,S,U,W,$\overline{A}$,$\overline{A}$,$\overline{C}$	"
	4	24.3	24.6	746.9	A,B,C,L,M,N,P,Q,$\underline{R}$,$\underline{U}$,$\underline{V}$,$\overline{A}$,$\overline{B}$	(Low)
	5	24.5	24.8	746.8	A,B,L,O,P,$\underline{S}$,U,X,$\overline{A}$,$\overline{B}$,$\overline{C}$	"
	6	24.7	24.9	746.6	A,L,M,S,X,$\overline{C}$	"
	7	24.9	25.0	746.5	A,P,S,U,V,X,$\overline{A}$	"
	8	25.0	25.2	746.4	L,O,Q,S,T,U,X,$\overline{A}$,$\overline{B}$	"
	9	25.1	25.2	746.1	M,O,P,S,U,W,X,$\overline{A}$,$\overline{C}$	"
	10	25.2	25.3	746.0	O,P,Q,S,T,U,W,$\overline{A}$,$\overline{A}$,$\overline{B}$,$\overline{C}$	"
	Date: 11/15/64			Thermotrol Setting: 647c/680f		Heater: 1 & 5(63%)
12	0	25.3	25.3	746.3	A,B,C,D,L,M,N,P,$\underline{U}$,$\overline{A}$	(High)
	1	25.3	25.4	746.3	A,B,M,O,P,$\underline{Q}$,$\underline{W}$,$\underline{X}$,$\overline{B}$	"
	2	25.4	25.6	746.1	A,L,M,U,X,$\overline{A}$,$\overline{A}$,$\overline{C}$	"
	3	25.6	25.8	746.0	A,M,Q,S,U,V,X,$\overline{A}$,$\overline{B}$,$\overline{C}$	"
	4	25.8	25.9	745.8	A,B,C,D,M,P,Q,R,W,$\underline{O}$,$\overline{A}$	(Low)
	5	25.9	26.0	745.7	A,B,L,M,N,Q,S,U,$\underline{X}$,$\overline{B}$,$\overline{C}$	"
	6	26.1	26.2	745.5	A,L,M,N,T,U,V,$\underline{X}$,$\overline{A}$,$\overline{B}$	"
	7	26.2	26.2	745.3	A,O,P,Q,$\underline{R}$,$\underline{T}$,$\underline{U}$,$\overline{C}$	"
	8	26.2	26.1	745.2	L,M,Q,T,$\overline{A}$,$\overline{B}$,$\overline{C}$	"
	9	26.1	26.0	745.1	M,N,S,T,$\underline{U}$,$\overline{A}$,$\overline{A}$,$\overline{C}$	"
	10	25.9	25.8	745.1	M,Q,U,V,$\overline{A}$	"

TABLE XIII (Continued)

T: 250°C Date: 11/16/64 $T_{air\ bath}$: 88°F

Run No.	r	T_{DWG}(°C)	T_{room} (°C)	P_{atm}(mm Hg)	DWG Reading	
13	0	25.0	25.1	751.9	A,B,C,D,L,M,N,P,T,U,W,X,$\overline{A}$,$\overline{B}$,$\overline{C}$	(High)
	1	25.2	25.1	752.1	A,B,L,O,Q,U,V,$\overline{A}$,$\overline{A}$,$\overline{B}$,$\overline{C}$,X	"
	2	25.2	25.1	752.0	A,L,M,O,Q,T,U,W,$\overline{C}$	"
	3	25.2	24.9	752.1	A,M,P,Q,S,W,X,$\overline{A}$,$\overline{A}$	"
	4	25.2	25.0	752.0	A,B,C,D,M,N,Q,R,T,U,V,$\overline{A}$,$\overline{C}$	(Low)
	5	25.2	25.0	752.0	A,B,L,M,N,Q,T,U,$\overline{A}$,$\overline{A}$	"
	6	25.3	25.0	751.9	A,L,M,O,P,S,T,U,V,X,$\overline{A}$	"
	7	25.3	24.9	751.5	A,O,P,S,U,$\overline{B}$,$\overline{C}$	"
	8	25.3	24.9	751.2	L,M,$\overline{A}$,$\overline{A}$,$\overline{C}$	"
	9	25.3	25.0	751.1	M,N,U,V,$\overline{A}$	"
	10	25.3	25.0	750.9	M,S,T,W	"
	Date: 11/17/64		Thermotrol Setting: 658c/640f		Heater: 1 & 5 (81%)	
14	0	24.9	24.7	748.2	A,B,C,L,M,Q,R,T,U,V,W	(High)
	1	25.0	24.8	747.9	A,B,M,O,S,W,X,$\overline{A}$,$\overline{A}$,$\overline{C}$	"
	2	25.4	25.0	748.0	A,L,O,Q,S,U,W,$\overline{A}$	"
	3	25.5	25.0	748.2	A,O,Q,S,U,W,$\overline{A}$,$\overline{A}$	"
	4	25.5	24.8	748.0	A,B,C,L,M,O,P,Q,R,T,W,X,$\overline{A}$,$\overline{B}$,$\overline{C}$	(Low)
	5	25.4	24.8	748.4	A,B,L,Q,S,T,U,X,$\overline{A}$,$\overline{C}$	"
	6	25.4	24.8	748.5	A,L,O,T,W,X	"
	7	25.6	24.9	748.2	L,M,N,P,Q,S,T,U,V,$\overline{A}$	"
	8	25.6	24.8	748.4	L,P,Q,S,T,U,V,$\overline{C}$	"
	9	25.6	24.9	748.4	M,O,Q,S,U,W,$\overline{A}$,$\overline{B}$	"
	10	25.7	25.0	748.6	O,P,Q,W,$\overline{A}$	"

TABLE XIII (Continued)

T: 275°C Date: 11/27/64 $T_{air\ bath}$: 90°F

Run No.	r	T_{DWG}(°C)	T_{room} (°C)	P_{atm}(mm Hg)	DWG Reading	
15	0	25.4	25.0	736.0	A,B,C,D,L,M,N,Q,R,T,$\underline{W}$,X,$\overline{B}$	(High)
	1	25.4	25.0	736.4	A,B,L,M,P,Q,S,T,W,X,$\overline{C}$	"
	2	25.5	25.1	236.8	A,L,M,O,P,Q,R,T,$\underline{U}$,$\underline{V}$,X,$\overline{A}$,$\overline{B}$,$\overline{C}$	"
	3	25.6	25.1	737.4	A,M,P,Q,R,T,U,W,$\overline{A}$,$\overline{A}$	"
	4	25.7	25.1	738.3	A,B,C,D,M,N,S,T,U,V,X,$\overline{A}$	(Low)
	5	25.8	25.1	738.4	A,B,L,M,O,P,S,T,$\underline{U}$,$\underline{V}$,W,$\overline{B}$	"
	6	25.7	25.0	740.0	A,L,M,O,S,$\underline{T}$,$\underline{W}$,X,$\overline{A}$,$\overline{C}$	"
	7	25.8	25.1	741.0	A,O,Q,W,X,$\overline{A}$,$\overline{B}$	"
	8	25.8	25.1	741.2	L,O,P,Q,U,$\overline{A}$,$\overline{A}$	"
	9	25.8	25.0	741.7	M,O,P,$\underline{Q}$,$\underline{S}$,T,X,$\overline{B}$,$\overline{C}$	"
	10	25.8	25.1	742.2	M,U,V,$\overline{B}$,$\overline{C}$	"
	Date: 11/28/64		Thermotrol Setting: 668c/720f		Heater: 1 & 5 (95%)	
16	0	24.5	24.0	758.3	A,B,C,L,M,P,T,U,X,$\overline{A}$,$\overline{B}$	(High)
	1	24.9	24.1	759.1	A,B,M,O,P,Q,$\underline{S}$,T,W,$\overline{B}$	"
	2	24.8	23.8	759.8	A,L,O,Q,R,$\underline{U}$,$\overline{A}$	"
	3	24.8	24.0	760.2	A,O,T,U,W,$\overline{A}$,$\overline{A}$	"
	4	24.7	23.7	761.1	A,B,C,L,M,Q,$\underline{S}$,$\underline{U}$,$\overline{B}$	(Low)
	5	24.9	24.0	761.4	A,B,M,N,U,$\underline{W}$,$\overline{A}$,$\overline{B}$,$\overline{C}$	"
	6	24.9	23.7	761.5	A,L,T,U,X,$\overline{C}$	"
	7	24.8	23.9	761.6	L,M,N,Q,X,$\overline{B}$,$\overline{C}$	"
	8	24.8	23.8	761.6	L,Q,R,T,$\underline{U}$,X	"
	9	24.9	24.0	761.7	M,O,T,W,$\overline{B}$,$\overline{C}$	"
	10	25.2	24.2	762.0	O,P,U,W,X,$\overline{A}$,$\overline{C}$	"

TABLE XIII (Continued)

T: 300°C Date: 11/30/64 $T_{air\ bath}$: 91°F

Run No.	r	T_{DWG}(°C)	T_{room} (°C)	P_{atm}(mm Hg)	DWG Reading	
17	0	25.2	24.9	754.1	A,B,C,D,L,M,N,Q,R,U,W,X,$\overline{A}$,$\overline{A}$	(High)
	1	25.2	24.9	753.8	A,B,L,M,O,P,Q,S,W,$\overline{A}$	"
	2	25.2	24.9	753.2	A,L,M,N,Q,T,U,V,$\overline{B}$	"
	3	25.1	24.8	752.8	A,M,P,Q,S,T,U,V	"
	4	25.1	24.8	752.6	A,B,C,D,M,O,S,T,W,X,$\overline{B}$	(Low)
	5	25.1	24.7	752.2	A,B,L,M,P,Q,U,X,$\overline{B}$	"
	6	25.1	24.6	752.1	A,L,M,Q,R,W,X,$\overline{B}$	"
	7	25.0	24.6	752.6	A,P,S,T,U,W,$\overline{A}$,$\overline{A}$,$\overline{C}$	"
	8	25.0	24.7	752.2	L,O,Q,S,T,W,$\overline{A}$,$\overline{A}$,$\overline{C}$	"
	9	25.0	24.9	752.0	M,O,P,S,U,$\overline{A}$	"
	10	25.0	24.9	751.9	O,P,Q,S,T,U,V,X	"
	Date: 12/1/64		Thermotrol Setting: 677c/847f		Heater: 1,2 & 5(40%)	
18	0	25.2	24.9	734.3	A,B,C,L,P,Q,U,W,$\overline{A}$,$\overline{A}$	(High)
	1	25.2	24.9	734.4	A,B,M,O,Q,$\overline{A}$,$\overline{B}$	"
	2	25.2	24.9	734.4	A,L,P,S,T,$\overline{A}$	"
	3	25.1	24.9	734.6	A,Q,S,W,X,$\overline{A}$,$\overline{A}$	"
	4	25.1	24.8	734.9	A,B,C,M,N,S,T,U,V,$\overline{A}$	(Low)
	5	25.1	24.8	735.2	A,B,O,P,Q,T,U,V,X,$\overline{A}$,$\overline{A}$,$\overline{C}$	"
	6	25.2	24.8	735.3	A,M,O,P,T,W,$\overline{A}$	"
	7	25.2	24.7	735.5	L,M,O,Q,U,$\overline{C}$	"
	8	25.2	24.7	735.8	M,N,P,Q,S,$\overline{A}$,$\overline{A}$	"
	9	25.1	24.6	736.0	M,P,S,U,V,$\overline{A}$,$\overline{C}$	"
	10	25.1	24.6	735.9	O,Q,T,U,W,$\overline{A}$,$\overline{A}$	"

TABLE XIII (Continued)

T: 325°C Date: 12/5/64 $T_{air\ bath}$: 93°F

Run No.	r	T_{DWG}(°C)	T_{room} (°C)	P_{atm}(mmHg)	DWG Reading	
19	0	25.1	24.6	747.4	A,B,C,D,L,M,Q,R,T,W,X,$\overline{A}$,$\overline{A}$,**N**	(High)
	1	25.1	24.6	747.9	A,B,L,M,N,Q,R,U,V,$\overline{A}$,$\overline{A}$	"
	2	25.0	24.6	748.5	A,L,M,N,Q,R,W,$\overline{A}$	"
	3	24.9	24.6	749.3	A,M,P,Q,W,$\overline{A}$,$\overline{A}$	"
	4	25.4	24.7	749.7	A,B,C,D,O,P,Q,R,T,U,X,$\overline{A}$,$\overline{B}$	(Low)
	5	25.4	24.7	750.2	A,B,L,O,P,Q,$\overline{A}$,$\overline{A}$	"
	6	25.3	24.7	750.6	A,L,O,P,S,T,U,V	"
	7	25.3	24.6	751.2	A,S,T,U,$\overline{A}$,$\overline{C}$	"
	8	25.2	24.6	751.7	L,O,U,X,$\overline{A}$	"
	9	25.2	24.6	752.1	M,O,Q,R,X,$\overline{B}$,$\overline{C}$	"
	10	25.2	24.5	752.3	O,P,Q,T,X,$\overline{B}$,$\overline{C}$	"
	Date: 12/6/64		Thermotrol Setting: 687c/495f		Heater: 1,2 & 5(70%)	
20	0	24.3	24.4	756.7	A,B,C,L,M,P,Q,U,V,X,$\overline{A}$,$\overline{A}$	(High)
	1	24.4	24.3	756.5	A,B,M,N,P,S	"
	2	24.7	24.5	756.4	A,L,O,Q,S,U,X,$\overline{A}$	"
	3	24.9	24.6	756.3	A,P,T,$\overline{A}$,$\overline{B}$	"
	4	24.6	24.7	756.3	A,B,C,M,N,Q,R,U,X,$\overline{B}$	(Low)
	5	24.8	24.6	756.2	A,B,O,P,Q,T,U,$\overline{C}$	"
	6	24.9	24.5	756.2	A,M,O,Q,R,T,U,$\overline{B}$	"
	7	25.1	24.5	756.1	L,M,O,S,U,W,$\overline{B}$,$\overline{C}$	"
	8	25.2	24.4	756.0	M,N,P,Q,U,W,$\overline{B}$,$\overline{C}$	"
	9	25.3	24.3	756.1	M,P,T,U,V,$\overline{C}$	"
	10	25.2	24.4	756.0	O,Q,U,V,$\overline{A}$,$\overline{B}$	"

TABLE XIII (Continued)

T: 350°C Date: 12/7/64 $T_{air\ bath}$: 94°F

Run No.	r	T_{DWG}(°C)	T_{room} (°C)	P_{atm}(mm Hg)	DWG Reading	
21	0	25.1	24.6	749.1	A,B,C,D,L,M,N,P,X,$\overline{A}$,$\overline{B}$	(High)
	1	25.2	24.6	748.4	A,B,L,M,N,P,Q,S,T,W,X,$\overline{B}$	"
	2	25.3	24.7	747.5	A,L,M,N,Q,R,U,W,X,$\overline{A}$,$\overline{B}$	"
	3	25.4	24.8	746.8	A,M,P,W,$\overline{B}$	"
	4	25.5	24.7	746.7	A,B,C,D,P,Q,T,U,V,X,$\overline{A}$,$\overline{B}$	(Low)
	5	25.6	24.6	746.6	A,B,L,P,Q,U,V,$\overline{A}$,$\overline{B}$	"
	6	25.6	24.6	746.6	A,L,P,Q,R,T,U,W,$\overline{A}$,$\overline{B}$	"
	7	25.5	24.6	746.5	L,M,N,P,Q,W,$\overline{A}$,$\overline{B}$,$\overline{C}$	"
	8	25.5	24.7	746.4	L,P,Q,U,W,$\overline{A}$,$\overline{B}$,$\overline{C}$	"
	9	25.5	24.7	746.4	M,O,Q,U,$\overline{A}$,$\overline{A}$,$\overline{C}$	"
	10	25.4	24.7	746.4	O,P,S,U,V,$\overline{A}$,$\overline{A}$,$\overline{C}$	"
	Date: 12/8/64		Thermotrol Setting: 695c/630f		Heater: 1,2 & 5(89%)	
22	0	25.2	24.5	745.2	A,B,C,L,M,P,Q,U,V,X,$\overline{A}$,$\overline{A}$	(High)
	1	25.2	24.5	745.3	A,B,M,N,P,S,U,V,X,$\overline{A}$,$\overline{A}$	"
	2	25.2	24.4	745.5	A,L,O,S,U,V,$\overline{B}$	"
	3	25.2	24.7	746.1	A,Q,T,W,$\overline{A}$,$\overline{C}$	"
	4	25.3	24.7	746.2	A,B,C,M,O,S,X,$\overline{B}$	(Low)
	5	25.2	24.7	746.2	A,B,P,Q,T,X,$\overline{A}$,$\overline{B}$	"
	6	25.3	24.7	746.3	A,M,P,Q,T,U,X,$\overline{A}$,$\overline{C}$	"
	7	25.3	24.4	746.9	L,M,P,S,T,U,W	"
	8	25.3	24.5	746.9	M,N,Q,R,U,V,$\overline{A}$,$\overline{C}$,X	"
	9	25.3	24.7	746.9	M,Q,R,W,$\overline{A}$,$\overline{B}$,$\overline{C}$	"
	10	25.3	24.7	747.0	O,S,U,W,X,$\overline{C}$	"

VITA

The author was born on September 26, 1935 in Seoul, Korea. He came to the United States in 1953 to study at the Citrus Junior College in Azusa, California, and received a A.A. degree in 1955. He enrolled in M.I.T. and received a B.S. degree in Chemical Engineering in 1957. He entered the graduate school of the University of Delaware and received a M.S. degree in Chemical Engineering in 1959. After working two years in industry, he enrolled in the University of Missouri in 1961.

The undersigned, appointed by the Dean of the Graduate Faculty, have examined a thesis entitled

P-V-T PROPERTIES OF METHYL CHLORIDE AT
HIGH TEMPERATURES AND PRESSURES

presented by Kyung Won Suh

a candidate for the degree of Doctor of Philosophy

and hereby certify that in their opinion it is worthy of acceptance.

Truman Storvick

George W. Preckshot

Floyd B Thomas